

Influence of Resonant and Foreign Gas Collisions on Line Shapes*

P. R. Berman† and Willis E. Lamb, Jr.

Physics Department, Yale University, New Haven, Connecticut 06520

(Received 21 April 1969)

In the limit of a dipole-dipole interaction between neutral atoms and the binary-collision approximation, we present a theory of pressure broadening in which the multiplet structure of the atomic levels is considered. The appropriate Schrödinger equations for the collision problem are numerically integrated to obtain solutions for both resonant and foreign gas broadening. The presence of radiation fields is neglected in the first half of the paper, where the collisional time rate of change of the density matrix is found. The pertinent collisional decay parameters are extracted from these equations. The ratios of the parameters of the average magnetic dipole to electric quadrupole moment obtained were 1.21 ± 0.02 for the relaxation of the entire ensemble in resonant broadening, 0.966 ± 0.012 for the relaxation of the initially excited atoms in resonant broadening, and 1.12 ± 0.02 for the relaxation of the initially excited atoms in foreign gas broadening. In the second half of the paper, the collisional broadening results are incorporated in a systematic evaluation of (i) spectral profiles (effects arising from the velocity and recoil of the emitting atom are neglected), (ii) Hanle-effect line shapes, and (iii) laser phenomena. For the case of resonant broadening, the radiation trapping process is reviewed and its influence on line shapes discussed. Finally, a detailed comparison of the theory with experimental findings as well as with previous theoretical results is made. We conclude that the dipole-dipole interaction is sufficient to explain most cases of resonant and some cases of foreign gas broadening.

I. INTRODUCTION

In the past decade, there has been increased interest in applying pressure broadening theory to obtain information about atomic systems. The earlier impact theories of Lindholm,¹ Foley,² and Anderson³ have been modified or extended by several authors.⁴⁻³² In effect, Lindholm and Foley neglected the multiplet structure of the atomic levels and explained the collision process in terms of collision-induced phase shifts in a two-level problem. For a given atom-atom interaction, this procedure led to a predicted value of the ratio of shift and width for collision-broadened spectral lines.

Anderson included multiplet structure and showed that its inclusion led to an interaction matrix that did not commute with itself at different times. The problem of noncommutativity led to several approximate methods of handling the problem. Either the noncommutativity was ignored, or the problem was solved by perturbative techniques using a cutoff procedure to treat close collisions. To check the errors introduced in such approximate methods, it is desirable to find numerical solutions of the Schrödinger equation for the collision problem.

In the impact approximation and in the limit of a dipole-dipole interaction between neutral atoms, we shall present such a numerical theory of pressure broadening in which we consider the multiplet structure of the pertinent atomic levels. Both res-

onant³³ and foreign gas broadening will be studied by similar techniques to obtain the various multipole decay parameters of the problem as well as the collisional time rate of change of the density matrix of the system under consideration.

Several similar calculations have appeared for the case of resonant broadening^{9,12,15,22,26,28,31} and there have been numerical discrepancies between some of these results. We hope that our results will resolve these differences. The techniques employed are essentially equivalent to those of Dyakonov and Perel,⁹ Omont,¹⁰ and Kazantsev¹⁵ which, in turn, reflect the work of Anderson. We include the resonant broadening results for the sake of unity of presentation and as an independent numerical check of previous results. In addition, we shall work in the magnetic quantum number representation for the density matrix as well as the irreducible representation commonly employed and shall incorporate our results in a systematic treatment of evaluating experimental line shapes.

An outline of the paper is given below.

- | | | |
|----------|---|--|
| Sec. I | – | Introduction |
| Sec. II | – | Approximations and method of approach |
| Sec. III | – | Solution for resonant broadening |
| Sec. IV | – | Solution for nonresonant broadening |
| Sec. V | – | A generalization of the theory of Secs. III–IV to allow for additional |

- virtual transitions and broadening of both upper and lower levels
- Sec. VI – Effect of interaction with radiation fields
- Sec. VII – Nonresonant line shapes
 - A. Spectral profiles
 - B. Depolarization effects (Hanle effect)
 - C. Laser phenomena
- Sec. VIII – Resonant line shapes
 - A. Depolarization effects (Hanle effect)
 - B. Spectral profiles
 - C. Laser phenomena
- Sec. IX – Comparison with other theories and experiments
- Sec. X – Discussion of results
- Appendix A Numerical solution for resonant case
- Appendix B Numerical solution for nonresonant case
- Appendix C Treatment of close collisions by an adiabatic approximation
- Appendix D Procedures for performing the needed averages over impact parameter, relative speed, and collision orientations

In Secs. II–V, we shall neglect all interactions of the atomic system with radiation fields and consider those changes in the system caused solely by collisions. This will give rise to a calculation of collision broadening parameters. In Secs. VI–VIII, we shall extend the calculations to allow for the presence of spontaneous emission and obtain line-shape formulas corresponding to various experimental situations. We shall see that the average electric-dipole-moment decay parameter associated with two radiative levels is responsible for the shift and width in spectral profiles. The various multipole decay parameters associated with a given atomic level will be relevant to a discussion of Hanle-effect line shapes. In addition, we shall indicate how a study of laser phenomena can be instrumental in determining broadening parameters. For the case of resonant broadening, we shall review the resonant trapping process,^{34–37} and exhibit its importance in line-shape calculations.

In Sec. IX, we shall compare the results with other theories and recent experiments,^{31, 38–54} and give values for certain oscillator strengths based on the theory and experimental results. A short discussion of the effects of very close collisions will also be given in Sec. IX, in which we argue against the use of some “intuitive” strong collision cutoffs previously used.^{10, 26, 31}

II. APPROXIMATIONS AND METHOD OF APPROACH

The physical system to be considered consists

of an excited atom (emitter) undergoing collisions with ground-state atoms (perturbers). In general, the interaction between the emitter and a perturber is an exceedingly complex function of their separation. However, if only those collisions in which the impact parameter is much larger than atomic dimensions are considered, the emitter-perturber interaction can be represented by the electrostatic multipole expansion. We shall retain only the leading dipole-dipole term of this expansion.

The assumption that the interaction can be approximated solely by the dipole-dipole term is not valid for very close collisions. To treat such collisions properly would require a demanding quantum treatment of the problem. The dipole-dipole approximation will be valid if close collisions do not contribute appreciably to the line shapes.

When the emitter and perturbers are atoms of the same kind (resonant perturbers), the dipole-dipole interaction will contribute in first order. If the oscillator strength of the resonant transition (the transition from the excited to ground state) is relatively large, one should expect the dipole-dipole term to provide a good approximation to the total interaction, since its effective range will be many times greater than atomic dimensions. On the other hand, if the emitter and perturber atoms are different (foreign gas or nonresonant perturbers), the lowest contribution from the interaction occurs in second order. In general, this will lead to an effective range for the dipole-dipole interaction on the order of or less than 10 \AA . At this range, one may already question the validity of the use of a pure dipole-dipole interaction. The only justification for its use in these cases will be found in the agreement between theory and experiment.

One should note that even in the case of resonant broadening, the second-order or nonresonant effects may be comparable with the first-order or resonant effects if the oscillator strength of the resonant transition is small. However, for resonant broadening perturbers, we shall consider only those cases where the resonant effects are dominant.

Figure 1 illustrates the general form of the interaction potential seen by the emitter in a collision with a single perturber. The time $t=0$ is chosen to coincide with the point of closest approach. The amplitude of the central peak is dependent upon an inverse power of the impact parameter b of the collision. Since the amplitude falls off rapidly with impact parameter, the significant collisions occur only with impact parameters on the order of some critical impact parameter b_0 . We can choose b_0 as that radius in a hard-sphere model which will produce optical cross sections equal to those predicted by the theory to be discussed in Secs. III–V. The radius b_0 is essentially equal to the Weisskopf or optical

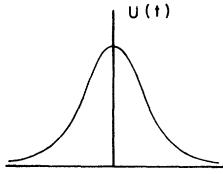


FIG. 1. General form of the emitter-perturber interaction potential.

collision radius⁵⁵ and will depend on the strength of the interaction and on the average relative speed of the emitter and perturber.

The collision time τ_c will be defined as the duration of the interaction pulse shown in Fig. 1, when the impact parameter is b_0 . As we have already noted, collisions with larger impact parameters (and larger collision times) will not prove to be very significant in the broadening problem. To a fair approximation, one may take $\tau_c = b_0/v$, where v is the average relative speed of the emitter and perturber. For a typical case, $b_0 \approx 10^{-7}$ cm and $v \approx 5 \times 10^4$ cm/sec giving $\tau_c \approx 2 \times 10^{-12}$ sec.

One need not consider collisions between three atoms if the time between binary collisions is much larger than the collision time. The time between collisions is approximately given by $[\mathfrak{N} \pi \times b_0^2 v]^{-1}$ where \mathfrak{N} is the perturber density. Thus, three-body collisions may be neglected if

$$[\mathfrak{N} \pi b_0^2 v]^{-1} \gg \tau_c \approx b_0/v, \quad \text{or} \quad \mathfrak{N} \pi b_0^3 \ll 1, \quad (1a)$$

which is the requirement that the average number of perturbers in a sphere having the optical collision radius b_0 be much less than unity. Since the time between collisions is also approximately the inverse of the "collision width" Γ_c , an alternate form of Eq. (1a) is

$$\tau_c \ll [\Gamma_c]^{-1}. \quad (1b)$$

Equations (1a) or (1b) are criteria for the "impact

approximation" of pressure broadening theory^{1,4,5,6,21} which, in this context, states that one is able to consider each collision as an independent event. For the purposes of this work, we shall restrict the discussion to pressures where the impact approximation is valid.

Finally, we note two additional assumptions which will be made. First, it will be assumed that the perturber atoms follow straight-line classical paths. Second, we shall make several assumptions on the relative magnitude of $(\tau_c)^{-1}$ compared with energy-level separations (to be discussed in Secs. III and IV) which effectively treat the collision as adiabatic with respect to the fine-structure separation and diabatic with respect to the Zeeman splitting. Neither these assumptions nor the dipole-dipole approximation are valid for very close collisions where the collision time is short. Such effects will manifest themselves in the wings of the lines, and we should not expect the theory to provide an adequate description in this region.

With the above assumptions, it is necessary to consider only binary collisions and we shall proceed as follows: (i) The Schrödinger equation for emitter-perturber system is obtained. (ii) A given collision geometry is chosen and the change in the wave function resulting from the collision is calculated. For distant collisions ($b \gg b_0$), the change in the wave function may be obtained by perturbation theory, but for intermediate collisions ($b \approx b_0$), a numerical solution is necessary. Very strong collisions ($b \ll b_0$) are treated by an additional adiabatic approximation to be discussed and justified in Appendix C. (iii) From the collisional change of the density matrix of the emitter-perturber system is found. (iv) The density matrix is contracted to provide the change in the density matrix of the emitter and perturber separately. (v) One then multiplies the change due to a single collision by the differential rate of such collisions and averages over all possible collision histories to obtain rate equations for the density matrix.

III. RESONANT CASE

The resonant case arises when the perturber and emitter possess identical energy schemes such as shown in Fig. 2.

The emitter is in a linear superposition of the states a , b , and s , and the perturber is in the ground state s before the collision. The transition $a \rightarrow s$ is the resonant one while state b has been introduced to allow for a study of optical transitions between excited states a and b . The level a will be taken to have total angular momentum $j=1$ and levels b and s to have $j=0$. We shall assume that the dominant broadening mechanism is the resonant dipole-dipole interaction between the states a and s . In that case, the levels shown are the only ones requiring consideration. At any time t during the collision, the state vector of the system of emitter and perturber may be written

$$|\psi(t)\rangle = \sum_m \{ [a_m(t)|m;s\rangle + w_m(t)|s;m\rangle] \exp(-iE_{ms}t/\hbar) \} + [c(t)|b;s\rangle + h(t)|s;b\rangle] \exp(-iE_{sb}t/\hbar)$$

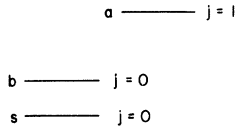


FIG. 2. Atomic structure of emitter or perturber for the resonant case. The transition $a \rightarrow s$ is the resonant one, where s is the ground state.

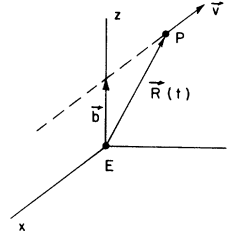


FIG. 3. Collision axes for the standard orientation Ω_0 . The emitter E is at the origin and the perturber P at $\vec{R}(t)$ in the xz plane. The perturber moves with relative speed v in the $-\hat{x}$ direction and the impact parameter \vec{b} is along the z axis.

$$+ \sum_{mm'} f_{mm'}(t) |m; m'\rangle \exp(-iE_{mm'}t/\hbar) + g(t) |s; s\rangle \exp(-iE_{ss}t/\hbar). \quad (2)$$

The first letter in each ket stands for the emitter state and the second for the perturber state. The m refers to a magnetic substate of the a level ($j=1$), and the b to the lower radiative state shown in Fig. 2. The energies E_{ab} are defined by

$$E_{ab} = E_a + E_b, \quad (3)$$

where the E 's are the energies of the various levels.

The first step in the calculation is to compute the effects of a given collision. At a later stage, an average over-all collision histories will be performed. For our given or "standard" collision orientation (designated by Ω_0), we take the impact parameter b along the z axis, and the perturber moving in the xz plane with speed v relative to the emitter. The axes are chosen with origin at the emitter as shown in Fig. 3. The dipole-dipole interaction is of the form

$$U(t) = [R(t)]^{-3} \{ \vec{p}_E \cdot \vec{p}_P - 3[\vec{p}_E \cdot \vec{R}(t)][\vec{p}_P \cdot \vec{R}(t)]/[R(t)]^2 \}, \quad (4)$$

where $\vec{p}_E = e \sum_i \vec{r}_i(E)$, and $\vec{p}_P = e \sum_j \vec{r}_j(P)$.

The separation of emitter and perturber is denoted by $\vec{R}(t)$, while $\vec{r}_i(E)$ and $\vec{r}_j(P)$ represent electronic coordinates of emitter and perturber, respectively. If we define $\vec{p}_E = e(x_E, y_E, z_E)$, $\vec{p}_P = e(x_P, y_P, z_P)$, and choose the time origin such that $\vec{R}(t) = b\hat{z} - vt\hat{x}$, the interaction takes the form

$$U(t) = \{ e^2/[R(t)]^5 \} \{ x_E x_P [(R(t))^2 - 3v^2t^2] + y_E y_P (R(t))^2 + z_E z_P [(R(t))^2 - 3b^2] + (x_E z_P + z_E x_P)(3bvt) \}. \quad (5)$$

Utilizing the fact that \vec{p} can be expressed in terms of components of an irreducible tensor of rank 1,⁵⁶ the nonvanishing matrix elements of $U(t)$ are found to be (the axis of quantization is taken along the z axis)

$$\begin{aligned} \langle n_1 00; n_2 00 | U(t) | n_3 1m_E; n_4 1m_P \rangle &= \frac{1}{6} [e^2 a_0^2 / (R(t))^5] [T_E(n_1 0, n_3 1) T_P(n_2 0, n_4 1)] \{ [\delta(m_E, -1) - \delta(m_E, 1)] \\ &\times [\delta(m_P, -1) - \delta(m_P, 1)] [(R(t))^2 - 3v^2t^2] - [\delta(m_E, 1) + \delta(m_E, -1)] [\delta(m_P, 1) + \delta(m_P, -1)] (R(t))^2 \\ &+ 2\delta(m_E, 0)\delta(m_P, 0) [(R(t))^2 - 3b^2] + 3(\sqrt{2})bvt \{ [\delta(m_E, -1) - \delta(m_E, 1)]\delta(m_P, 0) + [\delta(m_P, -1) \\ &- \delta(m_P, 1)]\delta(m_E, 0) \} \} = \langle n_3 1m_E; n_4 1m_P | U(t) | n_1 00; n_2 00 \rangle^*, \end{aligned} \quad (6)$$

and

$$\langle n_1 00; n_4 1m_P | U(t) | n_3 1m_E; n_2 00 \rangle = \frac{1}{6} [e^2 a_0^2 / (R(t))^5] [T_E(n_1 0, n_3 1) T_P^*(n_2 0, n_4 1)] \{ [\delta(m_E, -1)$$

$$\begin{aligned}
& -\delta(m_E, 1)[\delta(m_P, -1) - \delta(m_P, 1)] [(R(t))^2 - 3v^2t^2] + [\delta(m_E, 1) + \delta(m_E, -1)][\delta(m_P, 1) \\
& + \delta(m_P, -1)](R(t))^2 + 2\delta(m_E, 0)\delta(m_P, 0)[(R(t))^2 - 3b^2] + 3(\sqrt{2})bvt[\delta(m_E, -1) - \delta(m_E, 1)]\delta(m_P, 0) \\
& + [\delta(m_P, -1) - \delta(m_P, 1)]\delta(m_E, 0)\} = \langle n_3 1m_E; n_1 00 | U(t) | n_2 00; n_4 1m_P \rangle^*, \quad (7)
\end{aligned}$$

where $T(nj, n'j')$ is the reduced matrix element in units of the Bohr radius a_0 ⁵⁷ of the irreducible tensor of rank 1 formed from the components of \vec{p} between states nj and $n'j'$ of the atom in question, while $\delta(m, m')$ is the Kronecker δ .

The Hamiltonian for this two-particle system is $H = H_0 + U(t)$, where the unperturbed Hamiltonian H_0 satisfies the relationship $H_0 |m; s\rangle = E_{mS} |m; s\rangle$. It will be convenient to introduce the following notation for the interaction matrix of the two-particle system:

$$\begin{array}{cccccc}
a1^*;s0^* & s0^*;a1^* & b0^*;s0^* & s0^*;b0^* & a1^*;a1^* & s0^*;s0^* \\
U(t) = \begin{bmatrix} 0 & V(t) & 0 & 0 & 0 & 0 \\ V^\dagger(t) & 0 & 0 & 0 & 0 & 0 \\ 0 & 0 & 0 & 0 & F(t) & 0 \\ 0 & 0 & 0 & 0 & H(t) & 0 \\ 0 & 0 & F^\dagger(t) & H^\dagger(t) & 0 & G(t) \\ 0 & 0 & 0 & 0 & G^\dagger(t) & 0 \end{bmatrix} & & & & & (8)
\end{array}$$

In this notation, each label represents the njm values of emitter-perturber multiplets so that, for example, the matrix element between states $n_1 j_1^*; n_2 j_2^*$ and $n_3 j_3^*; n_4 j_4^*$ is itself a *matrix* of dimension $(2j_1 + 1)(2j_2 + 1)$ by $(2j_3 + 1)(2j_4 + 1)$. The matrix $U(t)$ can be thought to act on the corresponding wave vector given by

$$|\psi(t)\rangle = \begin{bmatrix} \vec{a}(t) \\ \vec{w}(t) \\ c(t) \\ h(t) \\ \vec{f}(t) \\ g(t) \end{bmatrix} \quad (9)$$

The elements of $|\psi(t)\rangle$ are each column vectors; for example, if $|\psi(t)\rangle$ is given by

$$\begin{aligned}
& \sum_{mm'} a_{mm'} |n_1 j_1 m; n_2 j_2 m'\rangle \exp(-iE_{12}t/\hbar) \\
& + \sum_{mm'} b_{mm'} |n_3 j_3 m; n_4 j_4 m'\rangle \exp(-iE_{34}t/\hbar) + \dots,
\end{aligned}$$

then the vector \vec{a} is composed of the $(2j_1 + 1)(2j_2 + 1)$ elements $a_{mm'}$ ($m = j_1, \dots, -j_1$; $m' = j_2, \dots, -j_2$), the vector \vec{b} is composed of the $(2j_3 + 1)(2j_4 + 1)$ elements $b_{mm'}$ ($m = j_3, \dots, -j_3$, $m' = j_4, \dots, -j_4$), etc.

We seek the change in $|\psi(t)\rangle$ caused by the collision. Since the collision occurs in a time $\tau_c(b) \approx b/v$, the Fourier transform of the interaction matrix $U(t)$ will have non-negligible frequency components up to the frequency

$$\omega_c(b) = [\tau_c(b)]^{-1} \approx v/b.$$

In order for the matrix $U(t)$ to contribute in first order, the difference in frequency ω_d between the emitter transition from its excited state to some lower state and the perturber transition from its ground state to some excited state must be less than $\omega_c(b)$. Such first-order processes may lead to the transfer of excitation from emitter to perturber. We shall make use of the adiabatic approximation which states that all such first-order processes contribute a negligible amount, except those of a resonant nature in which the emitter and perturber transition frequencies are identical (or nearly so). For the systems under consideration, the fine-structure separation of the pertinent levels is greater than 10^{14} sec^{-1} and we may take this as the value of ω_d .⁵⁸ The adiabatic approximation will begin to fail when $\omega_c \approx \omega_d$ or at $b \approx 10^{-8} \text{ cm}$ so it will surely be valid if the dipole-dipole approximation is valid. Selection rules may also inhibit first-order processes, but we shall always refer to the "adiabatic nature of the collision" as that condition which allows us to neglect such effects.

In this section, we have assumed that the first-order or resonant effects are dominant over all second-order effects. Under the adiabatic approximation, only the elements $V(t)$ and $V^\dagger(t)$ of the interaction matrix $U(t)$ represent resonant processes. Thus, we shall be concerned only with the change in the transition amplitudes represented by the vectors $\vec{a}(t)$ and $\vec{w}(t)$ in Eq. (9). The time-dependent Schrödinger equation, in the interaction representation, reduces to the two vector equations

$$i\hbar \dot{\vec{a}} = \vec{V}(t)\vec{w}, \quad i\hbar \dot{\vec{w}} = \vec{V}^\dagger(t)\vec{a}, \quad (10)$$

where the matrix $\tilde{V}(t)$ is given by

$$\tilde{V}(t) = \exp(i\mathcal{E}c_0 t/\hbar)V(t)\exp(-i\mathcal{E}c_0 t/\hbar). \quad (11)$$

Since the collision is localized in time about $t=0$, we can take the initial conditions at $t=-\infty$ (before the collision) and seek solutions for $t=+\infty$ (after the collision). The initial conditions are

$$\vec{a}(-\infty) = \vec{a}_0, \quad \vec{w}(-\infty) = 0.$$

The exponential factor in the matrix elements of $\tilde{V}(t)$ will be of the form $\exp(i\omega_z t)$, where ω_z is the Zeeman splitting of level a . For the significant collisions, we shall assume that the collision frequency $\omega_c(b_0) \approx 10^{12} \text{ sec}^{-1}$ is much larger than the Zeeman splitting. This implies that $\exp(i\omega_z t)$ is a slowly varying function of time compared with $V(t)$ and the exponential may be evaluated at $t=0$. Thus, collisions are always diabatic with respect to the magnetic sublevel separation of the emitter and, as will be shown, can always magnetically reorient the emitter.

With this assumption, Eqs. (10) become

$$i\hbar\dot{\vec{a}} = V(t)\vec{w}, \quad i\hbar\dot{\vec{w}} = V^\dagger(t)\vec{a}.$$

We introduce time evolution matrices $T(t)$ and $R(t)$ defined by

$$\vec{a}(t) = T(t)\vec{a}_0, \quad \vec{w}(t) = R(t)\vec{a}_0, \quad (12)$$

which obey the matrix differential equations

$$i\hbar\dot{T} = V(t)R, \quad i\hbar\dot{R} = V^\dagger(t)T, \quad (13)$$

with initial conditions $T(-\infty) = 1$, $R(-\infty) = 0$. The explicit form of $V(t)$ is determined by Eq. (7) to be

$$V(t) = \begin{bmatrix} X(t) & Y(t) & Z(t) \\ Y(t) - 2X(t) & -Y(t) & \\ Z(t) - Y(t) & X(t) & \end{bmatrix} = V^\dagger(t), \quad (14)$$

where

$$X(t) = e^2 a_0^{-2} |T(s_0, a_1)|^2 \{2[R(t)]^2 - 3v^2 t^2\} / 6[R(t)]^5,$$

$$Y(t) = -e^2 a_0^{-2} |T(s_0, a_1)|^2 bvt / (\sqrt{2})[R(t)]^5,$$

$$Z(t) = e^2 a_0^{-2} |T(s_0, a_1)|^2 v^2 t^2 / 2[R(t)]^5,$$

and the form for $\vec{a}(t)$ is

$$\vec{a} = \begin{bmatrix} a_1 \\ a_0 \\ a_{-1} \end{bmatrix}.$$

Sum and difference matrices $S(t) = T(t) + R(t)$ and $D(t) = T(t) - R(t)$ are introduced which transform Eq. (13) into

$$i\hbar\dot{S} = V(t)S, \quad (15a)$$

$$i\hbar\dot{D} = -V(t)D, \quad (15b)$$

$$S(-\infty) = D(-\infty) = 1. \quad (15c)$$

From Eqs. (15), it is easy to see that $D(t) = S^*(t)$, so that the matrices T and R can be expressed solely in terms of S as

$$T(t) = \text{Re}[S(t)], \quad R(t) = i\text{Im}[S(t)]. \quad (16)$$

Equation (15a) must be solved numerically since the matrix $V(t)$ does not commute with $V(t')$ for $t \neq t'$. The solution of Eq. (15a) is obtained in Appendix A. This solution, together with Eqs. (12) and (16), provides a complete determination of the change in the wave function as the result of a single collision. Rather than work with the wave function, it will prove more convenient to work with the density matrix of the emitter-perturber system. The density matrix is defined by

$$\rho(t) = |\psi(t)\rangle\langle\psi(t)|,$$

with $|\psi(t)\rangle$ given in Eq. (9).⁵⁹ As we shall see, the reduced density matrices of emitter and perturber will prove relevant. These matrices are defined by

$$\rho^{\text{I}} = \text{Tr}\rho, \quad (17)$$

$$\rho^{\text{II}} = \text{Tr}'\rho. \quad (18)$$

The trace in Eq. (17) is over all perturber states while that in Eq. (18) is over all emitter states. We denote by $\delta\rho^{\text{I}}$ and $\delta\rho^{\text{II}}$ the changes in ρ^{I} and ρ^{II} caused by a collision. Due to the adiabatic nature of the interaction, one gets contributions to $\delta\rho_{mm}^{\text{I}}$, only if the perturber is in its ground state after the collision and contributions to $\delta\rho_{mm}^{\text{II}}$, only if the emitter is in its ground state after the collision. The latter case corresponds to a transfer of excitation. The net result is that both $\delta\rho^{\text{I}}$ and $\delta\rho^{\text{II}}$ can be expressed directly in terms of the components of $|\psi(t)\rangle$. The value of $\rho(t)$ just prior to the collision will depend on the past collision history of the emitter and will be represented by $\rho(t, c)$. Furthermore, we shall write $\rho(-\infty, c) \equiv \rho(c)$. Thus, for our standard collision geometry,

$$\begin{aligned} \delta\rho_{mm}^{\text{I}}(b, v, \Omega_0, c) &= [\vec{a}(\infty, c)\vec{a}^\dagger(\infty, c) - \vec{a}(c)\vec{a}^\dagger(c)]_{mm}, \\ &= [T(t=\infty, b, v, \Omega_0)\rho^{\text{I}}(c) \\ &\quad \times T^\dagger(t=\infty, b, v, \Omega_0) - \rho^{\text{I}}(c)]_{mm}, \end{aligned} \quad (19)$$

$$\begin{aligned} \delta\rho_{mm}^{\text{II}}(b, v, \Omega_0, c) &= [\vec{w}(\infty)\vec{w}^\dagger(\infty) - \vec{w}(c)\vec{w}^\dagger(c)]_{mm}, \\ &= [R(t=\infty, b, v, \Omega_0)\rho^{\text{I}}(c) \\ &\quad \times R^\dagger(t=-\infty, b, v, \Omega_0)]_{mm}, \end{aligned} \quad (20)$$

where we have used $\vec{w}(c) = 0$. One should note

that the evolution matrix $T(t, b, v, \Omega)$ for the specific binary collision does not depend on the previous collision history.

In Sec. VIII, we shall need the quantities defined by

$$\rho(t) = \rho^{\text{I}}(t) + \rho^{\text{II}}(t),$$

$$\text{and } \delta\rho(t) = \delta\rho^{\text{I}}(t) + \delta\rho^{\text{II}}(t). \quad (21)$$

In terms of components, Eqs. (19)–(21) may be written⁶⁰

$$\delta\rho_{mm'}^{\text{I}}(b, v, \Omega_0, c) = \sum_{ll'} T_{mm'}^{ll'}(b, v, \Omega_0) \rho_{ll'}^{\text{I}}(c), \quad (22a)$$

$$\delta\rho_{mm'}^{\text{II}}(b, v, \Omega_0, c) = \sum_{ll'} R_{mm'}^{ll'}(b, v, \Omega_0) \rho_{ll'}^{\text{I}}(c), \quad (22b)$$

$$\delta\rho_{mm'}(b, v, \Omega_0, c) = \sum_{ll'} S_{mm'}^{ll'}(b, v, \Omega_0) \rho_{ll'}^{\text{I}}(c), \quad (22c)$$

where

$$T_{mm'}^{ll'}(b, v, \Omega) = T_{ml}(b, v, \Omega) T_{m'l'}^*(b, v, \Omega) - \delta_{l, m} \delta_{l', m'}, \quad (23a)$$

$$R_{mm'}^{ll'}(b, v, \Omega) = R_{ml}(b, v, \Omega) R_{m'l'}^*(b, v, \Omega), \quad (23b)$$

$$S_{mm'}^{ll'}(b, v, \Omega) = T_{mm'}^{ll'}(b, v, \Omega) + R_{mm'}^{ll'}(b, v, \Omega). \quad (23c)$$

We must now seek the average of the change $\delta\rho$ due to all possible collision histories. The first step is to find the change in ρ caused by a collision of arbitrary orientation. This change may be obtained from the results for a collision with the standard geometry Ω_0 . For the sake of definiteness, we shall work with Eq. (22a).

Let us suppose the emitter undergoes another collision with the same b and v but a different orientation. We choose a new coordinate system (primed) such that the collision is along the z' axis with relative velocity in the $x'z'$ plane. In this new coordinate system (quantized along the z' axis), the change in $\rho_{mm'}^{\text{I}}$ for this collision is given by

$$\delta\rho_{mm'}^{\text{I}'}(b, v, \Omega, c) = \sum_{pp'} T_{mm'}^{pp'}(b, v, \Omega_0) \rho_{pp'}^{\text{I}}(c), \quad (24)$$

and $T_{mm'}^{pp'}$ is unchanged since the physical scattering processes in the primed and unprimed systems are identical. To obtain the change in $\rho_{mm'}^{\text{I}}$ (i. e., in the initial coordinate system), we need

only carry out the transformations

$$\rho^{\text{I}'} = \mathfrak{D}(\Omega) \rho^{\text{I}} \mathfrak{D}^{-1}(\Omega), \quad (25a)$$

$$\delta\rho^{\text{I}'} = \mathfrak{D}(\Omega) \delta\rho^{\text{I}} \mathfrak{D}^{-1}(\Omega), \quad (25b)$$

where the $\mathfrak{D}(\Omega)$ are rotation matrices.⁵⁶ Substituting Eqs. (25) into Eq. (24) and using the orthogonality relations for the \mathfrak{D} matrices,⁵⁶ one solves for the change in $\rho_{mm'}^{\text{I}}$, and finds

$$\delta\rho_{mm'}^{\text{I}}(b, v, \Omega, c) = \sum_{pp'} T_{mm'}^{pp'}(b, v, \Omega) \rho_{pp'}^{\text{I}}(c), \quad (26)$$

where

$$T_{mm'}^{pp'}(b, v, \Omega) = \sum_{\mu\mu', \alpha\alpha'} \mathfrak{D}_{p\mu}^{j*}(\Omega) \mathfrak{D}_{m'\alpha}^{j'*}(\Omega) \times \mathfrak{D}_{m\alpha}^j(\Omega) \mathfrak{D}_{p'\mu'}^{j'}(\Omega) T_{\alpha\alpha'}^{\mu\mu'}(b, v, \Omega_0), \quad (27)$$

and j and j' are the j values associated with states m and m' .

Having obtained the change in $\rho_{mm'}^{\text{I}}$ due to an arbitrary collision, we can proceed to find the average collisional rate of change of $\rho_{mm'}^{\text{I}}$. Consider the change in $\rho_{mm'}^{\text{I}}$ in a time δt chosen small enough to contain at most one collision but large enough to contain the entire collision. The change in the average value of ρ^{I} is given by

$$\begin{aligned} [\delta\rho_{mm'}^{\text{I}}(b, v, \Omega, \delta t, c)]_{\text{av}} &= \langle \{ P_1(b, v, \Omega, \delta t) \\ &\times \sum_{pp'} T_{mm'}^{pp'}(b, v, \Omega) \rho_{pp'}^{\text{I}}(c) \}_{bv\Omega} \rangle_c \\ &= \sum_{pp'} \{ P_1(b, v, \Omega, \delta t) \\ &\times T_{mm'}^{pp'}(b, v, \Omega) \}_{bv\Omega} \langle \rho_{pp'}^{\text{I}}(c) \rangle_c, \end{aligned} \quad (28)$$

where $P_1(b, v, \Omega, \delta t)$ is the probability density of a collision specified by b, v, Ω occurring in a time δt , $\{ \dots \}_{bv\Omega}$ indicates an integration over b, v , and Ω , and $\langle \dots \rangle_c$ refers to an average over all possible histories up to time t .⁶¹ Explicitly,

$$P_1(b, v, \Omega, \delta t) = \delta t 2\pi b v \mathfrak{N}(\varphi) F(\Omega), \quad (29)$$

where \mathfrak{N} is the density of resonant perturbers, $\varphi(v)$ is the relative speed distribution, and $F(\Omega)$ is the probability density for a collision orientation Ω . Performing the average in Eq. (28), one finds

$$\delta\rho_{mm'}^{\text{I}}(t)/\delta t = \sum_{pp'} T_{mm'}^{pp'} \rho_{pp'}^{\text{I}}(t), \quad (30)$$

where $T_{mm'}^{pp'} = 2\pi \mathfrak{N} \int db dv d\Omega bv \varphi(v) F(\Omega)$

$$\times T_{mm'}^{pp'}(b, v, \Omega), \quad (31)$$

and the notation $\langle \rho_{mm'}(c) \rangle_c = \rho_{mm'}(t)$ has been used. For the present, we shall assume Eq. (30) may be replaced by the corresponding differential equation

$$\dot{\rho}_{mm'}^I(t) = \sum_{pp'} T_{mm'}^{pp'} \rho_{pp'}^I(t). \quad (30')$$

This topic will be discussed in Sec. VII.

In reality, there is more than one atom excited at $t=0$. Indeed, the average over collision histories has significance only because one observes radiation from many different atoms. That is, each emitter possesses its individual collision history; only the ensemble of emitters can be characterized by average collisional decay rates. However, we still assume that the density of excited atoms is always low enough to neglect any collisions between two excited atoms. If n_E is the density of excited atoms, we shall assume that

$$n_E/\mathcal{N} \ll 1, \quad (32)$$

where \mathcal{N} is the total density of resonant atoms.

In calculating the various line shapes, we shall see that each excited atom contributes to the line shape through its reduced density matrix so that we must calculate the sum of excited-atom reduced density matrices given by

$$\rho^{\text{IS}}(t) = \sum_i \rho_i^{\text{I}}(t), \quad (33)$$

where the sum is over all atoms that were initially excited. That Eq. (30') for $\dot{\rho}_{mm'}^I(t)$ is still valid for $\dot{\rho}_{mm'}^{\text{IS}}(t)$ follows from condition (32) and the fact that each emitter acts independently.

Similarly, we define ρ^{IIS} as

$$\rho^{\text{IIS}}(t) = \sum_j \rho_j^{\text{II}}(t), \quad (34)$$

where the sum is over all perturbers that were initially in their ground state. Following a procedure similar to that above, one finds

$$\dot{\rho}_{mm'}^{\text{IIS}}(t) = \sum_{pp'} R_{mm'}^{pp'} \rho_{pp'}^{\text{IS}}(t), \quad (35)$$

where the $R_{mm'}^{pp'}$ are given by an equation analogous to Eq. (31).

Equation (35) is not really complete since two additional effects must be taken into account. The first of these is that as soon as a ground-state atom is excited it begins to decay at the same rate as the initially excited atoms. The other effect is that the rate of transfer of excitation to ground-state atoms is dependent upon the number of excited atoms at time t . These atoms will include some which have become excited by trans-

fer collisions. If these effects are included, Eq. (35) is modified to read

$$\begin{aligned} \dot{\rho}_{mm'}^{\text{IIS}}(t) = & \sum_{pp'} [R_{mm'}^{pp'} \rho_{pp'}^{\text{IS}}(t) \\ & + T_{mm'}^{pp'} \rho_{pp'}^{\text{IIS}}(t) + R_{mm'}^{pp'} \rho_{pp'}^{\text{IIS}}(t)]. \end{aligned} \quad (36)$$

Finally, we define $\rho^{\text{S}}(t)$ by

$$\rho^{\text{S}}(t) = \rho^{\text{IS}}(t) + \rho^{\text{IIS}}(t), \quad (37)$$

with $\rho^{\text{IS}}(t)$ and $\rho^{\text{IIS}}(t)$ given by Eqs. (33) and (34). Combining Eqs. (30) and (36), we see that $\rho_{mm'}^{\text{S}}(t)$ satisfies the equation

$$\dot{\rho}_{mm'}^{\text{S}}(t) = \sum_{pp'} S_{mm'}^{pp'} \rho_{pp'}^{\text{S}}(t), \quad (38)$$

$$\text{where } S_{mm'}^{pp'} = T_{mm'}^{pp'} + R_{mm'}^{pp'}. \quad (39)$$

The $S_{mm'}^{pp'}$ and $T_{mm'}^{pp'}$ shall be called average scattering matrix elements for the entire system and initially excited atoms, respectively. We shall see that the decay of both $\rho^{\text{S}}(t)$ and $\rho^{\text{IS}}(t)$ are instrumental in determining experimental line shapes. (In what follows, we shall drop the superscript S.)

The evaluation of Eq. (31) for $T_{mm'}^{pp'}$, $R_{mm'}^{pp'}$, and $S_{mm'}^{pp'}$ elements is presented in Appendix D. The average collisional rates of change of $\rho_{mm'}^{\text{I}}(t)$ are given by the rate equations

$$\begin{aligned} \dot{\rho}_{11}^{\text{I}}(t) &= T_{11}^{11} \rho_{11}^{\text{I}}(t) + T_{11}^{00} \rho_{00}^{\text{I}}(t) + T_{11}^{-1-1} \rho_{-1-1}^{\text{I}}(t), \\ \dot{\rho}_{10}^{\text{I}}(t) &= T_{10}^{10} \rho_{10}^{\text{I}}(t) + T_{10}^{0-1} \rho_{0-1}^{\text{I}}(t), \\ \dot{\rho}_{-1-1}^{\text{I}}(t) &= T_{-1-1}^{-1-1} \rho_{-1-1}^{\text{I}}(t), \\ \dot{\rho}_{00}^{\text{I}}(t) &= T_{00}^{11} \rho_{11}^{\text{I}}(t) + T_{00}^{00} \rho_{00}^{\text{I}}(t) + T_{00}^{-1-1} \rho_{-1-1}^{\text{I}}(t), \\ \dot{\rho}_{mm'}^{\text{I}}(t) &= [\dot{\rho}_{m'm}^{\text{I}}(t)]^*, \end{aligned} \quad (40)$$

with the remaining equations obtained by interchanging 1 and -1 in all indices. The equations for $\dot{\rho}(t)$ analogous to Eq. (40) are

$$\begin{aligned} \dot{\rho}_{11}(t) &= S_{11}^{11} \rho_{11}(t) + S_{11}^{00} \rho_{00}(t) + S_{11}^{-1-1} \rho_{-1-1}(t) \\ \dot{\rho}_{10}(t) &= S_{10}^{10} \rho_{10}(t) + S_{10}^{0-1} \rho_{0-1}(t), \quad \text{etc.} \end{aligned} \quad (41)$$

Values of $T_{mm'}^{pp'}$ and $S_{mm'}^{pp'}$ are shown in Table I in units of the frequency

$$A = (2\pi/15) [|T(s0, a1)|^2 / 6] (\mathcal{N} e^2 a_0^2 / \hbar). \quad (42)$$

The errors quoted in Table I, as well as all other errors to be given, represent only those estimated

TABLE I. Resonant average scattering matrix elements in frequency units of $A = (2\pi/15) \mathfrak{A}(e^2 a_0^2 / \hbar) \frac{1}{6} |T(s0, a1)|^2$.

T_{00}^{00}	T_{11}^{11}	T_{11}^{00}	T_{10}^{0-1}	T_{10}^{10}	T_{1-1}^{1-1}	T_{11}^{-1-1}
-42.42	-41.62	4.53	0.799	-46.15	-46.95	3.73
± 0.21	± 0.23	± 0.08	± 0.088	± 0.21	± 0.23	± 0.12
S_{00}^{00}	S_{11}^{11}	S_{11}^{00}	S_{10}^{0-1}	S_{10}^{10}	S_{1-1}^{1-1}	S_{11}^{-1-1}
-29.98	-34.68	14.99	-4.70	-49.67	-44.97	19.69
± 0.31	± 0.32	± 0.13	± 0.12	± 0.29	± 0.32	± 0.20

numerical errors introduced in solving Eqs. (15a) and (31) and do not include errors introduced by incorrect physical assumptions of the model. To complete the table, the additional relationships

$$T_{mm'}^{pp'} = (T_{m'm}^{p'p})^*, \quad S_{mm'}^{pp'} = (S_{m'm}^{p'p})^*,$$

$$T_{mm'}^{pp'} = T_{-m-m'}^{-p-p'}, \quad S_{mm'}^{pp'} = S_{-m-m'}^{-p-p'},$$

and

$$T_{mm'}^{pp'} = T_{pp'}^{mm'}, \quad S_{mm'}^{pp'} = S_{pp'}^{mm'},$$

are needed.

The elements $T_{mm'}^{pp'}$ represent the rates at which emitter atoms alter their populations [as exhibited by the rate equations for diagonal element of $\rho^I(t)$] or coherence properties [as exhibited by the rate equations for the off-diagonal elements of $\rho^I(t)$] as the result of collisions. Collisions result either in a reorientation of the emitter sublevels or in a transfer of orientation information to the perturbing atom. One should note that both reorientation and excitation transfer are coherent processes; the state of the system after the collision is strongly dependent upon the state of the system before the collision with both the amplitude and phase information retained. The elements $R_{mm'}^{pp'}$ represent the rates at which perturber atoms acquire population and coherence properties as the result of collisions. Finally, the elements $S_{mm'}^{pp'}$ represent similar rates for the entire system of emitters and perturbers.

Equations (40) and (41) for the collisional decay rate of the density matrix are not in the most convenient form. These equations may be decoupled by taking a linear combination of the $\rho_{mm'}$ given by

$$\rho_{KQ}(\alpha j, a' j')$$

$$= \sum_{mm'} \rho_{\alpha jm, a' j' m'} (-1)^{j'-m'} \begin{bmatrix} j & j' & K \\ m & -m' & Q \end{bmatrix}. \quad (43)$$

The ρ_{KQ} are the coefficients in an expansion of the density matrix in terms of an irreducible tensor operator basis.⁶² Since the collisions are

isotropic, the ρ_{KQ} will decay exponentially with a decay parameter independent of Q .¹⁴ Thus, when the inverse of Eq. (43) is substituted into Eqs. (40) and (41), one finds

$$\dot{\rho}_{KQ}^I = -\Gamma_{K\rho}^I \rho_{KQ}^I, \quad K=0, 1, 2 \quad (44a)$$

$$\dot{\rho}_{KQ}^I = -\Gamma_{K\rho}^I \rho_{KQ}^I, \quad Q=K, \dots, -K \quad (44b)$$

where the decay parameters Γ_K are linear combinations of the average scattering matrix elements (see Appendix D). Using the fact that the reduced matrix element between the states a and s of the resonant transition is simply related to the transition probability per unit time $\gamma_{a,s}$ of that transition by

$$e^2 a_0^2 |T(s0, a1)|^2 / \hbar = 9\lambda^3 \gamma_{a,s} / 32\pi^3,$$

one finds

$$\Gamma_1^I = (0.0287 \pm 0.0002) \pi \lambda^3 \gamma_{a,s}, \quad (45a)$$

$$\Gamma_2^I = (0.0297 \pm 0.0002) \pi \lambda^3 \gamma_{a,s}, \quad (45b)$$

$$\Gamma_0^I = (0.0211 \pm 0.0003) \pi \lambda^3 \gamma_{a,s}, \quad (45c)$$

$$\Gamma_1 = (0.0344 \pm 0.0003) \pi \lambda^3 \gamma_{a,s}, \quad (45d)$$

$$\Gamma_2 = (0.0285 \pm 0.0002) \pi \lambda^3 \gamma_{a,s}, \quad (45e)$$

$$\Gamma_0 = 1.2 \times 10^{-6} \pi \lambda^3 \gamma_{a,s}, \quad (45f)$$

where λ is the wavelength of the resonant transition.

The Γ 's have a simple interpretation in terms of the various multipole moments of the given $j=1$ multiplet. It is easily shown that Γ_1 represents the decay rate of the average magnetic dipole moment, while Γ_2 represents the decay rate of the average electric quadrupole moment of level a . Whereas the Γ_K represent the decay rates of average multipole moments for the entire ensemble of excited emitters, Γ_K^I represent the corresponding decay rates for the ensemble of initially excited emitters only. (In resonant broadening

by isotopes, it is possible to measure the Γ_K^I .³¹⁾ The average monopole moment is a measure of the total population of the $j=1$ multiplets. Thus, Γ_0^I is the decay rate of the initially excited emitter population, and, as such, represents the rate of transfer of population from emitter to perturbers. The decay parameter Γ_0 gives the decay rate for the state a population of the entire system. Since the interaction is adiabatic, Γ_0 has theoretical value zero; the small value for Γ_0 obtained by our numerical methods is somewhat indicative of the accuracy of these numerical methods. The multipole moment decay constants are directly measurable in certain Hanle-effect experiments^{44,48,50} (see Sec. VIII).

We have not yet completed our calculation of the decay rates of density-matrix elements that are altered by collisions. As we shall see in Secs. VI–VIII, both $\delta\rho_{mb}$ and $\delta\rho_{ms}$ [see Fig. 2 (m refers to a magnetic quantum number of the $j=1$ state)] are important in determining the widths of the spectral lines. Since the perturber enters the collision in its ground state and since the collision is adiabatic with respect to levels b and s , it will be impossible for the perturber to acquire an electric dipole moment associated with states a and b during the collision. However, it is possible for the perturber to acquire a dipole moment associated with states a and s . We now make these statements quantitative.

First we calculate $\delta\rho_{mb}$. The perturber enters the collision in its ground state so that $h(-\infty)=0$ [see Eq. (2)]. Since the collision is adiabatic, one also finds

$$h(+\infty)=h(-\infty)=0$$

$$\text{so that } \delta\rho_{mb}^{\text{II}}(b, v, \Omega, c)=0; \quad (46)$$

that is, the perturber never acquires a dipole moment associated with states a and b during the collision. Level b of the emitter has been assumed to be unaffected by collisions so that $c(+\infty)=c(-\infty)$. Using this fact, one finds

$$\begin{aligned} \delta\rho_{mb}^{\text{I}}(b, v, \Omega_0, c) &= a_m(+\infty, c)c^*(+\infty, c) - a_m(c)c^*(c) \\ &= \sum_m T_{mm'}(b, v, \Omega_0) \rho_{m'b}^{\text{I}}(c) - \rho_{mb}^{\text{I}}(c). \end{aligned}$$

On averaging this equation, one obtains (see Appendix D)

$$\dot{\rho}_{mb}^{\text{I}}(t) = -\Gamma_{mb} \rho_{mb}^{\text{I}}(t), \quad (47a)$$

where

$$\begin{aligned} \Gamma_{mb} &= -(\delta t)^{-1} \{ P_1(b, v, \delta t) (-1 + \frac{1}{3} [T_{11}(b, v, \Omega_0) \\ &+ T_{-1-1}(b, v, \Omega_0) + T_{00}(b, v, \Omega_0)]) \}_{bv} \quad (47b) \end{aligned}$$

and the integral is over impact parameter and relative speed. The three components Γ_{mb} ($m=1, 0, -1$) can be shown to represent the decay rates of the components of the average electric-dipole-moment operator associated with the states a and b . Since the collisions are isotropic, Γ_{mb} is independent of m and may be written simply as Γ_{ab} . One finds its numerical value to be

$$\Gamma_{ab} = (0.0229 \pm 0.0001) \pi \lambda^3 \gamma_{a, s}. \quad (48)$$

It is important to note that $\Gamma_{ab} \neq \Gamma_0^I$, differing by about 8%. This point has been overlooked in some analyses of experimental results.^{45,49,53}

Finally, we calculate $\delta\rho_{ms}$. The wave vector is given by Eq. (2), and we seek

$$\begin{aligned} \delta\rho_{ms}^{\text{I}}(b, v, \Omega_0, c) \\ = a_m(+\infty, c)g^*(+\infty, c) - a_m(c)g^*(c), \end{aligned}$$

and

$$\begin{aligned} \delta\rho_{ms}^{\text{II}}(b, v, \Omega_0, c) \\ = w_m(+\infty, c)g^*(+\infty, c) - w_m(c)g^*(c), \end{aligned}$$

where g is the coefficient of $|s; s\rangle$ in the wave vector $|\psi(t)\rangle$ [see Eq. (2)] and initially $\vec{w}(c)=0$, $\vec{a}(c)=\vec{a}_0$, and $g(c)=g_0$. Adiabaticity implies that $g(+\infty, c)=g_0$. Therefore,

$$\begin{aligned} \delta\rho_{ms}^{\text{I}}(b, v, \Omega_0, c) \\ = \sum_m [T_{mm'}(b, v, \Omega_0) - \delta_{mm'}] \rho_{m's}^{\text{I}}(c) \end{aligned}$$

and

$$\delta\rho_{ms}^{\text{II}}(b, v, \Omega_0, c) = \sum_m R_{mm'}(b, v, \Omega_0) \rho_{m's}^{\text{I}}(c).$$

After performing all averages, we obtain

$$\partial\rho_{ms}^{\text{I}}(t)/\partial t = -\Gamma_{as}^{\text{I}} \rho_{ms}^{\text{I}}(t), \quad (49a)$$

$$\partial\rho_{ms}^{\text{II}}(t)/\partial t = -\Gamma_{as}^{\text{II}} \rho_{ms}^{\text{I}}(t) - \Gamma_{as}^{\text{II}} \rho_{ms}^{\text{II}}(t), \quad (49b)$$

$$\partial\rho_{ms}^{\text{I}}(t)/\partial t = -\Gamma_{as} \rho_{ms}^{\text{I}}(t), \quad (49c)$$

where

$$\begin{aligned} \Gamma_{as}^{\text{I}} &= -(\delta t)^{-1} \{ P_1(b, v, \delta t) (-1 + \frac{1}{3} [T_{11}(b, v, \Omega_0) \\ &+ T_{00}(b, v, \Omega_0) + T_{-1-1}(b, v, \Omega_0)]) \}_{bv}, \quad (50a) \end{aligned}$$

$$\begin{aligned} \Gamma_{as}^{\text{II}} &= -(\delta t)^{-1} \{ \frac{1}{3} P_1(b, v, \delta t) [R_{11}(b, v, \Omega_0) \\ &+ R_{00}(b, v, \Omega_0) + R_{-1-1}(b, v, \Omega_0)] \}_{bv}, \quad (50b) \end{aligned}$$

$$\Gamma_{as} = \Gamma_{as}^I + \Gamma_{as}^{II}, \quad (50c)$$

and the integral is over impact parameter and relative speed. Comparing Eqs. (47b) and (50a), we see that the real part of the average electric-dipole decay parameter is independent of the lower state. Since $R_{mm'}$ is purely imaginary, Γ_{as}^{II} is pure imaginary and may be written as $i\Delta_g$; we shall call Δ_g a "shift" although it is not now certain that Δ_g can be directly related to a shift in the emitted spectral line from state a to s . The origin of the shift resides in the ability of the excited atom to transfer its dipole moment to the perturber. Numerically, we find

$$i\Delta_g = \Gamma_{as}^{II} = i(2.10 \pm 0.01) \times 10^{-3} \lambda^3 \gamma_{a,s}, \quad (51)$$

so that

$$|\Delta_g/\Gamma_{as}^I| = |\Delta_g/\Gamma_{ab}| = 0.0918 \pm 0.0010, \quad (52)$$

which is in good agreement with some recent calculations of this shift.^{15,28}

IV. NONRESONANT CASE

The case of foreign-gas broadening requires a somewhat different analysis than that given for the resonant case. Let the energy schemes of the emitter and perturber be as depicted in Fig. 4. During the collision, both emitter and perturber undergo virtual transitions to allowed states, but after the collision, due to the adiabatic nature of the interaction, both atoms must have returned to their initial multiplets (we again assume the fine-structure splitting is much greater than the inverse collision time). For the purpose of this section, we shall assume that the perturber can undergo only the virtual transition $s' \rightarrow p$ and the emitter only the virtual transition $a \rightarrow s$; in addition, we shall assume that the b level is unaffected by the collision. The results will be generalized in Sec. V.

Under these assumptions, the wave vector may be written

$$|\psi(t)\rangle = \sum_m a_m(t) |m; s\rangle \exp(-iE_{ms}t/\hbar)$$

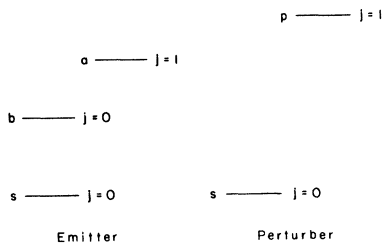


FIG. 4. Atomic structures of emitter and perturber for the nonresonant case.

$$\begin{aligned} & + \sum_q p_q(t) |s; q\rangle \exp(-iE_{sq}t/\hbar) \\ & + c(t) |b; s\rangle \exp(-iE_{bs}t/\hbar) \\ & + \sum_q f_q(t) |b; q\rangle \exp(-iE_{bq}t/\hbar), \end{aligned} \quad (53)$$

where the q represents the magnetic sublevels of state p . Following the same procedure as in the resonant case, one easily finds the vector equations

$$i\hbar \dot{\vec{a}} = \vec{V}_N(t) \vec{p}, \quad (54a)$$

$$i\hbar \dot{\vec{p}} = \vec{V}_N^\dagger(t) \vec{a}, \quad (54b)$$

where the matrix $V_N(t)$ is obtained from $V(t)$ by replacing $|T(s0, a1)|^2$ in Eq. (14) with $TP(s'0, p1) T_E^*(s0, a1)$ (the same standard orientation for the collision as in the resonant case has been used). From Eq. (11), we find (neglecting Zeeman splitting)

$$\vec{V}_N(t) = V_N(t) \exp(-i\tilde{\omega}_{ps}t), \quad (55)$$

$$\text{where } \tilde{\omega}_{ps} = \tilde{\omega}_{sp} = (E_p - E_a + E_s - E_s)/\hbar, \quad (56)$$

so that Eq. (54) may be formally integrated to give

$$\begin{aligned} \vec{a}(t) = & \vec{a}_0 + (i\hbar)^{-2} \int_{-\infty}^t dt' V_N(t') \int_{-\infty}^{t'} dt'' \\ & \times V_N^\dagger(t'') \vec{a}(t'') \exp[-i\tilde{\omega}_{ps}(t' - t'')], \end{aligned} \quad (57a)$$

$$\begin{aligned} \vec{p}(t) = & (i\hbar)^{-1} \int_{-\infty}^t dt' V_N^\dagger(t') \exp(i\tilde{\omega}_{ps}t') \vec{a}_0 \\ & + (i\hbar)^{-2} \int_{-\infty}^t dt' V_N^\dagger(t') \int_{-\infty}^{t'} dt'' \\ & \times V_N(t'') \vec{p}(t'') \exp[i\tilde{\omega}_{ps}(t' - t'')]. \end{aligned} \quad (57b)$$

The frequency $\tilde{\omega}_{ps}$ represents the frequency difference between the virtual transition of the perturber to state p and the virtual transition of the excited emitter to state s . We shall assume the interaction to be adiabatic with respect to this frequency, i.e.,

$$|\tilde{\omega}_{ps}| \tau_c \gg 1. \quad (58)$$

Thus, any accidental resonances are not considered. From this condition, it follows that both $V_N(t'')$ and $\vec{a}(t'')$ are slowly varying in time compared with $\exp(i\tilde{\omega}_{ps}t'')$. In doing the integral over t'' , we may evaluate both $V_N(t'')$ and $\vec{a}(t'')$ at $t'' = t'$ since the major contribution to the integral occurs at $t'' = t'$.⁶³ We have neglected the Zeeman splitting, but this procedure will be valid as long as $\tau_c^{-1} \gg$ Zeeman splitting. With these approxima-

tions, Eqs. (57) become

$$\vec{a}(t) = \vec{a}_0 + (i\hbar)^{-2} (i\tilde{\omega}_{ps})^{-1} \int_{-\infty}^t dt' V_N(t') V_N^\dagger(t') \vec{a}(t'), \quad (59a)$$

$$\vec{p}(\infty) \approx 0. \quad (59b)$$

That the perturber remains in its ground state is specified by Eq. (59b).

We define the evolution matrix $M(t)$ for foreign-gas collisions in a way similar to that in which $T(t)$ was defined for resonant collisions, namely,

$$\vec{a}(t) = M(t) \vec{a}_0, \quad (60a)$$

$$M(-\infty) = 1. \quad (60b)$$

From Eqs. (59a) and (60), one can easily show that $M(t)$ satisfies the matrix equation

$$M(t) = 1 + i\hbar^{-1} (\hbar\tilde{\omega}_{ps})^{-1} \int_{-\infty}^t dt' V_N(t') V_N^\dagger(t') M(t'),$$

or in differential form,

$$i\hbar dM/dt = - (\hbar\tilde{\omega}_{ps})^{-1} V_N(t) V_N^\dagger(t) M, \quad (61a)$$

$$\text{with } M(-\infty) = 1. \quad (61b)$$

The solution of Eq. (61a) is given in Appendix B. For the nonresonant case we are interested only in following the emitter, since the perturber remains in its ground state after the collision. The effect of a collision is to magnetically reorient the emitter in a certain manner. All the equations of Sec. III involving $\delta\rho^1$ are applicable to the nonresonant case with the replacement of $T_{mm'} p p'$ by $M_{mm'} p p' \equiv M_{mp} M_{m'p'}^*$. The elements $M_{mm'} p p'$, as derived in the Appendixes, are listed in Table II in units of frequency

$$\left(\frac{2}{15}\pi\right) N |B|^{2/5} \langle v^{3/5} \rangle_v, \quad (62)$$

where

$$B = \left(\frac{1}{36}\right) |T_P(s_0, p_1) T_E^*(s_0, a_1)|^2 \times (e^2 a_0^2 / \hbar)^2 (\tilde{\omega}_{ps})^{-1}, \quad (63)$$

$\langle v^{3/5} \rangle_v$ equals the average value of the $\frac{3}{5}$ power of the relative speed, and N is the density of foreign-gas perturbers.

As in the resonant case, we can expand the density matrix in terms of its irreducible tensor com-

ponents and find the decay constants Γ_1^N , Γ_2^N , and Γ_0^N which correspond to Γ_1^I , Γ_2^I , and Γ_0^I of the resonant case. From Appendix D we have

$$\Gamma_1^N = (7.62 \pm 0.08) N |B|^{2/5} \langle v^{3/5} \rangle_v, \quad (64a)$$

$$\Gamma_2^N = (6.80 \pm 0.08) N |B|^{2/5} \langle v^{3/5} \rangle_v, \quad (64b)$$

$$\Gamma_0^N = 3.75 \times 10^{-4} N |B|^{2/5} \langle v^{3/5} \rangle_v, \quad (64c)$$

$$\Gamma_1^N / \Gamma_2^N = 1.12 \pm 0.02. \quad (64d)$$

As in the resonant case, Γ_1^N and Γ_2^N can be interpreted as decay rates for the average magnetic dipole moment and electric quadrupole moment, respectively, of level a while Γ_0^N is the decay rate of excited-state population which has theoretical value zero (the emitter always remains in its excited state). The departure of the numerical value of Γ_0^N from zero is again somewhat indicative of the accuracy of the numerical methods employed.

Finally, we wish to calculate Γ_{ab}^N , the collisional decay rate of ρ_{mb} due to nonresonant collisions (Γ_{ab}^N is the decay rate of the average electric dipole moment associated with states a and b). Assuming no collisional perturbation of the b level, it is shown in Appendix D in a manner similar to that for the resonant case, that

$$\dot{\rho}_{ab}(t) = -\Gamma_{ab}^N \rho_{ab}(t), \quad (65)$$

$$\text{where } \Gamma_{ab}^N = \gamma_{ab}^N + i \Delta_{ab}^N, \quad (66a)$$

$$\gamma_{ab}^N = (8.97 \pm 0.04) |B|^{2/5} \langle v^{3/5} \rangle_v, \quad (66b)$$

$$\text{and } \Delta_{ab}^N = (6.51 \pm 0.03) |B|^{2/5} \langle v^{3/5} \rangle_v. \quad (66c)$$

We shall be able to interpret Δ_{ab}^N as a shift and γ_{ab}^N as collisional broadening of the emission line from state a to state b . If the quantity $\tilde{\omega}_{ps}$ of Eq. (56) is less than (greater than) zero the shift is to the red (violet).⁶⁴

It is interesting to note that the ratio

$$\Delta_{ab}^N / \gamma_{ab}^N = 0.726 \pm 0.007 \quad (67)$$

is precisely that of the simple Lindholm-Foley

TABLE II. Nonresonant average scattering matrix elements in frequency units of $(2\pi/15)N|B|^{2/5}\langle v^{3/5}\rangle_v$.

M_{00}^{00}	M_{11}^{11}	M_{11}^{00}	M_{10}^{0-1}	M_{10}^{10}	M_{1-1}^{1-1}	M_{11}^{-1-1}
-10.82	-11.80	5.41	-0.976	-17.21	-16.24	6.39
± 0.16	± 0.11	± 0.07	± 0.200	± 0.07	± 0.24	± 0.16

theory^{1,2} which neglects multiplet structure. We should point out, however, that this agreement seems to be a numerical coincidence. We should also mention that the neglect of noncommutativity in calculating the electric-dipole parameters for this case provides a good approximation ($\approx 1\%$) to the values obtained in Eqs. (66). (For the resonant case, the neglect of noncommutativity in calculating Γ_{ab}^I leads to errors $\approx 13\%$.)

V. GENERALIZATION OF THE THEORY

The theory of Secs. III and IV can be generalized to include the effects of additional virtual transitions and perturbations of the lower level b . The selection rules governing the virtual transitions of either the emitter or perturber are (a) $\Delta j = \pm 1$, 0 for transitions originating in a $j = 1$ state, (b) $\Delta j = +1$ for transitions originating in a $j = 0$ state, and (c) parity violating transitions are forbidden.

The time evolution of the emitter-perturber system is given by

$$i\hbar |\dot{\psi}(t)\rangle = [H_0 + U(t)] |\psi(t)\rangle, \quad (68)$$

where $U(t)$ and $|\psi(t)\rangle$ as defined by Eqs. (8) and

$$U'(t) = \begin{matrix} & \begin{matrix} a1*;s'0* & s0*;p1* & s0*;h1* & d2*;p1* & d2*;h1* & b0*;s'0* & a1*;p1* & a1*;h1* \end{matrix} \\ \begin{matrix} a1*;s'0* \\ s0*;p1* \\ s0*;h1* \\ d2*;p1* \\ d2*;h1* \\ b0*;s'0* \\ a1*;p1* \\ a1*;h1* \end{matrix} & \begin{bmatrix} 0 & A_{sp}(t) & A_{sh}(t) & D_{dp}(t) & D_{dh}(t) & 0 & 0 & 0 \\ A_{sp}^\dagger(t) & 0 & 0 & 0 & 0 & 0 & 0 & 0 \\ A_{sh}^\dagger(t) & 0 & 0 & 0 & 0 & 0 & 0 & 0 \\ D_{dp}^\dagger(t) & 0 & 0 & 0 & 0 & 0 & 0 & 0 \\ D_{dh}^\dagger(t) & 0 & 0 & 0 & 0 & 0 & 0 & 0 \\ 0 & 0 & 0 & 0 & 0 & 0 & F_{ap}(t) & F_{ah}(t) \\ 0 & 0 & 0 & 0 & 0 & F_{ap}^\dagger(t) & 0 & 0 \\ 0 & 0 & 0 & 0 & 0 & F_{ah}^\dagger(t) & 0 & 0 \end{bmatrix} \end{matrix} \quad (69)$$

The state vector associated with $U'(t)$ is given by

$$|\psi(t)\rangle = \begin{bmatrix} \vec{a}(t) \\ \vec{p}(t) \\ \vec{h}(t) \\ \vec{d}(t) \\ \vec{r}(t) \\ \vec{b}(t) \\ \vec{f}(t) \\ \vec{g}(t) \end{bmatrix}, \quad (70)$$

with initial conditions

$$\vec{a}(-\infty) = \vec{a}_0, \quad \vec{b}(-\infty) = \vec{b}_0,$$

and all other elements of $|\psi(t)\rangle$ at $t = -\infty$ are zero.

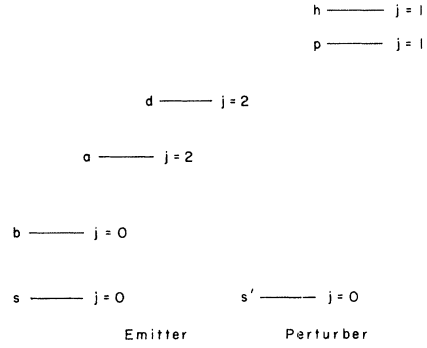


FIG. 5. Atomic structures of emitter and perturber for the generalized nonresonant case.

(9), have been expanded to include all possible states. It will be sufficient to consider a finite number of states for the emitter and perturber as depicted in Fig. 5. These states will be represented by a finite portion of the $U(t)$ matrix, denoted by $U'(t)$, and given by

The following notation is implied in Eq. (69):

$$A_{nm'}(t) = \langle a1*;s'0* | U(t) | n0*;n'1* \rangle, \quad \text{dimension } 3 \times 3, \quad (71a)$$

$$D_{rr'}(t) = \langle a1*;s'0* | U(t) | r2*;r'1* \rangle, \quad \text{dimension } 3 \times 15, \quad (71b)$$

$$F_{ff'}(t) = \langle b0*;s'0* | U(t) | f1*;f'1* \rangle, \quad \text{dimension } 1 \times 9, \quad (71c)$$

where $A_{nm'}(t)$, $D_{rr'}(t)$, and $F_{ff'}(t)$ are matrices as described in Sec. III. (We have suppressed the indices a , b , and s' in labeling these matrices.) In essence, the A 's represent the matrix elements

of virtual transitions from emitter state a to states with $j=0$, the D 's represent the matrix elements of virtual transitions from state a to states with $j=2$, and the F 's represent the matrix element of virtual transitions from state b to states with $j=1$; in addition, two possible perturber virtual transitions with $\Delta j=1$ have been included in this notation. The usefulness of this notation lies in the fact that all A matrices are scalar multiples of each other, differing in magnitude only by the ratio of reduced matrix elements. Similar remarks also apply to the D matrices and to the F matrices. It will also be convenient to define the following products of reduced matrix elements:

$$\mathcal{T}_{mm'}^A = T_P(s'0, n'1) T_E^*(n0, a1), \quad (72a)$$

$$\mathcal{T}_{rr'}^D = T_P(r'1, s'0) T_E^*(r2, a1), \quad (72b)$$

$$\mathcal{T}_{ff'}^F = T_P(s'0, f'1) T_E^*(s0, f1), \quad (72c)$$

and also the quantities

$$\mathcal{G}_{mm'}^A = \frac{1}{36} |\mathcal{T}_{mm'}^A|^2 (e^2 a_0^2 / \hbar)^2 (\tilde{\omega}_{mm'}^A)^{-1}, \quad (73a)$$

$$\mathcal{G}_{rr'}^D = \frac{1}{36} |\mathcal{T}_{rr'}^D|^2 (e^2 a_0^2 / \hbar)^2 (\tilde{\omega}_{rr'}^D)^{-1}, \quad (73b)$$

$$\mathcal{G}_{ff'}^F = \frac{1}{36} |\mathcal{T}_{ff'}^F|^2 (e^2 a_0^2 / \hbar)^2 (\tilde{\omega}_{ff'}^F)^{-1}, \quad (73c)$$

where

$$\tilde{\omega}_{mm'}^A = [E_n(j=0) + E_{n'}(j=1) - E_a - E_{s'}] / \hbar, \quad (74a)$$

$$\tilde{\omega}_{rr'}^D = [E_r(j=2) + E_{r'}(j=1) - E_a - E_{s'}] / \hbar, \quad (74b)$$

and

$$\tilde{\omega}_{ff'}^F = [E_f(j=1) + E_{f'}(j=1) - E_b - E_{s'}] / \hbar. \quad (74c)$$

These $\tilde{\omega}$'s represent the differences in frequency between the virtual transitions of emitter and perturber. The j values represent the angular momenta of the virtual states. (Note that, by definition, $\tilde{\omega}_{mm'} = \tilde{\omega}_{n'n}$.)

From the reduced nature of Eq. (69) for $U'(t)$, one immediately notices that the levels a and b are perturbed independently. Let us first consider the magnetic reorientation effects of the additional virtual transitions on $\rho_{mm'}$, where m

and m' are the magnetic substates of level a . If resonant effects dominate (i. e., if $E_p - E_{s'} = E_a - E_s$ and the oscillator strength of the transition is large), the results of Sec. III are still valid, since all matrices except $A_{sp}(t)$ and $A_{sp}^\dagger(t)$ contribute a negligible amount to the broadening. If nonresonant effects dominate, the previous results will be modified. The equations analogous to Eqs. (59b) and (61) for the evolution matrix $M(t)$ are

$$\vec{p}(+\infty) \approx \vec{h}(+\infty) \approx \vec{d}(+\infty) \approx \vec{r}(+\infty) \approx 0, \quad (75)$$

$$i\hbar \frac{dM}{dt} = - \left(\frac{A_{sp}(t)A_{sp}^\dagger(t)}{\hbar\tilde{\omega}_{sp}^A} + \frac{A_{sh}(t)A_{sh}^\dagger(t)}{\hbar\tilde{\omega}_{sh}^A} + \frac{D_{dp}(t)D_{dp}^\dagger(t)}{\hbar\tilde{\omega}_{dp}^D} + \frac{D_{dh}(t)D_{dh}^\dagger(t)}{\hbar\tilde{\omega}_{dh}^D} \right) M, \quad (76a)$$

$$\text{and } M(-\infty) = +1. \quad (76b)$$

A somewhat tedious calculation gives the matrix equation

$$D_{rr'}(t)D_{rr'}^\dagger(t)(\hbar\tilde{\omega}_{rr'}^D)^{-1} = d^2(rr', mm') \times A_{mm'}(t)A_{mm'}^\dagger(t)(\hbar\tilde{\omega}_{mm'}^A)^{-1} - \hbar q_{rr'}(t)1, \quad (77a)$$

where 1 is the unit matrix,

$$d^2(rr', mm') = \frac{3}{2} \frac{\mathcal{T}_{rr'}^D}{\mathcal{T}_{mm'}^A} \frac{\tilde{\omega}_{mm'}^A}{\tilde{\omega}_{rr'}^D} \quad (77b)$$

and the frequency $q_{rr'}(t)$ is given by

$$q_{rr'}(t) = 108 \mathcal{G}_{rr'}^D (R(t))^{-6}. \quad (77c)$$

Note that $q_{rr'}(t)$ is just a real scalar function of t .

The different A matrices are scalar multiples of each other and are related by

$$A_{mm'}(t)A_{mm'}^\dagger(t) = A_{mm'}(t)A_{mm'}^\dagger(t) (\mathcal{T}_{mm'}^A / \mathcal{T}_{mm'}^A), \quad (78)$$

so that

$$A_{mm'}(t)A_{mm'}^\dagger(t)(\hbar\tilde{\omega}_{mm'}^A)^{-1} = a^2(mm', mm') A_{mm'}(t)A_{mm'}^\dagger(t)(\hbar\tilde{\omega}_{mm'}^A)^{-1}, \quad (79a)$$

$$\text{where } a^2(mm', mm') = \frac{\tilde{\omega}^A_{mm'}}{\tilde{\omega}^A_{nm'}} \frac{\tau^A_{nm'}}{\tau^A_{mm'}}. \quad (79b)$$

Using Eqs. (77) and (79), Eq. (76) takes the simple form

$$i\hbar \frac{dM}{dt} = -\alpha^2 \frac{A_{sp}(t)A_{sp}^\dagger(t)}{\hbar\tilde{\omega}^A_{sp}} M - \hbar\mu(t)M, \quad (80)$$

where

$$\alpha^2 = 1 + a^2(sh, sp) + d^2(dp, sp) + d^2(dh, sp), \quad (81)$$

$$\text{and } \mu(t) = q_{dp}(t) + q_{dh}(t). \quad (82)$$

Using the transformation

$$M(t) = [\exp(i \int_{-\infty}^t \mu(t') dt')] \tilde{M}(t), \quad (83)$$

one obtains the following matrix equation for $\tilde{M}(t)$:

$$i\hbar \frac{d\tilde{M}(t)}{dt} = \alpha^2 \frac{A_{sp}(t)A_{sp}^\dagger(t)}{\hbar\tilde{\omega}^A_{sp}} \tilde{M}(t), \quad (84a)$$

$$\tilde{M}(-\infty) = 1. \quad (84b)$$

In Sec. IV, we solved [Eq. (61a)]

$$i\hbar dM/dt = -(\hbar\tilde{\omega}^A_{sp})^{-1} A_{sp}(t)A_{sp}^\dagger(t)M, \quad (61a')$$

which is identical in form to Eq. (84a). For calculation of reorientation effects, one always needs products of the form

$$\begin{aligned} M_{mp} M_{m'p'}^* &= M_{mm'}^{pp'} \\ &= \tilde{M}_{mp} \tilde{M}_{m'p'}^* = \tilde{M}_{mm'}^{pp'}. \end{aligned}$$

One sees that the exponential factor of Eq. (83) will not alter reorientation results and concludes that the final results (after all averaging) of Sec. IV for reorientation effects are still valid if the substitution $(\tilde{\omega}A_{sp})^{-1} \rightarrow \alpha^2(\tilde{\omega}A_{sp})^{-1}$ is made. This is equivalent to replacing B [see Eq. (63)] by

$$\mathfrak{B} = \mathfrak{B}_{ps}^A + \mathfrak{B}_{ph}^A + \frac{3}{2}(\mathfrak{B}_{db}^D + \mathfrak{B}_{dh}^D),$$

where the $\mathfrak{B}_{nm'}$'s are defined by Eqs. (73).

Virtual transitions from state a with $\Delta j = 0$ will be included by introducing the matrix $G_{nm'}(t)$

that connects state a to other $j=1$ states, i. e.,

$$G_{qq'}(t) = \langle a1*; s'0* | U(t) | q1*; q'1* \rangle. \quad (71')$$

The state q represents a $j=1$ emitter state not shown in Fig. 5. In analogy with Eqs. (73) and (74), we also define

$$\begin{aligned} \mathfrak{B}_{qq'}^G &= \left(\frac{1}{36}\right) | T_p(q'1, s'0) T_E^*(a1, q1) |^2 \\ &\times (e^2 a_0^2 / \hbar)^2 (\tilde{\omega}_{qq'}^G)^{-1}, \end{aligned} \quad (73')$$

where

$$\tilde{\omega}_{qq'}^G = (E_q + E_{q'} - E_a - E_{s'}) / \hbar. \quad (74')$$

The G matrices enter the theory in an identical manner as did the D matrices, so that the general result for all virtual transitions in the nonresonant case may be easily obtained. The reorientation results of Sec. IV are still valid if B is replaced by

$$\mathfrak{B}_a = \sum (\mathfrak{B}_a^A + \frac{3}{2} \mathfrak{B}_a^D - \frac{9}{2} \mathfrak{B}_a^G), \quad (85)$$

where the sum is over all allowed virtual transitions of the system. Thus, the averaged scattering matrix elements $M_{mm'}^{pp'}$ are given by Table II in units of $(2\pi/15)N|\mathfrak{B}_a|^{2/5}\langle v^{3/5} \rangle_v$ and Eqs. (64) are modified to read

$$\Gamma_1^N = (7.62 \pm 0.08) |\mathfrak{B}_a|^{2/5} \langle v^{3/5} \rangle_v, \quad (86a)$$

$$\Gamma_2^N = (6.80 \pm 0.08) |\mathfrak{B}_a|^{2/5} \langle v^{3/5} \rangle_v, \quad (86b)$$

$$\Gamma_0^N = 3.75 \times 10^{-4} |\mathfrak{B}_a|^{2/5} \langle v^{3/5} \rangle_v. \quad (86c)$$

One might have expected that the quantity \mathfrak{B}_a would be proportional to the London value⁶⁵ for the van der Waals constant; however, such a proportionality does not exist. The explanation of this feature resides in the fact that the London value is based on a static interaction, while ours involves a dynamic one. The time dependence of the interaction results in ratios between the contributions to \mathfrak{B}_a of the virtual transitions $\Delta j_E = +1$, $\Delta j_E = 0$, and $\Delta j_E = -1$ (the subscript E refers to the emitter) which are different from those of a static interaction. One should note several other points concerning Eq. (75) for \mathfrak{B}_a . First, one must adhere to the way in which the reduced matrix elements have been defined by Eqs. (72) and (73') since reversal of the arguments in such elements will introduce statistical factors. Second, in systems with total spin $S=0$ which also obey an LS coupling scheme, all the \mathfrak{B}_a^G are zero. Finally, it should be noted that an exact evaluation of \mathfrak{B}_a

is all but impossible, and approximation techniques are needed.

To complete this section, we compute the collisional effects on the spectral line $a \rightarrow b$ when there is a perturbation of both levels. We may find the change in the probability amplitude of level b due to collisions by the methods of Sec. IV (we assume that the broadening of level b is of a nonresonant nature). Using Eqs. (68)–(70), one can easily show that the amplitude b , which is the probability amplitude for the state $|b; s\rangle$, obeys the equation

$$i\hbar \frac{db}{dt} = - \left[\frac{F_{ap}(t)F_{ap}^\dagger(t)}{\hbar\tilde{\omega}_{ap}^F} + \frac{F_{ah}(t)F_{ah}^\dagger(t)}{\hbar\tilde{\omega}_{ah}^F} \right] b. \quad (87)$$

The appropriate matrix elements are given by Eq. (6), and a simple calculation yields

$$\frac{F_{ff'}(t)F_{ff'}^\dagger(t)}{\hbar\tilde{\omega}_{ff'}^F} = \frac{24\hbar\mathcal{G}_{ff'}^F}{[R(t)]^6},$$

which is a scalar function of t . Eq. (77) can be integrated trivially to give

$$b(+\infty) = \exp[9\pi i (\mathcal{G}_{ap}^F + \mathcal{G}_{ah}^F)/b^5 v] b_0, \quad (88)$$

where the \mathcal{G} 's are defined by Eq. (73c). Defining an evolution function for one collision $Q(t, b, v)$ by

$$b(t, b, v) = Q(t, b, v) b_0,$$

we have

$$Q(+\infty, b, v) = \exp[9\pi i (\mathcal{G}_{ap}^F + \mathcal{G}_{ah}^F)/b^5 v].$$

It is obvious that this result can be generalized to allow for all virtual transitions by putting

$$Q(+\infty) = \exp(9\pi i \mathcal{G}_b/b^5 v), \quad (89a)$$

$$\text{where } \mathcal{G}_b = \sum \mathcal{G}^F, \quad (89b)$$

the sum being over all transitions of type F [see discussion following Eq. (74)]. We have yet to average over impact parameter.

We seek the change

$$\delta\rho_{mb}(b, v, \Omega_0, c) = a_m(+\infty, c)$$

$$\times b^*(+\infty, c) - a_0 b_0^* = \sum_{m'} [-\delta_{mm'} + Q^*(b, v) M_{mm'}(b, v, \Omega_0)] \rho_{m'b}(c),$$

which must be averaged over impact parameter and all orientations of collisions (substitute T for M to get the resonant case). If the average over angles is performed (see Appendix D), we find

$$\delta\rho_{mb}^I(b, v, c) = \{-1 + \frac{1}{3} Q^*(b, v) [T_{11}^I(b, v, \Omega_0) + T_{00}(b, v, \Omega_0) + T_{-1-1}(b, v, \Omega_0)]\} \rho_{mb}^I(c) \quad (90a)$$

for the resonant case, and

$$\delta\rho_{mb}(b, v, c) = \{-1 + \frac{1}{3} Q^*(b, v) [M_{11}(b, v, \Omega_0) + M_{00}(b, v, \Omega_0) + M_{-1-1}(b, v, \Omega_0)]\} \rho_{mb}(c) \quad (90b)$$

for the nonresonant case.

For broadening by similar atoms, we shall assume that the resonant interaction dominates all nonresonant effects. Thus, we take the T_{mm} 's equal to those derived in the section on resonant broadening and set $Q^*(b, v) = 1$. For this case, inclusion of the nonresonant interaction in levels a and b would result in a slight increase in width and a small shift of the spectral line $a \rightarrow b$.

For foreign-gas broadening, the M elements are given by Eq. (83). The additional phase factor due to $\Delta j_E = +1$ virtual transitions, represented by

$$\Phi(b, v) = \exp[i \int_{-\infty}^{\infty} \mu(t') dt']$$

in Eq. (83), must now be considered. When one allows for all virtual transitions of the systems, it can be shown that the total phase factor is given by

$$\Phi(b, v) = \exp(i\lambda/b^5 v), \quad (91)$$

where $\lambda = (-\frac{9\pi}{2}) (\sum \mathcal{G}^D + \sum \mathcal{G}^G)$,

and the sums are over all virtual transitions of type D ($\Delta j_E = +1$) and G ($\Delta j_E = 0$). In terms of the phase factor Φ , Eq. (83) becomes

$$M(b, v, \Omega_0) = \Phi(b, v) \tilde{M}(b, v, \Omega_0). \quad (92)$$

As noted earlier the matrix \tilde{M} is just a generalization of the nonresonant M determined in Sec. IV. The generalization is effected by replacement of

$$\mathcal{G}_{ps}^A = \left(\frac{1}{36}\right) |T_P(s'0, p1) T_E^*(s0, a1)|^2 \times (e^2 a_0^2 / \hbar)^2 (\tilde{\omega}_{ps}^A)^{-1},$$

which appears in the expressions [see Eqs. (63) and (66)] for M in Sec. IV, by

$$\mathfrak{R}_a = \sum (\mathfrak{R}_{+\frac{3}{2}}^A \mathfrak{R}^D - \frac{\mathfrak{R}}{2} \mathfrak{R}^G),$$

the sum being over all virtual transitions of the system. This is the same replacement that was needed in generalizing the reorientation effects [see Eq. (85)].

With these changes, Eq. (90b) becomes

$$\begin{aligned} \delta\rho_{mb}(b, v, c) = & \left\{ -1 + \frac{1}{3} Q^*(b, v) \Phi(b, v) \right. \\ & \times [\tilde{M}_{11}(b, v, \Omega_0) + \tilde{M}_{00}(b, v, \Omega_0) \\ & \left. + \tilde{M}_{-1-1}(b, v, \Omega_0) \right\} \rho_{mb}(c). \end{aligned} \quad (93)$$

On averaging this equation over impact parameters, one obtains

$$\dot{\rho}_{mb}(t) = -\Gamma_{ab}^N \rho_{mb}(t), \quad (94a)$$

where

$$\begin{aligned} \Gamma_{ab}^N = & -(\delta t)^{-1} \{ P_1(b, v, \delta t) \\ & \times (-1 + \frac{1}{3} Q^*(b, v) \Phi(b, v) [\tilde{M}_{11}(b, v, \Omega_0) \\ & + \tilde{M}_{00}(b, v, \Omega_0) + \tilde{M}_{-1-1}(b, v, \Omega_0)] \} \}_{bv}. \end{aligned} \quad (94b)$$

The evaluation of Γ_{ab}^N is now quite complex since it requires a detailed knowledge of the relative strengths of the virtual transitions. To obtain a qualitative picture of the average, we introduce the parameter r as the ratio of the broadening parameters for levels a and b ,

$$r = \mathfrak{R}_a / \mathfrak{R}_b. \quad (95)$$

The general behavior of

$$\Gamma_{ab}^N = \gamma_{ab}^N + i\Delta_{ab}^N$$

as a function of r will then be given in Fig. 6 which is drawn assuming a fixed $B_b > 0$, $B_a > 0$, and neglecting $\Delta j_E = +1, 0$ transitions. Positive Δ_{ab} corresponds to a violet shift. (If level b had a greater energy than level a , the direction of shift would be reversed.) For $r < 1$, level b dominates the broadening, and one may analytically obtain the Lindholm-Foley result

$$\gamma_{ab}^N = 14.4N |\mathfrak{R}_b|^{2/5} \langle v^{3/5} \rangle_v, \quad (96a)$$

$$\Delta_{ab}^N = 10.4N |\mathfrak{R}_b|^{2/5} \langle v^{3/5} \rangle_v. \quad (96b)$$

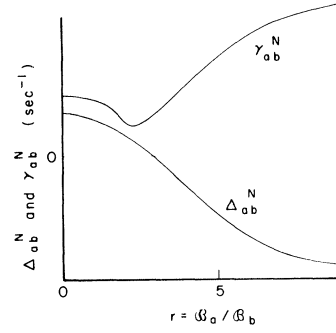


FIG. 6. Variation of Δ_{ab}^N and γ_{ab}^N as a function of the ratio r of level a and level b broadening parameters for the case of $\Delta j_E = -1$ virtual transitions only assuming a fixed $B_b > 0$. At $r=0$, $\Delta_{ab}^N / \gamma_{ab}^N = 0.726$ [see Eqs. (96)], while for $r \gg 1$, both Δ_{ab}^N and γ_{ab}^N vary as $r^{2/5}$ with $|\Delta_{ab}^N / \gamma_{ab}^N| = 0.76 \pm 0.007$ [see Eqs. (67)],

As r increases, the shift passes through zero and the width goes through a minimum. (A method of estimating where these phenomena occur, based on the perturbation solutions, is presented in Appendix B.) When level a dominates the broadening ($r \gg 1$), γ_{ab}^N and Δ_{ab}^N are given by Eqs. (66) (with B modified to include all $\Delta j_E = -1$ transitions). Had level b been the ground state, the system would most likely be in the region $r \gg 1$, where the predicted red shift is usually said to be typical of the attractive van der Waals forces. However, when both levels a and b represent excited states, it becomes almost meaningless to associate a definite sign to the shift for an arbitrary van der Waals interaction. Indeed, the shift can be towards either red or violet depending on the ratio r , and whether level b lies above or below level a in energy.

The effect of including the $\Delta j_E = +1, 0$ virtual transitions would be to increase the contributions of level a to both the width and shift of the line, and to alter the ratio $\Delta_{ab}^N / \gamma_{ab}^N$ in the region $r \gg 1$ from that given in Eq. (67). Thus, it is possible to get various ratios of shift to width and direction of shift within the confines of a dipole-dipole interaction. It should be noted, however, that both the shift and width are proportional to $\langle v^{3/5} \rangle_v$ and deviations from this dependence may indicate the need for additional interactions. In summary, one obtains the Lindholm-Foley values for the shift and width only in the case where the dominant broadening is that of a $j=0$ state. All other cases lead to more complicated formulas which require a knowledge of the atomic structure of the colliding atoms.

VI. INTERACTION WITH RADIATION FIELDS

The purpose of Secs. II-V of this work was to

develop a formalism that will prove useful in studying the general case of an atom in the presence of a radiation field which is undergoing collisions. We shall restrict this study to the case of spontaneous emission and assume, in a classical manner, that each atom has a prescribed center-of-mass motion. The Hamiltonian for the system, in dipole approximation for the radiation field, is given by

$$H(t) = H_{\text{atoms}} + H_f + H^C(t) + \sum_i [(e/mc) \vec{p}_i \cdot \vec{A}(\vec{R}_i(t)) + \frac{1}{2} (e^2/mc^2) A^2(\vec{R}_i(t))], \quad (97)$$

where H_{atoms} is the Hamiltonian for the free atoms, H_f is the Hamiltonian for the vacuum radiation field, \vec{p}_i is the total electronic momentum of the i th atom [i.e., \vec{p}_i is the $\sum_j \vec{p}_j(i)$, the sum is over all electronics of atom i], $\vec{A}[\vec{R}_i(t)]$ is the vector potential of the radiation field at the position $\vec{R}_i(t)$ of the i th atom, and $H^C(t)$ is the collision Hamiltonian which is a sum of binary collision Hamiltonians similar to that given in Eqs. (8) and (69). The time dependence of $H(t)$ enters implicitly through the factors $\vec{A}(\vec{R}_i(t))$ and $H^C(t)$ which depend on the position of the atoms. The factor $H^C(t)$ will effectively consist of a series of impulses representing the collisions.

In terms of the creation and annihilation operators for photons of frequency ω_k , direction of propagation \hat{k} , and polarization λ , represented by $a^\dagger_\lambda(\vec{k})$ and $a_\lambda(\vec{k})$, respectively, we can express H_f and \vec{A} as

$$H_f = \sum_{\vec{k}\lambda} \hbar\omega_k a^\dagger_\lambda(\vec{k}) a_\lambda(\vec{k}),$$

and

$$\vec{A}(\vec{R}_i) = \sum_{\vec{k}\lambda} (2\pi\hbar c^2/V\omega_k)^{1/2} [\vec{\epsilon}^\lambda(\vec{k}) a_\lambda(\vec{k}) \times \exp(i\vec{k} \cdot \vec{R}_i) + \vec{\epsilon}^\lambda(\vec{k}) a^\dagger_\lambda(\vec{k}) \exp(-i\vec{k} \cdot \vec{R}_i)],$$

where the $\vec{\epsilon}$'s are polarization vectors and V is an enclosing volume. Since we are treating the atomic trajectories classically, the vector potential is an implicit function of time through the factors $\exp[\pm i\vec{k} \cdot \vec{R}_i(t)]$. For the case of no collisions, these factors lead to the Doppler broadening of spectral lines. When collisions are present, $\vec{R}_i(t)$ depends on the specific collision history of atom i , and one must average the results over all such histories. A discussion of this averaging procedure will be given in Sec. VII.

In general, the term in A^2 in Eq. (97) can not be

neglected. It modifies the electrostatic collision interaction at large atom-atom separations (separations larger than the radiative wavelength). This corresponds to the well-known Casimir-Polder result⁶⁶ in which the radiation field precisely cancels out the R^{-6} dipole-dipole interaction at large separations, leaving the leading term of order R^{-7} . However, we are not concerned with such large atom-atom separations since they contribute negligibly to the broadening and shall drop the A^2 term. There may also be some question as to whether $\vec{A} \cdot \vec{p}$ or $\vec{E} \cdot \vec{x}$ is the correct interaction Hamiltonian to be used. For the case of optical spectra, both these interactions are equivalent except in the extreme line wings, a region that does not concern us here.

Letting

$$H_0 = H_{\text{atoms}} + H_f, \quad (98)$$

$$H^r(t) = (e/mc) \sum_i \vec{p}_i \cdot \vec{A}[\vec{R}_i(t)], \quad (99)$$

and neglecting the A^2 term, the Schrödinger equation for the system will be

$$i\hbar \partial |\psi\rangle / \partial t = H |\psi\rangle, \quad (100)$$

$$\text{where } H = H_0 + H^r(t) + H^C(t). \quad (101)$$

We expand the wave vector $|\psi\rangle$ in an interaction representation as

$$|\psi\rangle = \sum_\alpha b_\alpha(t) \exp(-iE_\alpha t/\hbar) |\varphi_\alpha\rangle, \quad (102)$$

where the $|\varphi_\alpha\rangle$ are eigenvectors and the E_α eigenenergies of H_0 . Substituting Eq. (102) into Eq. (100), we find that the probability amplitudes $b_\alpha(t)$ must satisfy the equation

$$i\hbar \dot{b}_\alpha = \sum_\beta \langle \varphi_\alpha | H^r(t) + H^C(t) | \varphi_\beta \rangle \exp(i\omega_{\alpha\beta} t) b_\beta(t). \quad (103)$$

The operator $H^C(t)$ is independent of the radiation field. Consequently, $H^C(t)$ may have nonvanishing matrix elements between states diagonal in the photon occupation number only. Matrix elements of $H^r(t)$ obey the selection rules for dipole transitions. There will be additional selection rules for matrix elements of $H^C(t)$ arising from the nature of the dipole-dipole interaction and the adiabaticity of collisions which will be discussed below. We now proceed to examine the solutions of Eq. (103) for spectral profiles, polarization effects (Hanle effect), and laser phenomena for the nonresonant and resonant cases.

VII. NONRESONANT LINE SHAPES

By using techniques similar to those which led to Eq. (61), one may eliminate all the states of the system in which the perturbers are in excited states and, for the case of nonresonant broadening, we shall

suppress the perturber-state labels with the understanding that perturber ground states are implied. The probability amplitudes under consideration, which specify states of the emitter and radiation field, obey the modified equation

$$i\hbar \dot{b}_\alpha = \sum_\beta \langle \varphi_\alpha | H^{\mathcal{Y}}(t) + H^{\mathcal{C}}(t) | \varphi_\beta \rangle \exp(i\omega_{\alpha\beta} t) b_\beta(t), \quad (104)$$

where $H^{\mathcal{C}}(t)$ is an effective real collision Hamiltonian, obtained by one iteration of Eq. (103), with a structure similar to that given in Eq. (61).⁶⁷ The interaction $H^{\mathcal{C}}(t)$ will have nonvanishing matrix elements only between states of the same multiplet.

A. Spectral Profiles

We wish to determine the spectral profile of spontaneous radiation emitted from level a , a degenerate $j=1$ state, to the ground-state level s shown in Fig. 7. Since we have treated the collisions by an effective Hamiltonian, there is no need to consider additional emitter states. We specify the initial conditions at $t=0$ by assuming that the substates m of level a and the state s have some given initial population distribution.

The spectral distribution is given by the probability of finding the emitter in state s and an emitted photon of frequency ω_k of type \vec{k}, λ after a long time has passed. This probability is denoted by $|b_{s\vec{k}\lambda}(\infty)|^2$. Using the selection rules, we obtain the time development of $b_{s\vec{k}\lambda}(t)$ from Eq. (104) as

$$i\hbar \dot{b}_{s\vec{k}\lambda}(t) = \sum_m H_{s\vec{k}\lambda; m}^{\mathcal{Y}}(t) \exp[i(\omega_k - \omega_0)t] b_m(t) + H_{s; s}^{\mathcal{C}}(t) b_{s\vec{k}\lambda}(t), \quad (105)$$

$$\text{where } \omega_0 = \omega_a - \omega_s. \quad (106)$$

The formal solution of this equation is

$$b_{s\vec{k}\lambda}(t) = \exp[-i\hbar^{-1} \int_0^t H_{s; s}^{\mathcal{C}}(t') dt'] \int_0^t dt' \sum_m (i\hbar)^{-1} \\ \times \exp[i\hbar^{-1} \int_0^{t'} H_{s; s}^{\mathcal{C}}(t'') dt''] H_{s\vec{k}\lambda; m}^{\mathcal{Y}}(t') \exp[i(\omega_k - \omega_0)t'] b_m(t').$$

Thus, the spectral profile is given by

$$|b_{s\vec{k}\lambda}(\infty)|^2 = \hbar^{-2} \sum_{mm'} \int_0^\infty dt \int_0^\infty dt' \exp[i\hbar^{-1} \int_0^t H_{s; s}^{\mathcal{C}}(t'') dt''] H_{s\vec{k}\lambda; m}^{\mathcal{Y}}(t) \\ \times \exp[i(\omega_k - \omega_0)(t - t')] \exp[-i\hbar^{-1} \int_0^{t'} H_{s; s}^{\mathcal{C}}(t''') dt'''] H_{m'; s\vec{k}\lambda}^{\mathcal{Y}}(t') b_m(t) b_{m'}^*(t'). \quad (107)$$

The time dependence of the $H^{\mathcal{Y}}(t)$ elements may be separated out by writing

$$(a) H_{s\vec{k}\lambda; m}^{\mathcal{Y}}(t) = \exp[-i\vec{k} \cdot \vec{R}(t)] H_{s\vec{k}\lambda; m}^{\mathcal{Y}} \quad \text{and} \quad (b) H_{m'; s\vec{k}\lambda}^{\mathcal{Y}}(t) = \exp[i\vec{k} \cdot \vec{R}(t)] H_{m'; s\vec{k}\lambda}^{\mathcal{Y}}, \quad (108)$$

where $\vec{R}(t)$ is the position of the emitter. One also recognizes that

$$H_{s\vec{k}\lambda; m}^{\mathcal{Y}} = H_{m'; s\vec{k}\lambda}^{\mathcal{Y}*}.$$

Substitution of Eqs. (108) and the factor of unity $[b_s(0) b_{s'}^*(0)]^{-1} b_s(0) b_{s'}^*(0)$ into Eq. (107) transforms it into

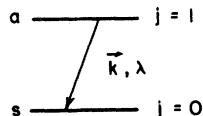


FIG. 7. Two-level atomic emitter structure employed to consider radiative interactions in the non-resonant case.

$$\begin{aligned}
|b_{s\vec{k}\lambda}(\infty)|^2 &= \hbar^{-2} \sum_{mm'} \int_0^\infty dt \int_0^\infty dt' [b_s(0)b_s^*(0)]^{-1} \exp[i\hbar^{-1} \int_0^t H_{s;s}^C(t'') dt''] \\
&\quad \times b_s^*(0) H_{s\vec{k}\lambda;m}^{\gamma'} \exp[-i\vec{k} \cdot \vec{R}(t)] \exp[i(\omega_k - \omega_0)(t-t')] \exp[-i\hbar^{-1} \int_0^{t'} H_{s;s}^C(t''') dt'''] \\
&\quad \times b_s(0) H_{s\vec{k}\lambda;m}^{\gamma'*} \exp[i\vec{k} \cdot \vec{R}(t')] b_m(t) b_m^*(t').
\end{aligned} \tag{109}$$

Using Eq. (104), it is easy to show that

$$b_s(t) = \exp[-i\hbar^{-1} \int_0^t H_{s;s}^C(t') dt'] b_s(0), \tag{110}$$

which expresses the collisional change in the ground state of the system. Substituting Eq. (110) into Eq. (109), and forming density-matrix elements gives

$$\begin{aligned}
|b_{s\vec{k}\lambda}(\infty)|^2 &= \hbar^{-2} \sum_{mm'} \int_0^\infty dt \int_0^\infty dt' [b_s(0)b_s^*(0)]^{-1} H_{s\vec{k}\lambda;m}^{\gamma'} H_{s\vec{k}\lambda;m'}^{\gamma'*} \\
&\quad \times \exp[i(\omega_k - \omega_0)(t-t')] \exp[-i\vec{k} \cdot [\vec{R}(t) - \vec{R}(t')]] \rho_{ms}(t) \rho_{m's'}^*(t').
\end{aligned}$$

Changing variables to $\tau = t - t'$, $t_0 = t'$, one can show that

$$|b_{s\vec{k}\lambda}(\infty)|^2 = 2\hbar^{-2} \text{Re} \int_0^\infty d\tau \exp[i(\omega_k - \omega_0)\tau] \varphi(\tau), \tag{111}$$

where, for $\tau > 0$,

$$\varphi(\tau) = \sum_{mm'} \int_0^\infty dt_0 [b_s(0)b_s^*(0)]^{-1} H_{s\vec{k}\lambda;m}^{\gamma'} H_{s\vec{k}\lambda;m'}^{\gamma'*} \exp[i\vec{k} \cdot [\vec{R}(t_0) - \vec{R}(t_0 + \tau)]] \rho_{ms}(t_0 + \tau) \rho_{m's'}^*(t_0). \tag{112}$$

The quantity $\varphi(\tau)$ is sometimes called the correlation function.⁴

The spontaneous emission from level a contributes an exponential decay in t_0 to the factors $\rho_{ms}(t_0 + \tau)$ and $\rho_{m's'}^*(t_0)$. Had this decay been neglected, one would find Eq. (111) to be divergent when averaged over all collision histories. Many pressure broadening theories do not properly consider spontaneous emission, and it has been customary to replace the time integral in Eq. (112) by an ensemble average over all collisions. The justification of this replacement is found not in the ergodic theorem as is commonly claimed,^{2,4} but rather by a systematic treatment of spontaneous emission.⁶⁸

We seek the value of $|b_{s\vec{k}\lambda}(\infty)|^2$ averaged over all collision histories and emitter velocities. Denoting this average by $I_{as}(\vec{k}\lambda)$, we have

$$I_{as}(\vec{k}\lambda) = 2\hbar^{-2} \text{Re} \int_0^\infty d\tau \exp[i(\omega_k - \omega_0)\tau] \langle \varphi(\tau) \rangle_{cu}, \tag{113}$$

where c and u indicate averages over collision history and emitter velocity, respectively. We are left with the difficult problem of determining⁶⁹

$$\begin{aligned}
\langle \varphi(\tau) \rangle_{cu} &= \sum_{mm'} \int_0^\infty dt_0 [b_s(0)b_s^*(0)]^{-1} H_{s\vec{k}\lambda;m}^{\gamma'} H_{s\vec{k}\lambda;m'}^{\gamma'*} \\
&\quad \times \langle \exp[i\vec{k} \cdot [\vec{R}(t_0) - \vec{R}(t_0 + \tau)]] \rho_{ms}(t_0 + \tau) \rho_{m's'}^*(t_0) \rangle_{cu}.
\end{aligned} \tag{114}$$

It will be useful to distinguish three interrelated effects contained in the average. First, there are the energy-level perturbations induced by collisions which will be termed impact effects. Second, there are velocity effects which require one to take account of the emitter's velocity in calculating the profile. Third, there are the changes in the emitter's velocity induced by collisions which will be called recoil effects. The velocity and recoil effects are contained in the exponential factor in Eq. (114). Recoil and impact effects occur at the same time and will be correlated leading to mathematical complexities in evaluating the average. Although formal expressions for $\langle \varphi(\tau) \rangle_{cu}$ have been derived,²⁰ explicit evaluations of it have been made only for unrealistic collision models.^{16,17,28-30} In the following discussion of spectral

profiles, we shall neglect all effects arising from the velocity and recoil of the emitter; that is, we shall replace $\exp\{i\vec{k} \cdot [\vec{R}(t_0) - \vec{R}(t_0 + \tau)]\}$ by unity. This is not to say that these effects are unimportant (they may, in fact, be dominant), but only that they will not be considered here. In order for an experimental spectral profile to agree with the results we shall obtain, all velocity and recoil effects must be correctly subtracted out of the profile. If one neglects recoil effects, the exponential factor no longer depends on collisions, giving the Doppler contribution $\exp(i\vec{k} \cdot \vec{v}\tau)$, and the spectral profile could be analyzed in terms of Voigt functions (convolution of a Gaussian with a Lorentzian line shape).⁷⁰ This procedure has often been carried out in analyzing spectra, but, as noted above, there is no sound theoretical basis for the use of Voigt profiles once recoil effects are included.

With the above approximation, Eq. (114) becomes

$$\langle \varphi(\tau) \rangle_c = \sum_{mm'} \int_0^\infty dt_0 [b_s(0)b_s^*(0)]^{-1} H_{s\vec{k}\lambda; m}^r H_{s\vec{k}\lambda; m'}^{r*} \langle \varphi_{mm'}(t_0, \tau) \rangle_c, \quad (115)$$

$$\text{where } \varphi_{mm'}(t_0, \tau) = \rho_{ms}(t_0 + \tau) \rho_{m's}^*(t_0). \quad (116)$$

Let us consider the change undergone by $\varphi_{mm'}(t_0, \tau)$ in the time interval between $t = \tau$ and $\tau + \delta\tau$. The quantity $\delta\tau$ is chosen small enough to contain at most one collision but large enough to contain the entire collision. The change in the average of φ will be given by

$$[\delta\varphi_{mm'}(t_0, \tau, \delta\tau, b, v, \Omega)]_{av} = \langle P_0(\delta\tau) \delta\varphi_{mm'}^0(t_0, \tau, \delta\tau) \rangle_c + \langle \{P_1(b, v, \Omega, \delta\tau) \delta\varphi_{mm'}^1(t_0, \tau, \delta\tau, b, v, \Omega)\}_{bv\Omega} \rangle_c, \quad (117)$$

where $P_0(\delta\tau)$ is the probability of no collisions in a time $\delta\tau$, $\delta\varphi_{mm'}^0(t_0, \tau, \delta\tau)$ is the change in $\varphi_{mm'}$ in time between τ and $\tau + \delta\tau$ if no collision occurs, $P_1(b, v, \Omega, \delta\tau)$ is the probability density for a collision specified by b, v, Ω occurring in a time $\delta\tau$, $\delta\varphi_{mm'}^1(t_0, \tau, \delta\tau, b, v, \Omega)$ is the change in $\varphi_{mm'}$ due to this collision. For $\delta\tau$ chosen as described above, $P_0(\delta\tau) \approx 1$. In the Wigner-Weisskopf approximation, neglecting energy shifts, one can show that the change $\delta\varphi_{mm'}^0$ is given by

$$\delta\varphi_{mm'}^0(t_0, \tau, \delta\tau) = -\frac{1}{2} \Gamma_a \delta\tau \varphi_{mm'}(t_0, \tau), \quad (118)$$

where Γ_a is the natural width of each sublevel of state a . On the other hand, from Secs. IV and V, we find the change $\delta\varphi_{mm'}^1$ as

$$\delta\varphi_{mm'}^1(t_0, \tau, \delta\tau, b, v, \Omega) = \sum_p [-\delta_{mp} + Q^*(b, v) M_{mp}(b, v, \Omega)] \varphi_{pm'}(t_0, \tau). \quad (119)$$

Substituting Eqs. (118) and (119) into (117) and averaging over all collision histories using the results of Secs. IV and V, one obtains

$$\langle \delta\varphi_{mm'}(t_0, \tau) \rangle_c / \delta\tau = -\frac{1}{2} (\Gamma_a + 2\Gamma_{as}^N) \langle \varphi_{mm'}(t_0, \tau) \rangle_c, \quad (120)$$

where Γ_{as}^N is the nonresonant average electric dipole decay parameter given in Eq. (94).

The transformation of Eq. (120) to a differential equation is valid only if $\delta\tau$ is much less than the oscillation frequency of the integrand in Eq. (111). This condition is fulfilled if

$$(\omega_k - \omega_0) \delta\tau \ll 1, \quad (121)$$

$$\text{and } \frac{1}{2} (\Gamma_a + 2\Gamma_{as}^N) \delta\tau \ll 1, \quad (122)$$

and since $\delta\tau$ is on the order of the collision time, Eqs. (121) and (122) represent the standard criteria for the adiabatic and impact approximations.^{4-6, 21} In that part of the line shape where Eq. (121) is valid, Eq. (120) may be replaced by a differential equation and integrated to yield

$$\langle \varphi_{mm'}(t_0, \tau) \rangle_c = \exp[-\frac{1}{2} (\Gamma_a + 2\Gamma_{as}^N) \tau] \langle \varphi_{mm'}(t_0, 0) \rangle_c. \quad (123)$$

Combining Eqs. (123), (113), (115), (116), and using the fact that $b_s(t)b_s^*(t) = b_s(0)b_s^*(0)$, gives the spec-

tral profile as

$$I_{as}(\vec{k}\lambda) = \frac{\hbar^{-2}[\Gamma_a + 2\text{Re}(\Gamma_{as}^N)] \sum_{mm'} \int_0^\infty dt {}_0 H^{\gamma}{}_{s\vec{k}\lambda; m} H^{\gamma*}{}_{s\vec{k}\lambda; m} \langle \rho_{mm'}(t_0) \rangle_c}{[\omega_k - \omega_0 - \text{Im}(\Gamma_{as}^N)]^2 + [\frac{1}{2}\Gamma_a + \text{Re}(\Gamma_{as}^N)]^2}. \quad (124)$$

Equation (124) verifies the assertion of Secs. III and IV that the real part and imaginary part of Γ_{as}^N correspond to broadening and shift, respectively. If we evaluate elements of H^{γ} at $\omega = \omega_0$ the line shape is a pure Lorentzian. One additional average may be made in Eq. (124). If the excitation is unpolarized, one should average over initial conditions using

$$\langle b_m(0) b_{m'}^*(0) \rangle_i = \frac{1}{3} D_0 \delta_{mm'}, \quad \text{where } D_0 = \sum_m |b_m(0)|^2, \quad (125)$$

and $\langle \dots \rangle_i$ indicates the average over initial conditions. If this average is performed, Eq. (114) becomes

$$\langle I_{as}(\vec{k}\lambda) \rangle_i = \frac{\frac{1}{3} D_0 \hbar^{-2} [\Gamma_a + 2\text{Re}(\Gamma_{as}^N)] \Gamma_a^{-1} \sum_m |H^{\gamma}{}_{s\vec{k}\lambda; m}|^2}{[\omega_k - \omega_0 - \text{Im}(\Gamma_{as}^N)]^2 + [\frac{1}{2}\Gamma_a + \text{Re}(\Gamma_{as}^N)]^2}. \quad (126)$$

The above procedure can be extended to the emitter structure shown in Fig. 8 and is used by Vaughan and Smith in their experiments.⁵⁴ Level a is a degenerate $j=1$ state while levels b and s are $j=0$ states, and the initial condition is $b_b(0)=1$ while all other b 's vanish at $t=0$. The spectral profile $I_{ba}(\vec{k}\lambda)$ of the emission line between states b and a may be calculated as

$$I_{ba}(\vec{k}\lambda) = \frac{\hbar^{-2} \Gamma_b^{-1} [\Gamma_b + \Gamma_a + 2\text{Re}(\Gamma_{ba}^N)] \sum_m |H^{\gamma}{}_{m\vec{k}\lambda; b}|^2}{[\omega_k - \omega_{ba} - \text{Im}(\Gamma_{ba}^N)]^2 + [\frac{1}{2}(\Gamma_b + \Gamma_a) + \text{Re}(\Gamma_{ba}^N)]^2}, \quad (127)$$

where Γ_b is the natural width of level b , Γ_a is the natural width of any sublevel of state a , and Γ_{ba}^N is the collisional decay rate of ρ_{ba} as calculated in Secs. IV-V. Again we see that it is the decay of ρ_{ba} alone which determines the contribution of collisions to the spectral characteristics of the emission line between states b and a . Velocity and recoil effects have also been neglected in Eq. (127). Had we included velocity effects but neglected recoil, both Eqs. (126) and (127) would go over into Voigt profiles instead of Lorentzians.

B. Polarization Effects (Hanle Effect)

The geometry of a Hanle-effect experiment is shown in Fig. 9. Emitter atoms in a scattering cell are excited by resonant radiation of polarization λ' , direction \hat{k}' . One observes the scattered (reemitted) radiation of polarization λ , direction \hat{k} . The scattering cell is located in a weak magnetic field. In this experiment, the detectors do not discriminate between different frequencies. We shall see that this condition enables one to bypass the difficulties presented by velocity and recoil effects.

Consider the emitter-level structure shown in Fig. 7. Level a is now nondegenerate due to the presence

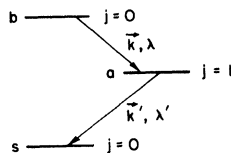


FIG. 8. Three-level emitter structure employed to consider radiative interactions for both the resonant and nonresonant cases. The radiation \vec{k}, λ is observed while the \vec{k}', λ' radiation is not detected. In the resonant case, the \vec{k}', λ' radiation is completely trapped in the medium.

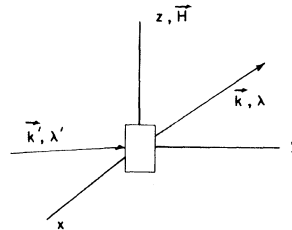


FIG. 9. Hanle-effect geometry, where \vec{k}, λ' represents the incident and \vec{k}, λ the scattered radiation from a sample cell at the origin. The system is in a weak magnetic field H directed along the z axis.

of the weak magnetic field. In Hanle-effect experiments, the excitation radiation usually has a broad spectral profile. If this is the case, one can simulate excitation radiation of direction \hat{k}' , polarization λ' by a proper choice of initial conditions. The nature of the excitation radiation is reflected in the ratio of the $b_m(0)$. For example, if the incident radiation is plane polarized in the y direction and is propagating in the x direction with the magnetic field along z , then we choose $b_0(0)=0$, $b_{+1}(0)=+b_{-1}(0)$. The probability of observing scattered radiation of frequency $\omega_{k\lambda}$ is given by Eq. (107), generalized to allow for the nondegeneracy of level a

$$|b_{s\vec{k}\lambda}(\infty)|^2 = \hbar^{-2} \sum_{mm'} \int_0^\infty dt \int_0^\infty dt' H^r_{s\vec{k}\lambda; m} H^{r*}_{s\vec{k}\lambda; m'} \exp[i(\omega_k + \omega_s)(t-t')] \exp\{i\hbar^{-1}[\int_0^t H^C_{s; s}(t'') dt'' - \int_0^{t'} H^C_{s; s}(t''') dt''']\} \exp[-i(\omega_m t - \omega_{m'} t')] \exp[-i\vec{k} \cdot [\vec{R}(t) - \vec{R}(t')]] b_m(t) b_{m'}^*(t'). \quad (128)$$

Since the detector does not discriminate different frequencies, we must sum Eq. (128) over all ω_k . The calculation is similar to that for isolated spontaneous emission profiles, and, in the Wigner-Weisskopf limit and the limit $v/c \ll 1$, one obtains

$$\sum_{\vec{k}} |b_{s\vec{k}\lambda}(\infty)|^2 = \frac{\omega_0^2}{\hbar^2 (2\pi c)^3} 2\pi V \sum_{mm'} \int_0^\infty dt H^r_{s\vec{k}_0\lambda; m} H^{r*}_{s\vec{k}_0\lambda; m'} \exp(i\omega_{m'} t) \rho_{mm'}(t), \quad (129)$$

where $k_0 = \omega_0/c$. Note that velocity and recoil effects no longer appear since the integration over ω_k gave a result proportional to $\delta(t-t')$. The removal of velocity and recoil effects make Hanle-effect experiments extremely useful in studying collision phenomena.

The intensity of radiation observed in the direction \hat{k} with polarization λ [denoted by $I(\hat{k}\lambda)$] is given by Eq. (129) averaged over all collision histories. Letting

$$C' = \hbar^{-2} \omega_0^2 (2\pi c)^{-3} 2\pi V, \quad (130)$$

one finds

$$I(\hat{k}\lambda) = C' \sum_{mm'} \int_0^\infty dt H^r_{s\vec{k}_0\lambda; m} H^{r*}_{s\vec{k}_0\lambda; m'} \exp(i\omega_{m'} t) \langle \rho_{mm'}(t) \rangle_c. \quad (131)$$

We must evaluate $\langle \rho_{mm'}(t) \rangle_c$. Using Eq. (104) in the Wigner-Weisskopf approximation, one can show that $\rho_{mm'}(t)$ obeys the differential equation

$$\dot{\rho}_{mm'}(t) = -\Gamma_a \rho_{mm'}(t) + (i\hbar)^{-1} [\exp(i\mathcal{E}_0 t/\hbar) H^C(t) \exp(-i\mathcal{E}_0 t/\hbar), \rho(t)]_{mm'}. \quad (132)$$

The radiation term is transformed away by use of the substitution

$$\rho_{mm'}(t) = \rho'_{mm'}(t) \exp(-\Gamma_a t), \quad (133)$$

leading to the differential equation for $\rho'_{mm'}(t)$

$$i\hbar \dot{\rho}'_{mm'}(t) = [\exp(i\mathcal{E}_0 t/\hbar) H^C(t) \exp(-i\mathcal{E}_0 t/\hbar), \rho'(t)]_{mm'}.$$

Thus, $\rho'_{mm'}(t)$ satisfies the equation of motion for the problem with no radiation field present. In Secs. IV and V, we have already derived differential equations from which one can obtain $\langle \rho'_{mm'}(t) \rangle_c$. The results are most conveniently expressed in terms of the irreducible components of $\langle \rho' \rangle_c$, given by

$$\langle \rho'_{mm'}(t) \rangle_c = \sum_{KQ} (-1)^{1-m'} \begin{bmatrix} 1 & 1 & K \\ m & -m' & Q \end{bmatrix} \langle \rho'_{KQ}(t) \rangle_c. \quad (134)$$

The $\langle \rho'_{KQ}(t) \rangle_c$ exhibit the simple exponential decay similar to that in Eq. (44),

$$\langle \rho'_{KQ}(t) \rangle_c = \exp(-\Gamma_K t) \rho_{KQ}(0). \quad (135)$$

Combining Eqs. (133)–(135), we obtain the desired result

$$\langle \rho_{mm'}(t) \rangle_c = \sum_{KQ} (-1)^{1-m'} \begin{bmatrix} 1 & 1 & K \\ m & -m & Q \end{bmatrix} \exp\{-(\Gamma_a + \Gamma_K^N)t\} \rho_{KQ}(0). \quad (136)$$

Substituting Eq. (136) into Eq. (131) and performing the trivial time integration, one obtains the Hanle-effect line shape as

$$I(\vec{k}\lambda) = C' \sum_{mm', KQ} \frac{H^r \vec{s}_{\vec{k}_0\lambda; m} H^{r*} \vec{s}_{\vec{k}_0\lambda; m'} (-1)^{1-m'} \begin{bmatrix} 1 & 1 & K \\ m & -m' & Q \end{bmatrix} \rho_{KQ}(0)}{i\omega_{mm'} + (\Gamma_K^N + \Gamma_a)} \quad (137)$$

This equation is a generalization of the Breit formula,⁷¹ which has been used in analyzing experimental results.

Equation (137) for the intensity depends on the excitation through the factor $\rho_{KQ}(0)$ and on the direction and polarization of the scattered light through the factor $H^r \vec{s}_{\vec{k}_0\lambda; m} H^{r*} \vec{s}_{\vec{k}_0\lambda; m'}$. The line shape is obtained by measuring intensity versus $\omega_{mm'}$; the frequency separation $\omega_{mm'}$ is varied by sweeping through the magnetic field. By suitable choices of experimental geometry (see Ref. 48), one can obtain a Lorentzian line shape with a width which is full width at half-maximum (FWHM) of $2(\Gamma_a + \Gamma_1^N)$ or a Lorentzian line shape with a width (FWHM) of $2(\Gamma_a + \Gamma_2^N)$. Thus, Hanle-effect experiments provide an excellent method of measuring the multipole decay constants.

C. Laser Phenomena

A theory of the laser developed by Lamb⁷² employed equations of motion for the density matrix of the emitters. Collision effects may be taken into account by simply adding the collisional rates of change of the emitter density matrix described in Secs. IV and V to the equations of the laser theory. The use of such a modified system of equations to analyze experimental results might lead to a determination of the relaxation parameters of the laser levels. Since laser action is observed between highly excited states, Hanle-effect experiments might not be suitable for the determination of these parameters.

By studying the pressure dependence of the dip in the curve of laser intensity versus cavity detuning, one will obtain information about the decay parameter of the average electric dipole moment associated with the two laser levels. Recoil effects, which have been neglected in the above treatment, must be included in this case. Somewhat artificial but soluble models of recoil effects have been utilized,^{17, 30} and we feel that a better treatment of recoil effects is necessary before theoretical predictions of the average electric dipole parameter take on added significance. On the other hand, we should not expect recoil effects to be as significant in determinations of Γ_1 and Γ_2 . In laser experiments, these parameters can be studied by mode competition effects in the Zeeman laser. The laser theory without collisions predicts neutral coupling for a $j=1 \rightarrow 0$ laser transition,⁷³ while the theory, modified to include collisions, correctly predicts the observed strong coupling.⁵² In effect, it is the collisional depolarization which causes the shift from neutral to strong coupling.

VIII. RESONANT BROADENING LINE SHAPES

The calculation of resonant broadening line shapes presents some additional difficulties. Each atom is assumed to have a prescribed motion for its center of mass, which will specify all collisions undergone by the system. Since both the perturber and emitter have some probability of being excited after a collision, we must consider each atom of the system as a possible source of radiation. In addition to the excitation exchange probability associated with collisions, the atoms can also exchange real photons. This phenomenon is commonly called radiation trapping and will be discussed in some detail below. The simultaneous consideration of collisions and radiation trapping will be

treated here in a somewhat phenomenological manner since a more rigorous approach would be exceedingly complex.

Since each atom of the system must be considered as a possible source of radiation, we must now label the state of each atom. However, if only one atom is initially excited, there are only three classes of system states which are energetically possible. First, there is the state written $|ia\rangle$ which means the i th atom is in an excited state a and the rest are in their ground states. Second, there is the state written $|b, \vec{k}, \lambda\rangle$ which means the i th atom is in some lower excited state b , a photon \vec{k}, λ is present, and the rest of the atoms are in their ground states. Finally, there is the state written $|\vec{k}, \lambda'\rangle$ which means all the

atoms are in their ground states with the photon \vec{k}' , λ' present.

Due to the adiabaticity of the interaction, it is easy to show that the reduced density matrix of the i th atom $\rho_{mm'}^i$ will be given by

$$\rho_{mm'}^i = \rho_{im';im'}, \quad (138)$$

since the right-hand side is the only term which contributes in the trace of the total system density matrix over perturber states. Thus, according to this notation, the definition of $\rho_{mm'}$ as a sum of reduced density matrices first given in Eq. (37) is

$$\rho_{mm'} = \sum_i \rho_{mm'}^i = \sum_i \rho_{im';im'}. \quad (139)$$

Having established the notation, we can proceed to calculate various experimental line shapes.

In order to provide some foundation for the calculation, we first present a short review of resonant trapping.³⁴⁻³⁷ Resonant trapping refers to the process in which radiation emitted by one atom is reabsorbed by other atoms. Consider an excited atom in a medium of resonant perturbers, all in their ground states. If the volume of perturbers is large enough, there is very little probability that an emitted photon will escape during the observation time of an experiment. This is the condition of complete trapping. Since complete trapping is already achieved at pressures where collision effects are still negligible,^{35, 48} we shall consider only this case.

For the moment, let us neglect collision effects. If, on the average, the radiation emitted from a given Zeeman sublevel were reabsorbed in the same Zeeman sublevel of another atom, all the average multipole decay constants of the entire system would be zero. Such is not the case, however, as radiation transfer results in a reorientation of the sample. This reorientation leads to nonzero values for some of the average multipole decay parameters. Thus, it is the trapping that causes a narrowing (decrease in the Γ 's) and the reorientation that causes a broadening (increase in the Γ 's) in the resultant line shapes.

Just as average collisional scattering elements have been introduced in Eqs. (38) and (39) [these have been denoted by $S_{mm'}^{pp'}$ but will be written here as $S_{mm'}^{pp'}(\text{col})$ for increased clarity], one can introduce average radiative scattering elements to be denoted by $S_{mm'}^{pp'}(\text{rad})$. For the case of Fig. 7, with no collision broadening, Doppler width much larger than natural width, and complete radiation trapping, Dyakonov and Perel³⁶ calculated these elements as

$$S_{11}^{11}(\text{rad}) = -0.3\gamma_{a,s},$$

$$S_{11}^{00}(\text{rad}) = 0.1\gamma_{a,s},$$

$$S_{11}^{-1-1}(\text{rad}) = 0.2\gamma_{a,s},$$

$$S_{10}^{10}(\text{rad}) = -0.4\gamma_{a,s}, \quad (140)$$

$$S_{00}^{00}(\text{rad}) = -0.2\gamma_{a,s},$$

$$S_{10}^{0-1}(\text{rad}) = 0.1\gamma_{a,s},$$

$$\text{and } S_{1-1}^{1-1} = -0.5\gamma_{a,s},$$

where $\gamma_{a,s}$ is the transition probability per unit time of the resonant transition.⁷⁴ Thus, on the average, radiation emitted from the $m=1$ state is 70% reabsorbed in $m=1$ states, 10% reabsorbed in $m=0$ states, and 20% reabsorbed in $m=-1$ states. Since the gas is assumed to be isotropic, the $S_{mm'}^{pp'}(\text{rad})$ elements possess the same symmetry properties with regard to index interchange as the collisional elements $S_{mm'}^{pp'}(\text{col})$. Hence, the trapping can be described by the three average multipole constants found by Dyakonov and Perel³⁶ and Omont³⁷ to be

$$\Gamma_0(\text{rad}) = 0.0, \quad (141a)$$

$$\Gamma_1(\text{rad}) = 0.5\gamma_{a,s}, \quad (141b)$$

$$\text{and } \Gamma_2(\text{rad}) = 0.3\gamma_{a,s}. \quad (141c)$$

Equation (141a) expresses the condition of complete trapping.

The results stated in Eqs. (140) and (141) were derived for pressures where the average separation of the atoms was much larger than the resonant radiative wavelength. It is possible that these values will change at collision broadening pressures where the average separation of the atoms is on the order of the resonant radiative wavelength (since trapping will still be complete, the value of Γ_0 will remain zero). However, for the experimental situations to be discussed, it will prove satisfactory to use the values given in Eqs. (140) and (141).⁷⁵ We shall now incorporate the above theory in the calculation of experimental line shapes for polarization effects, spectral profiles, and laser phenomena.

A. Polarization Effects (Hanle Effect)

In Hanle-effect experiments, one is interested in the probability of observing all the scattered radiation of direction \vec{k} , polarization λ of a system excited with resonant radiation of direction \vec{k}' , and polarization

λ' . In most cases, the excitation information can be simulated by a judicious choice of initial conditions for the density matrix of the system. To study resonant collision effects, we consider the structure, similar to that of lead, shown in Fig. 10, in which the frequency separation of levels b and s is assumed large compared with the inverse collision time. In the presence of a weak magnetic field, one may observe the untrapped radiation emitted between states a and b in order to obtain information about the orientation of level a . The probability for observing an untrapped photon of frequency $\omega_k \approx \omega_a - \omega_b$, direction \hat{k} , and polarization λ may be computed using Eq. (103) to be

$$\sum_i \rho_{ib, \vec{k}\lambda; ib, \vec{k}\lambda}^{(\infty)} = \sum_i |(i\hbar)^{-1} \sum_m \int_0^\infty dt H_{b, \vec{k}\lambda; m}^r \exp[-i\vec{k} \cdot \vec{R}_i(t)] \exp[i(\omega_k - \omega_{mb})t] b_{im}(t)|^2, \quad (142)$$

where m represents a substate of level a . The position vector of the i th atom is denoted by $\vec{R}_i(t)$. Note that all the position and time dependence has been factored from the radiative matrix elements and that the remaining term, $H_{b, \vec{k}\lambda; m}^r$ no longer depends on the atom label i . An additional feature of Eq. (142) is that matrix elements of $H^C(t)$ do not explicitly appear since the resonant collisions do not alter the state $|ib\rangle$.

The Hanle-effect line shape is obtained by integrating the expression (142) over all ω_k and averaging it over all histories. The resultant intensity is denoted by $I(\hat{k}\lambda)$ and may be calculated as

$$I(\hat{k}\lambda) = C'' \sum_i \sum_{mm'} \int_0^\infty dt H_{b, \vec{k}_1\lambda; m}^r H_{b, \vec{k}_1\lambda; m'}^{r*} \exp(-i\omega_{mm'}t) \langle \sum_i \rho_{im; im'}(t) \rangle_c \quad (143)$$

where $k_1 = \omega_{ab}/c$, $C'' = (\omega_{ab}/\omega_0)^2 C'$,

and C' is defined by Eq. (130). Equation (143) is valid as long as the average time between collisions is much greater than the time it takes untrapped radiation to travel the length of the system, a condition that will hold for the pressures and system sizes under consideration.

Using Eq. (103), it is a straightforward matter to show that, in the Wigner-Weisskopf approximation, elements of the density matrix have the time development given by

$$\dot{\rho}_{im; i'm'} = -(\gamma_{a,s} + \gamma_{a,b}) \rho_{im; i'm'} + \sum_{jj'} \sum_{pp'} [H(r, t)_{im; i'm'}^{jp; j'p'} + H(c, t)_{im; i'm'}^{jp; j'p'}] \rho_{jp; j'p'}, \quad (144)$$

where

$$H(r, t)_{im; i'm'}^{jp; j'p'} = \left[\left(-\frac{1}{2} C' \right) \sum_{\vec{k}_0 \lambda} H_{m; s, \vec{k}_0 \lambda}^r H_{p; s, \vec{k}_0 \lambda}^{r*} \exp(i\omega_{mp} t) \right. \\ \left. \times \exp\{i\vec{k}_0 \cdot [\vec{R}_i(t) - \vec{R}_{j'}(t)]\} \delta_{i'j'} \delta_{m'p'} + \text{c. c. of same term with } \begin{pmatrix} i \rightarrow i' & m \rightarrow m' \\ j \rightarrow j' & p \rightarrow p' \end{pmatrix} \right] (1 - \delta_{ij} \delta_{i'j'}), \quad (145)$$

$$H(c, t)_{im; i'm'}^{jp; j'p'} = (i\hbar)^{-1} [H^C(t)_{im; jp} \exp(i\omega_{mp} t) \delta_{i'j'} \delta_{m'p'} - H^C(t)_{i'm'; j'p} \exp(-i\omega_{m'p'} t) \delta_{ij} \delta_{m'p'}], \quad (146)$$

$$k_0 = (\omega_a - \omega_s)/c, \quad (147)$$

and $\gamma_{a,b}$ and $\gamma_{a,s}$ represent the transition probability per unit time for the transitions $a \rightarrow b$ and $a \rightarrow s$, respectively, for an isolated atom. If we consider the $(3n)^2$ elements of ρ for an n atom system to make up a column vector and form corresponding matrices from the elements

$$H(r, t)_{im; i'm'}^{jp; j'p'} \quad \text{and} \quad H(c, t)_{im; i'm'}^{jp; j'p'},$$

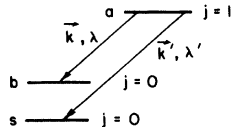


FIG. 10. Three-level atomic structure employed to consider radiative effects in the presence of resonant perturbers. The radiation \vec{k}, λ is observed while the \vec{k}', λ' radiation is completely trapped by the medium.

Eq. (144) may be written in vector form⁷⁶ as

$$\dot{\vec{\rho}} = -(\gamma_{a,s} + \gamma_{a,b})\vec{\rho} + [H(r,t) + H(c,t)]\vec{\rho}. \quad (148)$$

The first term on the right-hand side represents the normal radiative decay, the matrix $H(r,t)$ represents radiation transfer effects, and the matrix $H(c,t)$ represents collision effects.

As in the nonresonant case, we consider the change in ρ in a short time interval δt ,

$$[\delta\vec{\rho}(t)]_{\text{av}} = \langle \{ P_0(\delta t) P(\mathcal{R}, t) \delta\vec{\rho}_0(\mathcal{R}, \delta t) \}_{\mathcal{R}} \rangle_c + \langle \{ \{ P_1(b, v, \Omega, \delta t) P(\mathcal{R}, t) \delta\vec{\rho}_1(b, v, \Omega, \mathcal{R}, \delta t) \}_{\mathcal{R}} \}_{bv\Omega} \rangle_c,$$

where $P_0(\delta t)$ is the probability of no collisions in time δt , $P(\mathcal{R}, t)$ is the probability density for a specific arrangement \mathcal{R} of all the atoms in the system - the position of the atoms will affect the radiative trapping of the system, $\delta\vec{\rho}_0(\mathcal{R}, \delta t)$ is the change in $\vec{\rho}$ in time δt if the atoms have the arrangement \mathcal{R} and no collisions occur in that interval, $P_1(b, v, \Omega, \delta t)$ is the probability density of one collision of type b, v, Ω in time δt , $\delta\vec{\rho}_1(b, v, \Omega, \mathcal{R}, \delta t)$ is the change in $\vec{\rho}$ in the time δt for the arrangement of atoms \mathcal{R} if one collision of type b, v, Ω occurs, $\{ \dots \}_{\mathcal{R}}$ is an intergral over all atom arrangements \mathcal{R} , $\{ \dots \}_{bv\Omega}$ is an intergral over all possible b, v, Ω , and $\langle \dots \rangle_c$ is an average over all possible collision histories up to time t . For small δt , $P_0 \approx 1$. Integrating Eq. (148) for a time between t and $t + \delta t$, and substituting in above, one obtains

$$\begin{aligned} [\delta\vec{\rho}(t)]_{\text{av}} = & \langle \{ P(\mathcal{R}, t) [\exp(-\gamma_{a,b} \delta t) (\exp[-\gamma_{a,s} \delta t \\ & + \int_t^{t+\delta t} H(r, t') dt')_+ - 1] \vec{\rho}(t) \}_{\mathcal{R}} \rangle_c + \langle \{ \{ P_1(b, v, \Omega, \delta t) P(\mathcal{R}, t) \\ & \times [(\exp\{ \int_t^{t+\delta t} [-\gamma_{a,b} - \gamma_{a,s} + H(r, t') + H(c, b, v, \Omega, t')] dt')_+ - 1] \vec{\rho}(t) \}_{\mathcal{R}} \}_{bv\Omega} \rangle_c, \end{aligned} \quad (149)$$

where $(\dots)_+$ represents a time-ordered product. We can neglect the factor $-\gamma_{a,b} - \gamma_{a,s} + H(r, t')$ in the exponential with $H(b, v, \Omega, t')$ since it will contribute terms of order $(\delta t)^2$ only. Using an assumption of the impact theory, $\gamma_{a,b} \delta t \ll 1$, and forming the sum of elements needed in Eq. (143) from Eq. (149), one is led to the equation

$$\begin{aligned} \sum_i [\delta\rho_{im; im'}(t)]_{\text{av}} = & -\gamma_{a,b} \delta t \sum_i \langle \rho_{im; im'}(t) \rangle_c \\ & + \langle \{ P(\mathcal{R}, t) \sum_i \{ [(\exp[-\gamma_{a,s} \delta t + \int_t^{t+\delta t} H(r, t') dt')_+ - 1] \vec{\rho}(t) \}_{im; im'} \}_{\mathcal{R}} \rangle_c \\ & + \langle \{ P_1(b, v, \Omega, \delta t) \sum_i \{ [(\exp\{ \int_t^{t+\delta t} H(b, v, \Omega, t') dt')_+ - 1] \vec{\rho}(t) \}_{im; im'} \}_{bv\Omega} \rangle_c. \end{aligned} \quad (150)$$

The first term on the right-hand side represents the change in $\vec{\rho}$ in a time δt due to spontaneous emission from state a to b , the second term the change in $\vec{\rho}$ due to spontaneous emission and radiation trapping effects associated with states a and s , and the third term the change in $\vec{\rho}$ due to collisions.

As we have seen in Sec. III,

$$\begin{aligned} \langle \{ P_1(b, v, \Omega, \delta t) [(\exp\{ \int_t^{t+\delta t} H(b, v, \Omega, t') dt')_+ - 1] \vec{\rho}(t) \}_{bv\Omega} \rangle_c \\ = \{ P_1(b, v, \Omega, \delta t) [(\exp\{ \int_t^{t+\delta t} H(b, v, \Omega, t') dt')_+ - 1] \}_{bv\Omega} \langle \vec{\rho}(t) \rangle_c, \end{aligned} \quad (151)$$

i. e., each collision is independent of the past history.

The treatment of the first term of Eq. (149) is not so simple. Since the arrangement of atoms is a continuously varying function of time, $\vec{\rho}(t)$ will be affected by radiative trapping in a continuous manner [as opposed to the discrete changes in $\vec{\rho}(t)$ caused by collisions]. Thus, the fractional change in $\vec{\rho}(t)$ in the time δt will always be somewhat correlated with $\vec{\rho}(t)$, making the averaging of the first term of Eq. (149) quite difficult.

One can better understand the problem by studying the simpler equation $\dot{X}(b, t) = -\Gamma(b, t)X(b, t)$, where b is some parameter to be averaged over. It can be shown that, for fixed b , if $\Gamma(b, t)$ varies rapidly in a time much less than $\langle \Gamma(b, t) \rangle^{-1}$, then $\langle X(b, t) \rangle \approx -\langle \Gamma(b, t) \rangle \langle X(b, t) \rangle$. The average in these equations is over the parameter b for some fixed t . The rapid time variation of $\Gamma(b, t)$ minimizes the correlation between

$\Gamma(b, t)$ and $X(b, t)$.

Applying this idea to Eqs. (148) and (149), we see that if $H(r, t)$ is rapidly varying compared with $(\gamma_{a, s})^{-1}$, we shall have⁷⁷

$$\begin{aligned} & \langle \{P(\mathcal{R}, t)[(\exp\{-\gamma_{a, s} \delta t + \int_t^{t+\delta t} H(r, t') dt'\})_+ - 1] \vec{\rho}(t) \}_{\mathcal{R}} \rangle_c \\ &= \{P(\mathcal{R}, t)[(\exp\{-\gamma_{a, s} \delta t + \int_t^{t+\delta t} H(r, t') dt'\})_+ - 1]\}_{\mathcal{R}} \langle \vec{\rho}(t) \rangle_c. \end{aligned} \quad (152)$$

A study of Eq. (145) will indicate that $H(r, t)$ will change significantly in a time t_γ such that $k_0 t_\gamma v \gg 2\pi$, where v is an average relative speed of the atoms. We obtain the validity condition for Eq. (152) by also requiring $t_\gamma \ll (\gamma_{a, s})^{-1}$ and find it to be

$$k_0 v \gg 2\pi \gamma_{a, s} \quad (153a)$$

which, in effect, shows that Eq. (152) is valid if the Doppler width \gg natural width. An alternate form of Eq. (153) is

$$v(\gamma_{a, s})^{-1} \gg \lambda_0, \quad (153b)$$

which requires the perturber to travel a distance equal to the resonant radiative wavelength λ_0 in a time much less than the inverse partial decay rate of the resonant transition. For the case of lead, $\lambda_0 = 2833 \text{ \AA}$, $v \approx 4.0 \times 10^4 \text{ cm sec}^{-1}$, and $(\gamma_{a, s})^{-1} \approx 2.0 \times 10^{-8} \text{ sec}$ so that condition (153b) is approximately satisfied.

The quantities

$$\begin{aligned} & (\delta t)^{-1} \{P(\mathcal{R}, t)[(\exp\{-\gamma_{a, s} \delta t + \int_t^{t+\delta t} H(r, t') dt'\})_+ - 1]\}_{\mathcal{R}} \\ \text{and } & (\delta t)^{-1} \{P_1(b, v, \Omega, \delta t)[(\exp\int_t^{t+\delta t} H(b, v, \Omega, t') dt')_+ - 1]\}_{bv\Omega} \end{aligned}$$

represent the average scattering matrix elements for radiation and collisions, respectively. Using this fact and Eqs. (151) and (152), Eq. (150) may be written

$$\langle \sum_i \dot{\rho}_{im; im'} \rangle_c = -\gamma_{a, b} \langle \sum_i \rho_{im; im'} \rangle_c + \sum_{pp'} \{ [S(\text{rad})_{mm'}^{pp'} + S(\text{col})_{mm'}^{pp'}] \langle \sum_i \rho_{ip; ip'} \rangle_c \}, \quad (154)$$

where the $S(\text{col})_{mm'}^{pp'}$ are given in Table I. On expanding the density-matrix elements in terms of irreducible tensor components using

$$\sum_i \rho_{im; im'}^i = \sum_{KQ} (-1)^{1-m'} \begin{bmatrix} 1 & 1 & K \\ m & -m' & Q \end{bmatrix} \sum_i \rho_{KQ}^i,$$

one obtains the rate equations

$$\langle \sum_i \dot{\rho}_{KQ}^i \rangle_c = -[\gamma_{a, b} + \Gamma_K(\text{rad}) + \Gamma_K(\text{col})] \langle \sum_i \rho_{KQ}^i \rangle_c, \quad (155)$$

where the collisional $\Gamma_K(\text{col})$ are given in Eqs. (45). Equations (154) and (155) show that, on the average, radiative and collision effects are independent. This is true only because of the assumption that the relative orientation of perturbers and emitters is rapidly changing; thus, any correlations between radiative and collisional effects are quickly forgotten.

Using Eqs. (143), (154), and (155), we arrive at the Hanle-effect line shape

$$I(\hat{k}\lambda) = C'' \sum_{mm', KQ} \frac{H_{b, \vec{k}, \lambda; m}^r H_{b, \vec{k}, \lambda; m'}^{r*} (-1)^{1-m'} \begin{bmatrix} 1 & 1 & K \\ m & -m' & Q \end{bmatrix} \sum_i \rho_{KQ}^i(0)}{i\omega_{mm'} + [\gamma_{a, b} + \Gamma_K(\text{rad}) + \Gamma_K(\text{col})]} \quad (156)$$

This equation is similar in form to the corresponding Eq. (137) of the nonresonant broadening case, and the comments following it still apply. In attempting a comparison with experimental results in Sec. IX, we shall use the values of $\Gamma_K(\text{rad})$ given in Eqs. (141). It should be noted that Happer and Saloman⁴⁸ used an equation equivalent to Eq. (156) in analyzing their experimental results.

An alternate method of observing resonant collision broadening phenomena has been attempted by Omont and Meunier.³¹ They considered the emitter-perturber structure shown in Fig. 11 which corresponded to the case of a Hg emitter perturbed by other Hg isotopes. Here, if $\Delta\omega = (\omega_a - \omega_s) - (\omega_{a'} - \omega_{s'})$ satisfies

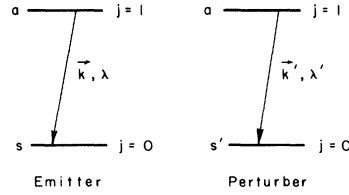


FIG. 11. Emitter and perturber atomic structures pertinent to resonant broadening of one element by its isotopes. One observes the \vec{k}, λ radiation which is untrapped. If a perturber becomes excited as a result of a collision, the \vec{k}', λ' radiation it emits will be completely trapped.

the inequalities Doppler broadening $\ll |\Delta\omega| \ll$ inverse collision time, the emitter radiation is never trapped and collision effects are as before. Since the emitter radiation is not trapped one need only follow emitter atoms in this case. It can be shown that the line shape will be given by

$$I(\hat{k}\lambda) = C' \sum_{mm', KQ} \frac{H_{s, \vec{k}_0\lambda; m}^{\gamma} H_{s, \vec{k}_0\lambda; m}^{\gamma*} (-1)^{1-m'} \begin{bmatrix} 1 & 1 & K \\ m & -m' & Q \end{bmatrix} \rho_{KQ}^{(0)}}{i\omega_{mm'} + [\gamma_{a,s} + \Gamma_K^I(\text{col})]}, \quad (157)$$

where ρ_{KQ} is the emitter density matrix, and the $\Gamma_K^I(\text{col})$ are the average collision multipole decay constants of the initially excited atoms given in Eqs. (45).

B. Spectral Profiles

Again we consider the structure shown in Fig. 10 with level a now taken as degenerate. The spectral profile is given by Eq. (142) averaged over all histories which, after a simple change of variable, becomes

$$I_{ab}(\vec{k}\lambda) = 2\hbar^{-2} \sum_i \sum_{mm'} \text{Re} \int_0^\infty d\tau \exp\{i(\omega_k - \omega_{ab})\tau\} H_{b, \vec{k}\lambda; m}^{\gamma} H_{b, \vec{k}\lambda; m'}^{\gamma*} \times \int_0^\infty dt \langle \exp[-i\vec{k} \cdot [\vec{R}_i(t_0 + \tau) - \vec{R}_i(t_0)]] b_{im}(t_0 + \tau) b_{im}^*(t_0) \rangle_c. \quad (158)$$

Neglecting all velocity effects, we are left with the problem of evaluating the correlation function

$$\varphi_{mm'}(t_0, \tau) = \sum_i \varphi_{im; im'}(t_0, \tau) = \langle \sum_i b_{im}(t_0 + \tau) b_{im}^*(t_0) \rangle_c. \quad (159)$$

In order to understand the nature of the correlation function, one must look at the physical processes involved. Initially, an atom is excited, which then decays to either state b or state s . If it decays to state b , the radiation is observable, but if the decay is to state s , the radiation is absorbed by some other atoms which repeat the decay process. Each atom that receives excitation through radiation trapping or collisions acts as a newly excited atom; the density matrix of the newly excited atom contains information on the orientation of its exciter, but this is not especially relevant in calculating the correlation function $\varphi_{mm'}(t_0, \tau)$. However, since the population of level b remains unchanged in all transfers of excitation, no information on the electric dipole moment associated with states a and b can be exchanged; this condition is reflected in the correlation function by the absence of terms like $b_{im}(t_0 + \tau) b_{jm}^*(t_0)$ for $i \neq j$.

The observed spectral intensity is given as a sum of the individual contributions from each atom. (In Hanle-effect experiments, we were interested in the orientation of the excited-state population of the entire ensemble.) In Sec. III, where the case of collisions only was considered, we found that the average electric dipole moment of the initially excited atoms followed a simple exponential decay. This occurred because it was highly unlikely for an excited atom to become deexcited in a collision and then undergo a collision with another excited atom. The situation with respect to radiation transfer is not so simple. When the average separation of the atoms is on the order of or less than the resonant radiative wavelength, the decay rate for a specific atom is not the same as that for an isolated one. The emitter atom will, in general, decay with a linear superposition of several decay modes characterizing the emitter-perturber system. Consider, however, the case when the emitter-perturber separation remains less than or equal to a distance on the order of the resonant radiative wavelength only for times much less than the lifetime of the emitter. In that case, the perturbers have only a small probability of excitation and, in return, can have little effect on the emitter. Thus, the radiative decay of a given emitter will be unaffected by the resonant transfer process as long as the atoms are moving fast enough. This means that the perturber must cover a distance of the radiative wavelength in a time much less than the emitter lifetime. That is, one requires

$$\lambda_0/v \ll (\gamma_{a,s})^{-1},$$

which is the same condition stated in Eq. (153b). Thus, condition (153b) leads to relatively simple results in line-shape calculations for both spectral profiles and polarization effects.

If we assume Eq. (153b) to hold, then, following the procedure of Sec. VII, it is easy to show that

$$\begin{aligned} \varphi_{mm'}(t_o, \tau) &= \varphi_{mm'}(t_o, 0) \exp\left[-\frac{1}{2}[\gamma_{a,b} + \gamma_{a,s} + 2\Gamma_{ab}^I(\text{col})]\tau\right] \\ &= \langle \sum_i \rho_{im; im'}(t_o) \rangle_c \exp\left[-\frac{1}{2}[\gamma_{a,b} + \gamma_{a,s} + 2\Gamma_{ab}^I(\text{col})]\tau\right], \end{aligned} \quad (160)$$

where $\Gamma_{ab}^I(\text{col})$ is the average collisional electric-dipole decay constant for initially excited atoms given in Eq. (48). Combining Eqs. (158)–(160), one obtains the equation for the spectral profile as

$$I_{ab}(\vec{k}\lambda) = \frac{\hbar^{-2}[\gamma_{a,b} + \gamma_{a,s} + 2\Gamma_{ab}^I(\text{col})] \sum_{mm'} H_{b, \vec{k}\lambda; m}^r H_{b, \vec{k}\lambda; m'}^{r*} \sum_i \int_0^\infty dt_o \langle \rho_{im; im'}(t_o) \rangle_c}{(\omega_k - \omega_{ab})^2 + [\frac{1}{2}(\gamma_{a,b} + \gamma_{a,s}) + \Gamma_{ab}^I(\text{col})]^2}. \quad (161)$$

To further reduce Eq. (161), we must expand $\langle \sum_i \rho_{im; im'}(t_o) \rangle_c$ in terms of its irreducible components. Then, using Eq. (154), we can write the numerator of Eq. (161) as

$$\begin{aligned} &\hbar^{-2}[\gamma_{a,b} + \gamma_{a,s} + 2\Gamma_{ab}^I(\text{col})] \sum_{mm', KQ} H_{b, \vec{k}\lambda; m}^r H_{b, \vec{k}\lambda; m'}^{r*} [\gamma_{a,b} + \Gamma_K(\text{rad}) \\ &+ \Gamma_K(\text{col})]^{-1} (-1)^{1-m'} \begin{bmatrix} 1 & 1 & K \\ m - m' & Q & \end{bmatrix} \sum_i \rho_{i, KQ}^i(0). \end{aligned}$$

This term can be averaged over initial conditions. We shall assume that the excitation is unpolarized which is equivalent to taking

$$\langle \sum_i \rho_{i, KQ}^i(0) \rangle_{\text{initial}} = (\sqrt{3})^{-1} \delta_{K0} \delta_{Q0}.$$

With this initial polarization, Eq. (161) for the spectral profile, averaged over initial conditions, becomes

$$\langle I_{ab}(\vec{k}\lambda) \rangle_{\text{initial}} = \frac{\frac{1}{3} \hbar^{-2} [\gamma_{a,b} + \gamma_{a,s} + 2\Gamma_{ab}^I(\text{col})] (\gamma_{a,b})^{-1} \sum_m |H_{b, \vec{k}\lambda; m}^r|^2}{[\omega_k - \omega_{ab}]^2 + [\frac{1}{2}(\gamma_{a,b} + \gamma_{a,s}) + \Gamma_{ab}^I(\text{col})]^2}, \quad (162)$$

where we have used $\Gamma_0(\text{rad}) = \Gamma_0(\text{col}) = 0$. This intuitive result is valid only when condition (153b) is met. Had we included velocity effects but neglected recoil, the line shape would have been a Voigt profile.

Finally, we wish to consider the emitter-perturber structure shown in Fig. 8 which has been used by several experimentalists.^{42, 45, 49, 53} The radiation between states b and a is observed while that between states a and s is completely trapped. In this case, the spectral profile will be given by the probability of finding any atom excited in level a and a photon of type \vec{k}, λ present. Explicitly, the profile is given by

$$I_{ba}(\vec{k}\lambda) = \langle \sum_i \sum_m \rho_{im, \vec{k}\lambda; im, \vec{k}\lambda}(\infty) \rangle_c.$$

Under the same assumptions that were used above, including condition (153a) and neglecting velocity and recoil effects, it is a straightforward matter to calculate the spectral profile as

$$I_{ba}(\vec{k}\lambda) = \frac{\hbar^{-2}[\gamma_{b,a} + \gamma_{a,s} + 2\Gamma_{ba}^I(\text{col})] (\gamma_{b,a})^{-1} \sum_m |H_{m, \vec{k}\lambda; b}^r|^2}{[\omega_k - \omega_{ba}]^2 + [\frac{1}{2}(\gamma_{b,a} + \gamma_{a,s}) + \Gamma_{ba}^I(\text{col})]^2}. \quad (163)$$

Due to the assumption of Eq. (153b), radiation trapping plays no role in this result.

C. Laser Phenomena

A typical laser structure is shown in Fig. 12 with the assumed laser action between levels a and b . In general, the oscillator strength between

level a and the ground state s is so small that resonant broadening and transfer effects are unimportant; the resonant perturbers, in essence, act like foreign-gas broadeners. However, if resonant effects were significant, one could use the re-

tory.

The numerical results of Omont and Meunier, carried out along lines similar to those presented here, appeared while this work was in progress. As can be seen in Table III, the agreement, in general, is excellent. It appears, however, that some error has been made in their calculation of Δ_g . Actually, the quoted values are not those given in the work of Omont and Meunier, but rather those of Omont's thesis²⁶ which employed the same asymptotic average values as those used in this work (see Appendixes A and C). The asymptotic average values represent the values of decay parameters averaged over impact parameter for close collisions. These values are dependent upon the form of the interaction and the path of the perturber. Omont has argued that since one cannot properly describe close collisions, the use of intuitive or equipartition values is justified. These intuitive values were obtained on the assumption that after each strong collision, on the average, it is equally likely to find the emitter in any of its magnetic substates. Equivalently, each strong collision, on the average, is assumed to produce equipartition. Based on these asymptotic average values, Omont and Meunier produced the results given in Ref. 31, which differ only by a few percent from those given in Table III.

We do not feel that the equipartition values have a sound theoretical basis although their use results in only slight numerical differences. All one can expect strong collisions to do is to produce a rapid rate of approach to equipartition. There is no *a priori* reason to believe that the effect of an average strong collision will also be to produce equipartition. For a dipole-dipole interaction and straight-line paths, this is definitely not the case (see Appendixes A and C) and will probably not be the case for the actual total interaction.

Indeed, the use of equipartition values will tend to lower the value of Γ_1/Γ_2 which leads to poorer agreement between theory and experiment in both the resonant and nonresonant cases. In summary, we feel that it is as good, if not better, to use the straight-line path dipole-dipole asymptotic average values than the equipartition ones. This will be true especially for resonant collisions where the use of the dipole-dipole interaction and straight-line paths is still valid for a large range of close collisions (collisions with impact parameter less than the optical collisions radius).

Of the approximate methods displayed, Omont's results¹⁰ (his approximation No. 2) give the best values. This method involves using the perturbation values of the parameters for distant impacts and the asymptotic average values for close impacts, with both solutions extended to join in the intermediate impact region. Omont used the equipartition asymptotic average values for strong collisions and this method gave agreement within 10%

of the exact results. Had the correct asymptotic average values been employed, the agreement would have been much worse (up to 34% deviation). Thus, an accidental choice of asymptotic average values leads to better agreement than the correct one. Some other choice may yield even better agreement, but it should be clear that cutoff procedures in the resonant case have little basis without a comparison with the numerically integrated results. Another approximate technique involving the neglect of noncommutativity^{8, 10, 31} leads to errors which average $\approx 15\%$ ($\approx 40\%$ error in Γ_1/Γ_2). It appears that the numerical integration procedure can not be bypassed if one desires reasonable accuracy in the results.

Experiments on resonant broadening provide satisfactory corroboration of the theory. Direct observation of spectral line profiles, using atomic structures similar to that in Fig. 8, have provided empirical values for the collision width $2\Gamma_{ab}$. The collision width is twice the average electric-dipole decay parameter. To conform with the notation of Kuhn and Vaughan,³⁸ we use the relationship $\lambda^3\gamma_{a,s} = \frac{8}{3}\pi^2 r_0 c \lambda f_{as}$ to rewrite Eq. (48)

$$\Gamma_{ab} = 4.82\mathfrak{R}\left[\frac{1}{6}(r_0 c f_{as} \lambda)\right], \quad (164)$$

where f_{as} is the average oscillator strength from the $j=1$ state to the ground state, and r_0 is the classical radius of the electron. The collision width of the line in Hz is given by

$$2\Gamma_{ab}/2\pi = K\mathfrak{R}\left[\frac{1}{6}(r_0 c \lambda f_{as})\right], \quad (165)$$

with $K=1.5$. Theoretical values for K are as follows:

Vdovin and Galitskii ²⁸	$1.48 \pm 2\%$,
Kazantsev ¹⁵	$1.54 \pm ?$,
Meunier and Omont ³¹	$1.54 \pm ?$,
This work	$1.54 \pm 1\%$.

The error in Kasantsev's and Omont and Meunier's work is probably 1–2%, so it appears that their values are in excellent agreement with the present calculation, but that the results of Vdovin and Galitskii differ somewhat. Several authors^{45, 49, 53} have used a value $K=1.44$ based on theoretical values for Γ_0 rather than Γ_{ab} .

Several measurements of Γ_{ab} in rare-gas resonant broadening have been made.^{42, 45, 49, 53} Resonant collisions have large optical collision diameters ($> 20 \text{ \AA}$) so that the dipole-dipole interaction is probably valid. Experiments have shown that collision widths are not affected by temperature, and negligible shifts have been observed for resonant transitions with appreciable oscillator strengths. In addition, when the lower level is the resonant one, the collision width was found to be independent of the upper level of the transitions, in agreement with theory. Using the experimental

values for the collision widths and our value of $K=1.54$ in Eq. (164), we can calculate the oscillator strengths of various transitions which have been examined experimentally. The results are given in Table IV along with some theoretical and empirical determinations of these strengths. In all these experiments, it is the lower level which is broadened by resonant collisions. The errors in our values of f are due basically to errors in measured widths. Except for the case of krypton, the results are in good agreement with theory and other experimental determinations.

The above experiments have yielded some interesting side results. The stated experimental values of Γ_{ab} were obtained after an analysis of the spectral profile in terms of Voigt functions had been made. We have already noted that velocity and recoil effects might lead to a modification of the Voigt profile. For the cases studied, such deviations were not appreciable.⁷⁹ The values of Γ_{ab} were obtained by finding the slope of the curve of Lorentzian width versus pressure, and the good agreement with theory indicates that the many-mode effects which were discussed in Sec. VIII

TABLE IV. Calculated values for oscillator strengths. These values were obtained by using the theory in conjunction with resonant broadening experimental results.

Element	Observed transitions	Observed broadening ^a	Resonant transition	Calculated oscillator strength	Other determinations	
					Experimental	Theoretical
He	$3^1S_0 \rightarrow 2^1P_1$	2.5 ± 0.15^b	$2^1P_1 \rightarrow 1^1S_0$	0.260 ± 0.016	0.26 ± 0.12^c	0.2761 ± 0.0001^g
					0.31 ± 0.04^d	
Ne	$2p_1 \rightarrow 1^1P_1$	1.89 ± 0.08^h	$1^1P_1 \rightarrow 1^1S_0$	0.158 ± 0.006	0.26 ± 0.07^e	$0.14 \pm ?^j$
	$2p_6 \rightarrow 1^1P_1$				0.16 ± 0.014^i	0.12 ± 0.02^k
	$2p_4 \rightarrow 1^1P_1$					
Ar	$3p^5(^2P_{1/2})4p[\frac{1}{2}]_1 \rightarrow 3^3P_1$	0.90 ± 0.16^l	$3^3P_1 \rightarrow 1^1S_0$	0.057 ± 0.009	0.273 ± 0.011^f	0.05 ± 0.01^m
	$3p^5(^2P_{3/2})4p[\frac{1}{2}]_0 \rightarrow 3^3P_1$				$0.075 \pm ?^j$	
Ar	$3p^5(^2P_{1/2})4p[\frac{1}{2}]_1 \rightarrow 1^1P_1$	4.53 ± 0.22^n	$1^1P_1 \rightarrow 1^1S_0$	0.266 ± 0.013		0.20 ± 0.04^m
	$3p^5(^2P_{3/2})4p[\frac{1}{2}]_0 \rightarrow 1^1P_1$				$0.15 \pm ?^j$	
Kr	$4p^5(^2P_{3/2})5p[\frac{1}{2}]_0 \rightarrow 3^3P_1$	3.78 ± 0.21^o	$3^3P_1 \rightarrow 1^1S_0$	0.189 ± 0.011	0.159 ± 0.01^p	$0.20 \pm ?^j$
Kr	$4p^5(^2P_{1/2})5p[\frac{1}{2}]_0 \rightarrow 1^1P_1$	3.24 ± 0.15^o	$1^1P_1 \rightarrow 1^1S_0$	0.172 ± 0.008	$0.166 \pm ?^q$	$0.20 \pm ?^j$
Xe			$3^3P_1 \rightarrow 1^1S_0$		0.28 ± 0.05^r	$0.28 \pm ?^j$
					0.27 ± 0.02^s	
					0.256 ± 0.008^t	
Xe			$1^1P_1 \rightarrow 1^1S_0$		0.25 ± 0.05^r	$0.25 \pm ?^j$
					0.26 ± 0.02^s	
					0.238 ± 0.15^t	

^aBroadening in units of 10^{-9} Hz(atoms/cm³)⁻¹.

^bReference 45.

^cF. A. Korolyov and V. I. Odintsov, Opt. i Spektroskopiya **18**, 968 (1964) [English transl.: Opt. Spectry. (USSR) **18**, 547 (1965)].

^dJ. Geiger, Z. Physik **175**, 530 (1963).

^eR. Lincke and H. R. Griem, Phys. Rev. **143**, 66 (1966).

^fW. L. Williams and E. S. Fry, Phys. Rev. Letters **20**, 1335 (1968); Phys. Rev. (to be published).

^gB. Schiff and C. L. Pekeris, Phys. Rev. **134**, A638 (1964).

^hReference 49.

ⁱF. A. Korolyov and V. I. Odintsov, Opt. i Spektroskopiya **16**, 555 (1964) [English transl.: Opt. Spectry. (USSR) **16**, 304 (1964)].

^jP. F. Gruzdev, Opt. i Spektroskopiya **22**, 313 (1967) [English transl.: Opt. Spectry. (USSR) **22**, 170 (1967)].

^kA. Gold and R. Knox, Phys. Rev. **113**, 834 (1959).

^lReference 42 modified to include a small nonresonant effect (see Ref. 24).

^mR. Knox, Phys. Rev. **110**, 375 (1958).

ⁿReference 42.

^oReference 53.

^pP. G. Wilkinson, J. Quant. Spectry. Radiative Transfer **5**, 503 (1965).

^qR. Turner, Phys. Rev. **140**, A426 (1965).

^rG. I. Chaschina and E. Y. Shreider, Opt. i Spektroskopiya **20**, 511 (1966) [English transl.: Opt. Spectry. (USSR) **20**, 283 (1965)].

^sP. G. Wilkinson, J. Quant. Spectry. Radiative Transfer **6**, 823 (1966).

^tD. K. Anderson, Phys. Rev. **137**, A21 (1965).

have either saturated or are very slowly varying over the pressure regions studied.

The value of Γ_{ab} determines a value for the natural width of the resonant transition through Eq. (165). However, an extrapolation to zero pressure in the above experiments produced values of the natural width which were 1.3–1.6 times that of the prediction. Kuhn, Vaughan, and Stacey⁸⁰ tried to explain this residual-width anomaly by the many-mode effect, attributing a larger decay parameter to the dominant decay mode. Zaidi,³² using a photon propagator approach, made an estimate of this effect. Using his calculation, we found that, at most, a residual width equal to 0.1, the natural width, could be attributed to the many-mode effect. This result, in addition to the discussion of Sec. VIII which showed that many-mode effects should be small when Doppler width \gg natural width, leads one to doubt the above explanation of residual widths. However, if no such residual widths are found in similar experiments on foreign gas broadening, one must conclude that either radiative transfer or recoil mechanisms are producing effects nonlinear in the pressure at very low density.

A better check of the theory is afforded by Hanle-effect experiments where velocity and recoil effects do not influence the results. Table V shows the results of some of these experiments in comparison with our theoretical predictions. The errors in the theoretical values reflect experimental errors in determinations of the natural linewidth [recall that $\Gamma_K \propto \gamma_{a,s}$ from Eqs. (47)]. The results of Happer and Saloman⁴⁸ from the resonant experiment in lead are in excellent agreement with theory. At the pressures considered, the radiative Γ 's of Eqs. (141) seem to provide good agreement with experiment. The different theoretical values quoted are based on different empirical values for the natural width. The larger value, from the work of de Zafra and Marshall⁸¹

is probably the better choice. Omont and Meunier³¹ observed the resonant broadening of a given isotope of Hg by other of its isotopes, reflecting the situation shown in Fig. 11. The difference in the transition frequencies of the isotopes is large enough to prevent resonant trapping, yet small enough to allow for all the phenomena of resonant broadening. By measuring the radiation from one isotope only, they obtained the quantities pertinent to the decay of ρ^I . The quoted values represent the average value of Hg₂₀₂ broadened by Hg₂₀₄, Hg₂₀₀ broadened by Hg₂₀₂, and Hg₂₀₀ broadened by Hg₂₀₄. Again the agreement with theory is good.

In summary, we feel that resonant broadening phenomena is adequately explained by the theory. The use of condition (153b) to simplify the theory seems to be justified, as does the use of the radiative decay parameters given in Eqs. (140) and (141) at the pressures under consideration.

B. Nonresonant Case

As far as we know, all previous treatments of nonresonant broadening have employed some form of cutoff approximation. Byron and Foley⁸ and Omont¹⁰ have treated the problem using cutoff procedures and an approximation to the van der Waals constant.

The results of several approximate methods are given in Table VI. Methods 1 and 2 represent cutoff procedures using equipartition and correct asymptotic average values, respectively. Again we see that use of the incorrect equipartition values leads to better agreement. Method 3 represents a calculation neglecting noncommutativity, and we see that although it provides excellent accuracy for γ_{ab} and Δ_{ab} , the value of Γ_1/Γ_2 is 50% off. Again it is somewhat unclear if any approximate techniques can be used with confidence, since their validity is established only after a comparison with the numerical results.

TABLE V. Comparison of theoretical and experimental values for resonant broadening parameters in units of 10^{-9} sec⁻¹ (atoms/cm³)⁻¹.

Parameter	Emitter	Perturber	Observed transitions	Resonant transition	Experimental results	Theoretical results
Γ_2/\mathfrak{N}	Pb ₂₀₈	Pb ₂₀₈	$^3P_1 \rightarrow ^3P_1$		38 ± 8^a	30.5 ± 3.6^b
			$^3P_1 \rightarrow ^3P_2$	$^3P_1 \rightarrow ^3P_0$		35.5 ± 5.4^c
Γ_1/Γ_2	$\left\{ \begin{array}{l} \text{Hg}_{202} \\ \text{Hg}_{200} \\ \text{Hg}_{200} \end{array} \right.$	$\left\{ \begin{array}{l} \text{Hg}_{204} \\ \text{Hg}_{202} \\ \text{Hg}_{204} \end{array} \right.$	$^3P \rightarrow ^1S_0$	$^3P_1 \rightarrow ^1S_0$	1.21 ± 0.05^a	1.21 ± 0.02
Γ_1^I/\mathfrak{N}					3.77 ± 0.40^d	4.03 ± 0.08^e
Γ_2^I/\mathfrak{N}					3.88 ± 0.40^d	4.08 ± 0.08^e
Γ_1^I/Γ_2^I					0.95 ± 0.03^d	0.966 ± 0.012

^aReference 48, error approximated from graph.

^bValue of $\gamma_{a,s}$ used in calculation taken from Ref. 48.

^cValue of $\gamma_{a,s}$ used in calculation taken from Ref. 81.

^dReference 31.

^eValue of $\gamma_{a,s}$ used in calculation taken from Ref. 35.

TABLE VI. Values for nonresonant decay parameters in frequency units of $N|B|^{2/5} \langle v^{3/5} \rangle_v$.

Element	Method 1 ^a	Method 2 ^b	Method 3 ^c	Numerical results ^d
Γ_1^N	8.17	10.3	8.20	7.62
Γ_2^N	7.21	6.02	4.91	6.80
Γ_1^N/Γ_2^N	1.11	1.70	1.67	1.12
γ_{ab}^N	8.80	8.80	8.93	8.97
Δ_{ab}^N	5.80	5.80	6.48	6.51
$\Delta_{ab}^N/\gamma_{ab}^N$	0.661	0.661	0.726	0.726

^aCutoff procedure using equipartition strong values.

^bCutoff procedure using correct strong values.

^cNeglect of noncommutativity.

^dNumerical integration of the equations – this work.

Only recently have experiments been performed that can provide meaningful tests of the theory. The measurement of the temperature dependence of both shift and width by examination of spectral profiles shows that the $T^{3/10}$ variation predicted by theory does not hold in some cases.^{43, 54} Specifically, with krypton as the emitter, the collision parameters for He, Ne, and Ar as perturbers did not obey the $T^{3/10}$ prediction while that for Kr as a (foreign gas) perturber did obey it.⁵⁴ The result is somewhat surprising since the optical collision radii for He-Kr is 8.7 Å and that for Ar-Kr is 12 Å, while that for Kr-Kr is 14 Å. One might expect that recoil effects are distorting the results since the optical collision radii seem large enough to have the dipole-dipole interaction dominate.

In a Hanle-effect experiment on Hg perturbed by inert gases, it was found that the temperature dependence of decay parameters associated with Ar, Kr, and Xe collisions are consistent with a dipole-dipole interaction, while those with He and Ne are not.⁴⁷ Since the optical collision radius is 3.5 Å for He-Hg and 7.5 Å for Xe-Ar, these results are reasonable. That is, one must deal with higher multipoles and wave-function overlap in the He-Hg and Ne-Hg systems.

Equation (85) for the broadening parameter \mathcal{B}_a shows that a determination of the absolute magnitude of cross sections requires a complete knowledge of the atomic system. However, the ratio Γ_1^N/Γ_2^N should be independent of the structure of the system (assuming a pure dipole-dipole interaction). Measurement of Γ_1^N/Γ_2^N for foreign gas broadening of the $^3P_1(6s6p)$ state of Hg and the $^3P_1(5s5p)$ state of Cd have been made. The results are given in Table VII. Although there is fair agreement with the value of 1.12 ± 0.02 predicted by theory, it would seem that the dipole-dipole interaction is not entirely sufficient to explain nonresonant broadening. It is surprising to note that the values of Γ_1^N/Γ_2^N for Ar, Kr, and

Xe perturbing Hg differ considerably from theory, since an independent measurement⁴⁷ on temperature effects indicates that the dipole-dipole interaction might be valid for these cases. The inert gas – Cd collisions have a slightly larger optical cross section than inert gas – Hg collisions, which, in addition to the fact that Cd is a smaller atom than Hg, may partially explain the better agreement with theory for inert gas – Cd collisions.

An experiment involving the use of a Zeeman laser⁵² yielded the ratio $\Gamma_1^N/\Gamma_2^N = 1.28 \pm 0.03$ in fair agreement with theory. The parameters Γ_1^N and Γ_2^N are the broadening constants for the $2s_2(j=1)$ level of neon perturbed by both helium and neon. The Weisskopf radius for these collisions (in which both helium and neon act as nonresonant perturbers) is on the order of 3 Å, indicating that the dipole-dipole interaction is not a good approximation to the true interaction.

A more detailed explanation of nonresonant effects will not be attempted in this paper. There are several possibilities for improvement of the theory. Some authors have tried to fit data by a Lennard-Jones potential^{23, 24, 54}; however, the results are not overly sensitive to the form of the repulsive part of the interaction. One can also modify the results by putting in some phenomenological dependence on velocity⁴³ which would supposedly account for deviations from a pure dipole-dipole interaction at small impact parameter. A more detailed solution would involve a completely quantum-mechanical description of the collision at small impact parameter. Increased experimental research in the form of measurements of Γ_1^N/Γ_2^N would be useful, since theoretical values for this ratio can be predicted without a knowledge of the atomic parameters of the system. Additional experiments on the temperature dependence of shift and width would also be useful. Such experiments on systems known to interact primarily through the dipole-dipole interaction might prove useful in studying the effects of recoil on spectral profiles. Finally, it should be noted that if one desires to predict absolute magnitudes of cross sections, he is faced with the task of evaluating the

TABLE VII. Experimental values for Γ_1^N/Γ_2^N in foreign gas broadening. The theoretical value is 1.12 ± 0.02 .

Perturber	Hg ₂₀₂ emitter (Ref. 44)	Cd ₁₁₂ emitter (Ref. 50)
He	1.15 ± 0.07	1.15 ± 0.10
Ne	1.26 ± 0.12	1.12 ± 0.10
Ar	1.21 ± 0.06	1.16 ± 0.10
Kr	1.16 ± 0.03	1.12 ± 0.10
Xe	1.03 ± 0.08	1.14 ± 0.10

broadening parameters of Sec. V.

X. DISCUSSION

In the limit of a dipole-dipole interaction between neutral atoms and the impact approximation for pressure broadening, we have numerically determined the effects of collisions on spectral line characteristics. A comparison with the results of approximate methods has indicated that the accuracy of any method can be tested only after the exact numerical calculation has been made. We have found that two apparently reasonable methods, cutoff with correct asymptotic average values and neglect of noncommutativity, lead to considerable errors ($\approx 30\%$ or more) in many of the parameters.

In all of the experiments mentioned, the perturber density and width of line profiles satisfied the needed requirements for the validity of the impact approximation. It appears, however, that the pure dipole-dipole interaction is valid only for resonant and certain foreign gas collisions. The situation for nonresonant broadening is somewhat unclear at the present time. For example, the optical collision radii for Kr-Hg and Xe-Hg systems are 6.5 and 7.5 Å, respectively, yet the corresponding experimental ratios for magnetic dipole to electric quadrupole decay Γ_1^N/Γ_2^N are 1.16 ± 0.03 and 1.03 ± 0.08 . It is difficult to suggest a cause for such a variance.

One should note that we have neglected recoil effects which may be significant in the broadening problem.^{16, 17, 20, 28-30} The good agreement of theory and experiment for the broadening parameters in the resonant case does not rule out the possibility that recoil effects contribute significantly to the spectral profiles observed in nonresonant broadening. The importance of recoil effects in laser experiments, using realistic models, is still to be determined.⁸²

It is fairly easy to extend the theory to allow for transitions other than $j=1$ to $j=0$ and to allow for different interaction potentials.⁸³ In particular, one can solve for simultaneous resonant and nonresonant broadening of atomic levels; for this case the equations analogous to Eqs. (10) or (61) would be of an integrodifferential nature. Such calculations seem a bit premature at this time considering the experimental and theoretical uncertainties in foreign gas broadening which are still present.

APPENDIX A: RESONANT SOLUTION

In this appendix we shall find the explicit solutions of Eq. (15a). Following Dyakonov and Perel,⁹ we make the substitutions $\cos\theta = -vt/R$, $\sin\theta = b/R$, which transforms Eq. (15a) into

$$idS(\theta)/d\theta = V'(\theta)S(\theta), \quad S(0) = 1, \quad (\text{A1})$$

where V' is given by a modified form of Eq. (14)

with X , Y , and Z replaced by

$$\begin{aligned} X' &= \alpha(2\sin\theta - 3\cos^2\theta\sin\theta), \\ Y' &= 3(\sqrt{2})\alpha\cos\theta\sin^2\theta, \\ Z' &= 3\alpha\cos^2\theta\sin\theta, \end{aligned}$$

and the dimensionless quantity α is given by

$$\alpha = \frac{1}{6}(e^2 a_0^2 / \hbar) |T(s0, a1)|^2 (b^2 v)^{-1}. \quad (\text{A2})$$

Equation (A1) is equivalent to the three sets of equations

$$idS_{1m}^+ / d\theta = X'S_{1m}^+ + Y'S_{0m}^+ + Z'S_{-1m}^+, \quad (\text{A3a})$$

$$idS_{0m}^+ / d\theta = Y'S_{1m}^+ - 2X'S_{0m}^+ - Y'S_{-1m}^+, \quad (\text{A3b})$$

$$idS_{-1m}^+ / d\theta = Z'S_{1m}^+ - Y'S_{0m}^+ + X'S_{-1m}^+, \quad (\text{A3c})$$

where m can be 1, 0, or -1, and initial conditions are $S_{mm}^+(0) = \delta_{mm}$. Introducing new variables $S_m^+ = S_{1m}^+ + S_{-1m}^+$, $S_m^- = S_{1m}^- - S_{-1m}^-$, the above equations become

$$idS_m^+ / d\theta = (X' + Z')S_m^+, \quad (\text{A4a})$$

$$idS_m^- / d\theta = (X' - Z')S_m^- + 2Y'S_{0m}^+, \quad (\text{A4b})$$

$$idS_{0m}^- / d\theta = Y'S_m^- - 2X'S_{0m}^+, \quad (\text{A4c})$$

$$\begin{aligned} \text{with } S_1^+(\theta=0) &= S_{-1}^+(\theta=0) = -S_{-1}^-(\theta=0) \\ &= S_1^-(\theta=0) = S_{00}(\theta=0) = 1 \end{aligned}$$

$$\text{and } S_0^+(\theta=0) = S_0^-(\theta=0) = 0.$$

We seek solutions for $t = +\infty$, or equivalently for $\theta = \pi$.

Equation (A4a) integrates immediately to give

$$S_1^+(\pi) = S_{-1}^+(\pi) = e^{-4i\alpha}, \quad S_0^+(\pi) = 0. \quad (\text{A5})$$

The remaining equations must be solved numerically. One needs to solve the equations only for the cases $m=0, 1$ since it follows directly from Eqs. (A3):

$$\begin{aligned} S_{11}(\theta) &= S_{-1-1}(\theta), \quad S_{-11}(\theta) = S_{1-1}(\theta), \\ S_{01}(\theta) &= -S_{0-1}(\theta), \end{aligned} \quad (\text{A6})$$

and the numerical results yield

$$S_{-10}(\pi) = S_{01}(\pi). \quad (\text{A7})$$

The solution of Eqs. (A4b) and (A4c) will be considered for three regions of α .

Region I $0.0 \leq \alpha \leq 0.02$

In this region we obtain solutions by iteration. Constructing elements of T_{mm}, D, D' and S_{mm}, P, P' ,

as given by Eq. (23), one obtains the following results:

$$T_{11}^{-11}(b, v, \Omega_0) = -8\alpha^2 + O(\alpha^4),$$

$$T_{00}^{00}(b, v, \Omega_0) = -16\alpha^2 + O(\alpha^4),$$

$$T_{00}^{-11}(b, v, \Omega_0) = (\frac{2}{3})\pi^2\alpha^4 + O(\alpha^6),$$

$$T_{10}^{-10}(b, v, \Omega_0) = -12\alpha^2 + O(\alpha^4),$$

$$T_{11}^{-1-1}(b, v, \Omega_0) = 16\alpha^4 + O(\alpha^6),$$

$$S_{11}^{-11}(b, v, \Omega_0) = -4\alpha^2 + O(\alpha^4),$$

$$S_{00}^{00}(b, v, \Omega_0) = -9\pi^2\alpha^4 + O(\alpha^6),$$

$$S_{00}^{-11}(b, v, \Omega_0) = (\frac{2}{3})\pi^2\alpha^4 + O(\alpha^6),$$

$$S_{10}^{-10}(b, v, \Omega_0) = -20\alpha^2 + O(\alpha^4),$$

$$S_{11}^{-1-1}(b, v, \Omega_0) = 4\alpha^2 + O(\alpha^4),$$

$$W = -1 + \frac{1}{3}[T_{00}^{-11}(b, v, \Omega_0) + T_{11}^{-11}(b, v, \Omega_0)$$

$$+ T_{-1-1}^{-11}(b, v, \Omega_0)] = -\frac{16}{3}\alpha^2 + O(\alpha^4),$$

$$\Delta \equiv \frac{1}{3}[R_{00}^{-11}(b, v, \Omega_0) + R_{11}^{-11}(b, v, \Omega_0)$$

$$+ R_{-1-1}^{-11}(b, v, \Omega_0)] = O(\alpha^3).$$

Region II $0.02 \leq a \leq 4.9$

In this region, computer solutions of Eqs. (A4b) and (A4c) were obtained. The accuracy of these solutions, which was tested by halving the step size, was found to be on the order of 0.5%.

Region III $4.9 \leq a \leq \infty$

This region corresponds to impact parameter less than $\frac{1}{3}$ the Weisskopf radius.⁵⁵ For resonant broadening the approximation of a dipole-dipole interaction may begin to fail in this region. However, since the contribution from this region will account for only 3% of final values, this assumption of a dipole-dipole interaction throughout this region will lead to little additional error.

The behavior of a typical element as a function of α is shown in Fig. 13. The other elements behave similarly. At large α , the solutions are nearly periodic. The average value of the elements over a period in α was computed for the two regions; $\alpha = [3.4, 5.0]$ and $\alpha = [8.9, 10.5]$. The difference in values for these two regions was found

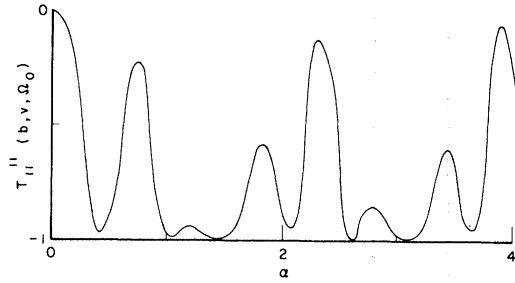


FIG. 13. Variation of the scattering matrix element $T_{11}^{-11}(b, v, \Omega_0)$ as a function of $\alpha = (e^2 a_0^2 / \hbar) (\frac{1}{b}) \times |T(s_0, a_1)|^2 (b^2 v)^{-1}$. For large α , $T_{11}^{-11}(b, v, \Omega_0)$ is nearly periodic with a period in α of ≈ 1.6 . The computer solution was extended to $\alpha = 10.5$.

to be negligible and we present these values as asymptotic average values. The asymptotic average values will be denoted by script letters $s_{mm'}^{pp'}(\Omega_0)$; for the resonant case these are given in Table VIII. These asymptotic average values may also be predicted analytically as is done in Appendix C. By using the technique given in Appendix D, one can perform an average over all collision orientations to obtain asymptotic average values $s_{mm'}^{pp'}$ which are independent of Ω_0 . These values are also given in Table VIII along with the quantities $s_{mm'}^{pp'}(eq)$ which would have been obtained if, on the average, a strong collision produced equipartition. One notes that, in general, $s_{mm'}^{pp'} \neq s_{mm'}^{pp'}(eq)$, i.e., an average strong collision does not produce equipartition as has been discussed in Sec. IX.

APPENDIX B: NONRESONANT SOLUTION

The calculation of Appendix A must be repeated for the foreign gas case. The equations corresponding to Eq. (61) of the text and analogous to Eqs. (A4) are

$$idM_m^+/d\theta = -(F+K)M_m^+, \quad (B1a)$$

$$idM_m^-/d\theta = (-F+K)M_m^- + 2GM_{0m}^-, \quad (B1b)$$

$$idM_{0m}^-/d\theta = GM_m^- - LM_{0m}^-, \quad (B1c)$$

$$M_1^+(0) = M_1^-(0) = M_{-1}^+(0)$$

$$= -M_{-1}^-(0) = M_{00}(0) = 1, \quad M_0^+(0) = M_0^-(0) = 0,$$

$$\text{where } M_m^+ = M_{1m}^+ + M_{-1m}^+, \quad M_m^- = M_{1m}^- - M_{-1m}^-,$$

$$F = 2\eta \sin^4\theta (2 + 3 \cos^2\theta), \quad G = 6(\sqrt{2})\eta \cos\theta \sin^5\theta,$$

$$K = 6\eta \sin^4\theta \cos^2\theta, \quad L = 4\eta \sin^4\theta (4 - 3 \cos^2\theta),$$

TABLE VIII. Asymptotic average values of resonant scattering matrix elements for close collisions. The argument Ω_0 indicates values of the elements for collisions with the standard geometry while an average over all collision orientations has been made to obtain the elements without argument. The argument eq indicates the values that would have been obtained if an average strong collision produced equipartition.

$\mathcal{T}_{00}^{00}(\Omega_0)$	\mathcal{T}_{00}^{00}	$\mathcal{T}_{00}^{00}(eq)$	$\mathcal{S}_{00}^{00}(\Omega_0)$	\mathcal{S}_{00}^{00}	$\mathcal{S}_{00}^{00}(eq)$
-0.50	$-\frac{23}{30}$	$-\frac{25}{30}$	0.00	$-\frac{8}{15}$	$-\frac{10}{15}$
$\mathcal{T}_{11}^{11}(\Omega_0)$	\mathcal{T}_{11}^{11}	$\mathcal{T}_{11}^{11}(eq)$	$\mathcal{S}_{11}^{11}(\Omega_0)$	\mathcal{S}_{11}^{11}	$\mathcal{S}_{11}^{11}(eq)$
-0.75	$-\frac{27}{30}$	$-\frac{25}{30}$	-0.50	$-\frac{12}{15}$	$-\frac{10}{15}$
$\mathcal{T}_{11}^{00}(\Omega_0)$	\mathcal{T}_{11}^{00}	$\mathcal{T}_{11}^{00}(eq)$	$\mathcal{S}_{11}^{00}(\Omega_0)$	\mathcal{S}_{11}^{00}	$\mathcal{S}_{11}^{00}(eq)$
0.00	$\frac{4}{30}$	$\frac{5}{30}$	0.00	$\frac{4}{15}$	$\frac{5}{15}$
$\mathcal{T}_{10}^{0-1}(\Omega_0)$	\mathcal{T}_{10}^{0-1}	$\mathcal{T}_{10}^{0-1}(eq)$	$\mathcal{S}_{10}^{0-1}(\Omega_0)$	\mathcal{S}_{10}^{0-1}	$\mathcal{S}_{10}^{0-1}(eq)$
0.00	$-\frac{4}{30}$	0.00	0.00	$-\frac{4}{15}$	0.00
$\mathcal{T}_{10}^{10}(\Omega_0)$	\mathcal{T}_{10}^{10}	$\mathcal{T}_{10}^{10}(eq)$	$\mathcal{S}_{10}^{10}(\Omega_0)$	\mathcal{S}_{10}^{10}	$\mathcal{S}_{10}^{10}(eq)$
-1.25	$-\frac{31}{30}$	$-\frac{30}{30}$	-1.50	$-\frac{16}{15}$	$-\frac{15}{15}$
$\mathcal{T}_{1-1}^{1-1}(\Omega_0)$	\mathcal{T}_{1-1}^{1-1}	$\mathcal{T}_{1-1}^{1-1}(eq)$	$\mathcal{S}_{1-1}^{1-1}(\Omega_0)$	\mathcal{S}_{1-1}^{1-1}	$\mathcal{S}_{1-1}^{1-1}(eq)$
-0.75	$-\frac{27}{30}$	$-\frac{30}{30}$	-0.50	$-\frac{12}{15}$	$-\frac{15}{15}$
$\mathcal{T}_{11}^{-1-1}(\Omega_0)$	\mathcal{T}_{11}^{-1-1}	$\mathcal{T}_{11}^{-1-1}(eq)$	$\mathcal{S}_{11}^{-1-1}(\Omega_0)$	\mathcal{S}_{11}^{-1-1}	$\mathcal{S}_{11}^{-1-1}(eq)$
0.25	$\frac{8}{30}$	$\frac{5}{30}$	0.50	$\frac{8}{15}$	$\frac{5}{15}$
	\mathcal{W}	$\mathcal{W}(eq)$		Δ	$\Delta(eq)$
	-1.00	-1.00		0.00	0.00

and the dimensionless quantity η is given by

$$\eta = B(b^5 v)^{-1}, \quad (\text{B2})$$

with B given by Eq. (63). We can solve Eq. (B1a) exactly to obtain

$$M_1^+(\pi) = M_{-1}^+(\pi) = e^{3i\pi\eta/2}, \quad M_0^+(\pi) = 0. \quad (\text{B3})$$

Equations (A6) and (A7) are also valid for the non-resonant M elements, so we are left with the problem of obtaining solutions of Eqs. (B1b) and (B1c) for the cases $m=0, 1$. Again the solutions are obtained in specific regions.

Region I $0.0 \leq \eta \leq 0.02$

Using perturbation theory in this region one obtains

$$M_{00}^{00}(b, v, \Omega_0) = O(\eta^4),$$

$$M_{00}^{11}(b, v, \Omega_0) = O(\eta^4)$$

$$M_{10}^{10}(b, v, \Omega_0) = -\frac{(369)}{64}\pi^2\eta^2 + O(\eta^4),$$

$$M_{11}^{-1-1}(b, v, \Omega_0) = \frac{(9)}{64}\pi^2\eta^2 + O(\eta^4),$$

$$M_{11}^{11}(b, v, \Omega_0) = -\frac{(9)}{64}\pi^2\eta^2 + O(\eta^4),$$

$$W' = -1 + \frac{1}{3}[M_{11}(b, v, \Omega_0) + M_{00}(b, v, \Omega_0) + M_{-1-1}(b, v, \Omega_0)] = 3\pi\eta i - \frac{(93)}{16}\pi^2\eta^2 + O(\eta^3).$$

We can also find the perturbation solutions for the case of lower-level broadening and additional virtual transitions. The equation of interest is

$$\begin{aligned} \delta\rho_{ms}(b, v, c)/\rho_{ms}(b, v, c) &\equiv W'' \\ &= -1 + \frac{1}{3}Q^*(b, v)\Phi(b, v)[\tilde{M}_{11}(b, v, \Omega_0) \\ &\quad + \tilde{M}_{00}(b, v, \Omega_0) + \tilde{M}_{-1-1}(b, v, \Omega_0)], \end{aligned} \quad (\text{B4})$$

which is Eq. (94). In the perturbation limit,

$$\begin{aligned} W'' &= \{\pi[\mathcal{R}_a + \frac{(27)}{2}\mathcal{R}_\varphi - 3\mathcal{R}_b][b^5 v]^{-1}\}i - \pi^2[\frac{(93)}{16}\mathcal{R}_a^2 \\ &\quad + \frac{(6561)}{8}\mathcal{R}_\varphi^2 + \frac{(81)}{2}\mathcal{R}_b^2 - 27\mathcal{R}_a\mathcal{R}_b + \frac{(243)}{2}\mathcal{R}_a\mathcal{R}_\varphi \\ &\quad - \frac{(729)}{2}\mathcal{R}_b\mathcal{R}_\varphi][b^5 v]^{-2} + O([b^5 v]^{-3}), \end{aligned} \quad (\text{B5})$$

where \mathcal{R}_a as given by Eq. (85) in the a -level

broadening parameter, \mathfrak{R}_b given by Eq. (89a) is the b -level broadening parameter, and $\mathfrak{R}_\varphi = \sum \times (\mathfrak{R}^G + \mathfrak{R}^D)$ with \mathfrak{R}^G and \mathfrak{R}^D given by Eqs. (73b) and (73') resulted from the additional phase contributions of the added virtual transitions. Thus, in a crude approximation, the shift will vanish when the coefficient of $[b^5v]^{-1}$ is zero and the width will have a minimum when the coefficient of $[b^5v]^{-2}$ vanishes. If there is no lower-level broadening ($\mathfrak{R}_b = 0$), the effect of the virtual transitions $\Delta j_E = 0, +1$ is to increase both the shift and width; the ratios of shift to width is altered from the numerically obtained Lindholm-Foley value of Eq. (67) which was gotten assuming $\mathfrak{R}_b = \mathfrak{R}_\varphi = 0$. We will average Eq. (B4) only in the limits $\mathfrak{R}_b = \mathfrak{R}_\varphi = 0$ and $\mathfrak{R}_a = \mathfrak{R}_\varphi = 0$.

Region II $0.02 \leq \eta \leq 4.9$

In these regions, computer solutions with accuracy of better than 0.5% in all $M_{mm'}^{pp'}$ elements have been used.

Region III $4.9 \leq \eta < \infty$

This region corresponds to collisions with impact parameters less than about 0.6 of the Weisskopf radius and contributes about 25% of the broadening. From experimental cross sections, it is quite probable that the dipole-dipole interaction fails for most systems at these impact parameters (it may also fail at larger impact parameters); however, in the spirit of the model, we shall assume its validity for all impact parameter. As in the resonant case, the nonresonant elements are periodic at small impact parameter (large η). The value of $M_{mm'}^{pp'}$ averaged over its period in η , denoted by $M_{mm'}^{pp'}(\Omega_0)$, for three periods is given in Table IX. From these results we can infer the asymptotic average values $\mathfrak{M}_{11}^{11}(\Omega_0) = -0.5$ and $\mathfrak{M}_{10}^{10}(\Omega_0) = -1.5$. In addition, we shall assume the final asymptotic average values for other elements as $\mathfrak{M}_{11}^{00}(\Omega_0) = 0$, $\mathfrak{M}_{00}^{00}(\Omega_0) = 0$, and $\mathfrak{M}_{11}^{-1-1}(\Omega_0) = 0.5$ whose choice will be verified in Appendix C. In view of this assumption, an attempt was made to fit the average of the elements over periods $\eta = 4.0-4.9$ and $\eta = 8.4-9.3$ to the following expressions for the asymptotic averages:

$$\mathfrak{M}_{11}^{00}(\eta, \Omega_0) = \epsilon_1 \exp(-A_1 \eta),$$

$$\mathfrak{M}_{11}^{-1-1}(\eta, \Omega_0) = 0.5[1 - \epsilon_2 \exp(-A_2 \eta)], \quad (\text{B6})$$

$$\mathfrak{M}_{00}^{00}(\eta, \Omega_0) = -2\mathfrak{M}_{11}^{00}(\eta, \Omega_0).$$

One obtains $\epsilon_1 = 0.245$, $A_1 = 0.0357$, $\epsilon_2 = 0.560$, and $A_2 = 0.0462$. A check of this solution at the period $\eta = [2.0, 2.9]$ yields agreement to within 10%, indicating some validity in the method. If the fit had been made to a power law, the results would not differ by a significant amount. An allowance for error extremes will be presented in Appendix D. Of course, more accurate results could have been obtained by integrating Eqs. (B1) at larger η ; however, such a procedure is costly (step integration size $\sim \eta^{-1}$) and, as mentioned above, is probably not particularly significant. On averaging over collision orientations, one obtains asymptotic average values $\mathfrak{M}_{mm'}^{pp'}$ which are numerically equal to the corresponding $s_{mm'}^{pp'}$ elements of the resonant theory given in Table VIII.

APPENDIX C: STRONG COLLISIONS

In this appendix, we indicate a method for analytically obtaining the asymptotic average values for the elements described in Appendixes A and B. The method is based on an additional adiabatic hypothesis to be discussed below.^{26, 84, 85}

It may seem surprising that strong collisions give rise to an adiabatic effect. However, in this appendix, we are considering adiabaticity relative to sublevels of a given state rather than relative to two optically separated levels. It is the collision interaction that breaks the sublevel degeneracy and allows for the use of an adiabatic theory.

Resonant Case

Consider Eqs. (10) which describe a single collision

$$i\hbar \dot{\vec{a}} = V(t)\vec{w}, \quad (\text{C1a})$$

$$i\hbar \dot{\vec{w}} = V(t)\vec{a}, \quad \vec{a}(-\infty) = \vec{a}_0, \quad \vec{w}(-\infty) = 0. \quad (\text{C1b})$$

TABLE IX. Average values of nonresonant scattering matrix elements for several periods in η .

Element	$\eta = [2.0, 2.9]$	$\eta = [4.0, 4.9]$	$\eta = [8.4, 9.3]$
$\mathfrak{M}_{11}^{11}(\Omega_0)$	-0.454	-0.480	-0.495
$\mathfrak{M}_{11}^{00}(\Omega_0)$	0.230	0.210	0.179
$\mathfrak{M}_{11}^{-1-1}(\Omega_0)$	0.223	0.271	0.316
$\mathfrak{M}_{10}^{10}(\Omega_0)$	-1.43	-1.47	-1.50
$\mathfrak{M}_{00}^{00}(\Omega_0)$	-0.461	-0.420	-0.357

We introduce a unitary matrix $D(t)$ which instantaneously diagonalizes the matrix $V(t)$; that is,

$$D(t)V(t)D^\dagger(t) = V'(t), \quad (C2)$$

where $V'(t)$ is diagonal. We may rewrite Eqs. (C1)

$$i\hbar \dot{\vec{a}}' - i\hbar \dot{D}(t)\vec{a} = V'(t)\vec{w}', \quad (C3a)$$

$$i\hbar \dot{\vec{w}}' - i\hbar \dot{D}(t)\vec{w} = V'(t)\vec{a}', \quad (C3b)$$

where $\vec{a}'(t) = D(t)\vec{a}(t)$ and $\vec{w}'(t) = D(t)\vec{w}(t)$. The adiabatic assumption, whose validity will be discussed below, allows us to neglect the $\dot{D}(t)$ terms in Eqs. (C3). Thus, in this adiabatic approximation, Eqs. (C3) read

$$i\hbar \dot{\vec{a}}' = V'(t)\vec{w}', \quad (C4a)$$

$$i\hbar \dot{\vec{w}}' = V'(t)\vec{a}'. \quad (C4b)$$

Since $V'(t)$ is now diagonal the problems of non-commutativity do not enter here, and Eqs. (C4) may be trivially integrated to yield

$$\begin{aligned} \vec{a}'(\infty) &= \cos[\hbar^{-1} \int_{-\infty}^{\infty} V'(t)dt] \vec{a}'(-\infty) \\ &\quad - i \sin[\hbar^{-1} \int_{-\infty}^{\infty} V'(t)dt] \vec{w}'(-\infty), \end{aligned} \quad (C5a)$$

$$\begin{aligned} \vec{w}'(-\infty) &= -i \sin[\hbar^{-1} \int_{-\infty}^{\infty} V'(t)dt] \vec{a}'(-\infty) \\ &\quad + \cos[\hbar^{-1} \int_{-\infty}^{\infty} V'(t)dt] \vec{w}'(-\infty). \end{aligned} \quad (C5b)$$

It remains to diagonalize $V(t)$. Equations (C5) are independent of representation and, for this problem, it is convenient to choose the basis

$$\begin{aligned} |x; s\rangle &= (-1/\sqrt{2})[|1; s\rangle - |-1; s\rangle], \\ |y; s\rangle &= (i/\sqrt{2})[|1; s\rangle + |-1; s\rangle], \\ |z; s\rangle &= |0; s\rangle, \end{aligned} \quad (C6)$$

so that the matrix $V(t)$, for a collision of the standard geometry, takes the form

$$V(t) = \{e^2 a_0^2 |T(s0, a1)|^2 / 3 [R(t)]^5\} \begin{matrix} x; s & y; s & z; s \\ \times y; s & \begin{bmatrix} R^2(t) - 3v^2 t^2 & 0 & 3bvt \\ 0 & R^2(t) & 0 \\ 3bvt & 0 & R^2(t) - 3b^2 \end{bmatrix} \\ z; s \end{matrix} \quad (C7)$$

In diagonalizing $V(t)$, one obtains eigenvalues

$$\lambda_1(t) = -2[R(t)]^2,$$

$$\lambda_2(t) = \lambda_3(t) = [R(t)]^2. \quad (C8)$$

and the corresponding eigenvectors

$$a'_x(t) = [-vt a_x(t) - b a_z(t)] [R(t)]^{-1}, \quad (C9a)$$

$$a'_y(t) = a_y(t), \quad (C9b)$$

$$a'_z(t) = [b a_x(t) - vt a_z(t)] [R(t)]^{-1}, \quad (C9c)$$

with similar expressions for $\vec{w}'(t)$. We are interested only in the times $t = \pm\infty$ for which

$$\begin{aligned} a'_x(-\infty) &= a_x(-\infty), & a'_x(\infty) &= -a_x(\infty), \\ a'_z(-\infty) &= a_z(-\infty), & a'_z(\infty) &= -a_z(\infty), \end{aligned} \quad (C10)$$

with similar expressions for the w 's. Letting

$$\chi_1(b) = \frac{1}{3} \hbar^{-1} e^2 a_0^2 |T(s0, a1)|^2 \int_{-\infty}^{\infty} [R(t)]^{-3} dt, \quad (C11)$$

$$\chi_2(b) = \frac{1}{3} \hbar^{-1} e^2 a_0^2 |T(s0, a1)|^2 \int_{-\infty}^{\infty} [-2[R(t)]^{-3}] dt,$$

and using the fact that $\vec{w}'(-\infty) = 0$, Eqs. (C5), (C8), (C10), and (C11) enable us to write the wave function after the collision as

$$\begin{aligned} |\psi(\infty)\rangle &= -a_x(-\infty) \cos[\chi_1(b)] |x; s\rangle \\ &\quad + a_y(-\infty) \cos[\chi_2(b)] |y; s\rangle \\ &\quad - a_z(-\infty) \cos[\chi_2(b)] |z; s\rangle \\ &\quad + i a_x(-\infty) \sin[\chi_1(b)] |s; x\rangle \\ &\quad - i a_y(-\infty) \sin[\chi_2(b)] |s; y\rangle \\ &\quad + i a_z(-\infty) \sin[\chi_2(b)] |s; z\rangle, \end{aligned} \quad (C12)$$

whereas the initial wave function was

$$\begin{aligned} |\psi(-\infty)\rangle &= a_x(-\infty) |x; s\rangle \\ &\quad + a_y(-\infty) |y; s\rangle + a_z(-\infty) |z; s\rangle. \end{aligned} \quad (C13)$$

Equations (C12) and (C13) then enable us to calculate the change in the density matrix as a result of the collision. To obtain the asymptotic average values we average over $\chi_1(b)$ and $\chi_2(b)$. Since χ_1 and χ_2 are rapidly varying functions of b for small b , we take

$$\langle \cos[\chi_i(b)] \rangle_{\text{av}} = \langle \sin[\chi_i(b)] \rangle_{\text{av}} = 0, \quad i=1,2 \quad (\text{C14a})$$

$$\begin{aligned} \langle \cos[\chi_i(b)] \cos[\chi_j(b)] \rangle_{\text{av}} \\ = \langle \sin[\chi_i(b)] \sin[\chi_j(b)] \rangle_{\text{av}} = \frac{1}{2} \delta_{ij}, \\ i, j = 1, 2. \end{aligned} \quad (\text{C14b})$$

We shall do one such calculation. Using Eqs. (C12), (C13), and (C6), it is a straightforward calculation to show that

$$\begin{aligned} \langle \delta \rho_{11}^{\text{I}} \rangle_{\text{av}} = \frac{1}{2} \langle |a_x(-\infty) \cos \chi_1 \\ + i a_y(-\infty) \cos \chi_2|^2 \rangle_{\text{av}} - \rho_{11}^{\text{I}}(-\infty). \end{aligned}$$

Using Eqs. (C14) and (C6), one obtains

$$\begin{aligned} \langle \delta \rho_{11}^{\text{I}} \rangle_{\text{av}} &= \frac{1}{4} [|a_x(-\infty)|^2 + |a_y(-\infty)|^2] - \rho_{11}^{\text{I}}(-\infty) \\ &= \frac{1}{4} [\rho_{11}^{\text{I}}(-\infty) + \rho_{-1-1}^{\text{I}}(-\infty)] - \rho_{11}^{\text{I}}(-\infty) \\ &= -\frac{3}{4} \rho_{11}^{\text{I}} + \frac{1}{4} \rho_{-1-1}^{\text{I}}, \end{aligned}$$

so that $\mathcal{T}_{11}^{11}(\Omega_0) = -\frac{3}{4}$ and $\mathcal{T}_{11}^{-1-1}(\Omega_0) = \frac{1}{4}$ in agreement with Appendix A. Similarly, all the other asymptotic average values may be verified.

We have used an adiabatic assumption for strong collisions and shall now show that it is valid in this region. The assumption was to neglect the $\dot{D}(t)$ terms in Eqs. (C3). The $D(t)$ matrix rotates the basis vectors so that the axis of quantization instantaneously lies along the line connecting the colliding atoms. Thus, in a rough approximation $\dot{D}(t) \approx (v/b)D(t)$. From Eqs. (C3) and (C7), we are led to the condition of applicability of the adi-

abatic approximation

$$\hbar(v/b) \ll b^{-3} e^2 a_0^{-2} |T(s_0, a_1)|^2,$$

or

$$b \ll [e^2 a_0^{-2} |T(s_0, a_1)|^2 / \hbar v]^{1/2} \approx b_0. \quad (\text{C15})$$

The quantity b_0 is the optical collision radius for resonant collisions. For strong collisions ($b \ll b_0$), the adiabatic approximation is valid; this explains the agreement obtained with the results of Appendix A.

One should note the difference between this adiabatic approximation and the one made throughout the main body of the paper. The latter is always valid due to the large optical separation of the levels. On the other hand, the separation of the energy levels of the instantaneous eigenfunctions presented in this appendix arises from the emitter-perturber electrostatic interaction. For close collisions, this separation becomes large enough so that the collision can no longer induce transitions between the instantaneous eigenstates. At this point, the adiabatic assumption, in the sense of this appendix, becomes valid.

Nonresonant Case

Here we must start with Eq. (59) (in differential form),

$$i\hbar \dot{\vec{a}} = (\hbar\omega)^{-1} V(t) V^\dagger(t) \vec{a}.$$

The procedure is the same as for the nonresonant case. The same matrix $D(t)$ can be used to diagonalize $V(t) V^\dagger(t)$. One easily verifies the asymptotic average values of Appendix B. In this case, the adiabatic approximation is valid for impact parameters much less than the optical collision radius for nonresonant collision.

APPENDIX D: AVERAGES OVER COLLISION ORIENTATION, IMPACT PARAMETERS, AND RELATIVE SPEED

In this appendix, we evaluate the average scattering matrix elements given in Eq. (31) as

$$X_{mm'}^{pp'} = 2\pi N \int db dv d\Omega \varphi(v) F(\Omega) b v X_{mm'}^{pp'}(b, v, \Omega), \quad (\text{D1})$$

where X can be any one of the elements T, R, S , or M .

A. Angular Average

We first evaluate

$$X_{mm'}^{pp'}(b, v) = \int d\Omega F(\Omega) X_{mm'}^{pp'}(b, v, \Omega). \quad (\text{D2})$$

The quantity $F(\Omega)$ is the probability density for a given collision orientation and is easily shown to equal

$(8\pi^2)^{-1}$.⁸⁶ Using this result and Eq. (27), Eq. (D2) becomes

$$X_{mm'}^{pp'}(b, v) = (8\pi^2)^{-1} \int d\Omega \sum_{\mu\mu'} \sum_{\alpha\alpha'} \mathfrak{D}_{p\mu}^{j*}(\Omega) \mathfrak{D}_{m'\alpha'}^{j'*}(\Omega) \mathfrak{D}_{m\alpha}^j(\Omega) \mathfrak{D}_{p'\mu'}^{j'}(\Omega) X_{\alpha\alpha'}^{\mu\mu'}(b, v, \Omega_0), \quad (D3)$$

where j and j' are the j values associated with m and m' . Using the formulas in Ref. 56, the average over angles in Eq. (D3) is easily performed to yield

$$X_{mm'}^{pp'}(b, v) = \sum_{\mu\mu'} \sum_{\alpha\alpha'} (-1)^{p'-\alpha'+m'-\mu'} X_{\alpha\alpha'}^{\mu\mu'}(b, v, \Omega_0) \sum_{JMN} (2J+1) \times \begin{pmatrix} j' & j & J \\ p' & -p & M \end{pmatrix} \begin{pmatrix} j' & j & J \\ \alpha' & -\alpha & N \end{pmatrix} \begin{pmatrix} j' & j & J \\ m' & -m & M \end{pmatrix} \begin{pmatrix} j' & j & J \\ \mu' & -\mu & N \end{pmatrix}, \quad (D4)$$

where the quantities under the summation sign are Wigner 3- J symbols.

Case 1 - $j = j' = 1$

In this case, one obtains parameters relevant to density-matrix elements involving substates of the $j = 1$ level only. Using elementary properties of the 3- J symbols and Eqs. (D4), (A6), (A7), and (23), it can be shown that the only contributing elements of $X_{mm'}^{pp'}(b, v, \Omega_0)$ are

$$\begin{aligned} X_{00}^{00}(b, v, \Omega_0), \quad X_{-1-1}^{11}(b, v, \Omega_0) &= X_{11}^{-1-1}(b, v, \Omega_0), \\ X_{0-1}^{10}(b, v, \Omega_0) &= X_{01}^{-10}(b, v, \Omega_0) = X_{10}^{01}(b, v, \Omega_0) = X_{10}^{0-1}(b, v, \Omega_0), \\ X_{00}^{11}(b, v, \Omega_0) &= X_{11}^{00}(b, v, \Omega_0) = X_{00}^{-1-1}(b, v, \Omega_0) = X_{-1-1}^{00}(b, v, \Omega_0), \\ X_{11}^{11}(b, v, \Omega_0) &= X_{-1-1}^{-1-1}(b, v, \Omega_0), \quad X_{1-1}^{1-1}(b, v, \Omega_0) = X_{-11}^{-11}(b, v, \Omega_0), \\ X_{10}^{10}(b, v, \Omega_0) &= [X_{01}^{01}(b, v, \Omega_0)]^* = [X_{0-1}^{0-1}(b, v, \Omega_0)]^* = X_{-10}^{-10}(b, v, \Omega_0), \end{aligned} \quad (D5)$$

and

$$X_{00}^{11}(b, v, \Omega_0) = X_{0-1}^{10}(b, v, \Omega_0), \quad X_{11}^{11}(b, v, \Omega_0) = X_{1-1}^{1-1}(b, v, \Omega_0). \quad (D6)$$

Thus, we need evaluate only five $X_{mm'}^{pp'}(b, v, \Omega_0)$ elements. The averaged elements $X_{mm'}^{pp'}$ obey all the equalities of Eq. (D5) but not those of Eq. (D6). An explicit calculation of Eq. (D4) yields the matrix equation

$$15 \begin{bmatrix} X_{00}^{00}(b, v) \\ X_{11}^{11}(b, v) \\ X_{00}^{11}(b, v) \\ X_{0-1}^{10}(b, v) \\ X_{10}^{10}(b, v) \\ X_{1-1}^{1-1}(b, v) \\ X_{-1-1}^{11}(b, v) \end{bmatrix} = \begin{bmatrix} 3 & 8 & 0 & 4 & 4 \\ 2 & 7 & 10 & 6 & 1 \\ 1 & 1 & 10 & -2 & 3 \\ -1 & -1 & 10 & 2 & -3 \\ 1 & 6 & 0 & 8 & -2 \\ 2 & 7 & 10 & 6 & 1 \\ 2 & 2 & 0 & -4 & 6 \end{bmatrix} \begin{bmatrix} X_{00}^{00}(b, v, \Omega_0) \\ X_{11}^{11}(b, v, \Omega_0) \\ X_{00}^{11}(b, v, \Omega_0) \\ \text{Re}[X_{10}^{10}(b, v, \Omega_0)] \\ X_{-1-1}^{11}(b, v, \Omega_0) \end{bmatrix}. \quad (D7)$$

All $X_{mm'}^{pp'}(b, v)$ not equal to any of the above by Eqs. (D5) will vanish.

Case 2 - $j = 1, j' = 0$ or $j = 0, j' = 1$

In this case, one obtains parameters relevant to density-matrix elements involving both the $j = 1$ and $j = 0$ levels. Using Eq. (D4) one finds

$$X_{m0}^{m0}(b, v) = \frac{1}{3} \sum_m X_{m'0}^{m'0}(b, v, \Omega_0) = -1 + \frac{1}{3} Q^*(b, v) \sum_m X_{m'm}^{m'm}(b, v, \Omega_0), \quad (D8)$$

and all other $X_{m0}^{n0}(b, v)$ vanish. [The 0's refer to the $j = 0$ state, and $Q(b, v)$ is the evolution operator for the $j = 0$ state.] One notes that $X_{m0}^{m0}(b, v)$ is independent of m .

B. Average Over Impact Parameter

We are left with evaluation of

$$X_{mm'}^{pp'} = 2\pi N \int db dv \varphi(v) b v X_{mm'}^{pp'}(b, v). \quad (D9)$$

Resonant Case

Using the results of Appendix A and the definitions of the constant A [see Eq. (42)], we perform the integration indicated by Eq. (D9). The transformation to an integration over α [see Eq. (A2)] is given by

$$2\pi N \int dv \int b db \varphi(v) v X_{mm'}^{pp'}(b, v) = \pi A \int_0^\infty d\alpha X_{mm'}^{pp'}(\alpha) \alpha^{-2}.$$

The integration in region I was done analytically using the perturbation solution for $X_{mm'}^{pp'}(\alpha)$. In region II, Simpson's rule was used with step sizes of 0.01 in the range $\alpha = [0.01, 0.1]$ and 0.1 in the range $\alpha = [0.1, 4.9]$. In region IV, $X_{mm'}^{pp'}(\alpha)$ is varying rapidly compared with α^{-2} , and we replace $\int d\alpha X_{mm'}^{pp'}(\alpha) \alpha^{-2}$ by $\mathfrak{X}_{mm'}^{pp'} \int d\alpha \alpha^{-2}$, where $\mathfrak{X}_{mm'}^{pp'}$ is the appropriate asymptotic average given in Table VIII. Summing the contributions from the three regions leads to the numerical values of $T_{mm'}^{pp'}$ and $S_{mm'}^{pp'}$ listed in Table I.

Values for the multipole decay constants in terms of the average scattering matrix elements may be calculated using Eqs. (30), (38), (43), and (44) to be

$$\begin{aligned} \Gamma_1^I &= -(T_{10}^{10} + T_{10}^{0-1}), & \Gamma_2^I &= -(T_{10}^{10} - T_{10}^{0-1}), & \Gamma_0^I &= -(T_{11}^{00} + T_{11}^{-1-1} + T_{11}^{11}), \\ \Gamma_1^{II} &= -(R_{10}^{10} + R_{10}^{0-1}), & \Gamma_2^{II} &= -(R_{10}^{10} - R_{10}^{0-1}), & \Gamma_0^{II} &= -(R_{11}^{00} + R_{11}^{-1-1} + R_{11}^{11}), \\ \Gamma_i &= \Gamma_i^I + \Gamma_i^{II}, \quad i = 0, 1, 2, \\ \Gamma_{ab} &= -T_{mb}^{mb} \text{ (independent of } m), \quad \text{and} \quad \Delta_g = iR_{mb}^{mb} \text{ (independent of } m). \end{aligned} \quad (D10)$$

The numerical values of these elements are given in Sec. III and Table III.

The errors quoted in these tables were obtained by consideration of errors introduced in (a) the computer solution of Eqs. (A4); (b) the use of Simpson's rule; (c) the replacement of $X_{mm'}^{pp'}(b, v)$ with its asymptotic average value in region IV; and (d) possible errors in asymptotic choices. Error (d) is not large because of the rapid convergence of the integral in the resonant case.

Nonresonant Case

The procedure is identical to that for the resonant case. The transformation to an integral over η is given by

$$2\pi N \int dv \int b db \varphi(v) v X_{mm'}^{pp'}(b, v) = \frac{1}{5} N |\mathfrak{B}_\alpha|^{2/5} \langle v^{3/5} \rangle_v \int_0^\infty d\eta X_{mm'}^{pp'}(\eta) \eta^{-7/5}.$$

For the nonresonant case the integration in region IV must also be done numerically, since our choice of average asymptotic solutions in this region leads to an incomplete γ function.

The numerical results for the average scattering matrix elements $M_{mm'}^{pp'}$ are listed in Table II. The parameters Γ_0^N , Γ_1^N , and Γ_2^N can be obtained by use of Eqs. (D10) with $T_{mm'}^{pp'}$ replaced by $M_{mm'}^{pp'}$. The quoted errors reflect the error considerations of the resonant case, as well as an allowance for a nonexponential decay of \mathfrak{M}_{11}^{00} , \mathfrak{M}_{00}^{00} , and \mathfrak{M}_{11}^{-1-1} [see Eqs. (B6)].

Finally, we wish to calculate γ_{ab}^N and Δ_{ab}^N . In these calculations, the average asymptotic values $\text{Re}(\mathfrak{w}'') = -1$ and $\text{Im}(\mathfrak{w}'') = 0$ in Eq. (B4) are well established by $\eta = 4.9$. As in the text, we shall assume that the $j=0$ level is the lower level. If the $j=1$ state dominates the broadening and if the virtual transitions of the emitter are solely of the form $\Delta_{jE} = -1$ [i. e., if $|\mathfrak{a}_a| \gg |\mathfrak{a}_b|$ and $|\mathfrak{a}_a| \gg |\mathfrak{a}_\varphi|$ in Eq. (B5)], using the results of Appendix B for $M_{m0}^{m0}(b, v, \Omega_0)$ in Eqs. (D8) and (D9), we obtain

$$\gamma_{ab}^N = (8.97 \pm 0.04)N |\mathfrak{a}_a|^{2/5} \langle v^{3/5} \rangle_v, \quad \Delta_{ab}^N = (-6.51 \pm 0.03)N |\mathfrak{a}_a|^{2/5} \langle v^{3/5} \rangle_v,$$

$$|\Delta_{ab}^N / \gamma_{ab}^N| = 0.726 \pm 0.007, \quad (\text{D11})$$

while if the $j=0$ state dominates ($|\mathfrak{a}_b| \gg |\mathfrak{a}_a|$ and $|\mathfrak{a}_b| \gg |\mathfrak{a}_\varphi|$), the Lindholm-Foley result may be analytically obtained as

$$\gamma_{ab}^N = 14.3N \mathfrak{a}_b^{2/5} \langle v^{3/5} \rangle_v, \quad \Delta_{ab}^N = +10.4N \mathfrak{a}_b^{2/5} \langle v^{3/5} \rangle_v,$$

$$|\Delta_{ab}^N / \gamma_{ab}^N| = 0.726. \quad (\text{D12})$$

A positive Δ indicates a shift to the violet. Had the upper level been the $j=0$ state, the shifts change sign. The equality of the ratio of $|\Delta_{ab}^N / \gamma_{ab}^N|$ for these two cases seems to be an accidental occurrence as has been noted in Sec. IV.

*Research sponsored by Yale University, the Air Force Office of Scientific Research, Office of Aerospace Research, under AFOSR grants 249-67 and 1324-67, and the National Aeronautics and Space Administration, grant No. NGR-07-004-035. This paper is based on material submitted by P. R. Berman in partial fulfillment of the requirements for the degree of Doctor of Philosophy at Yale University.

†Sterling Fellow.

¹E. Lindholm, *Arkiv Mat. Astron. Fysik* **32A**, 17 (1945).

²H. M. Foley, *Phys. Rev.* **69**, 616 (1946).

³P. W. Anderson, *Phys. Rev.* **76**, 647 (1949).

⁴Additional discussion of and references to earlier works may be found in S. Chen and M. Takeo, *Rev. Mod. Phys.* **29**, 20 (1957); R. Breene, *ibid.* **29**, 94 (1957); H. Margeneau and M. Lewis, *ibid.* **31**, 569 (1959).

⁵M. Baranger, in *Atomic and Molecular Processes*, edited by D. R. Bates (Academic Press Inc., New York, 1962), Chap. 13; *Phys. Rev.* **111**, 481 (1958); **111**, 494 (1958).

⁶H. R. Griem, *Plasma Spectroscopy* (McGraw-Hill Book Co., Inc., New York, 1964).

⁷U. Fano, *Phys. Rev.* **131**, 259 (1963).

⁸F. W. Byron, Jr., and H. M. Foley, *Phys. Rev.* **134**, A625 (1964).

⁹M. I. Dyakonov and V. I. Perel, *Zh. Eksperim. i Teor. Fiz.* **48**, 345 (1965) [English transl.: *Soviet Phys. - JETP* **21**, 227 (1965)].

¹⁰A. Omont, *J. Phys. (Paris)* **26**, 26 (1965).

¹¹G. P. Reck, H. Takebe, and C. A. Mead, *Phys. Rev.* **137**, A683 (1965).

¹²T. Watanabe, *Phys. Rev.* **138**, A1573 (1965); **140**, AB5 (1965).

¹³A. W. Ali and H. R. Griem, *Phys. Rev.* **140**, A1044

(1965); **144**, A366 (1966).

¹⁴A. Ben-Reuven, *Phys. Rev.* **141**, 34 (1966); **145**, 7 (1966).

¹⁵A. P. Kazantsev, *Zh. Eksperim. i Teor. Fiz.* **51**, 1751 (1966) [English transl.: *Soviet Phys. - JETP* **24**, 1183 (1967)].

¹⁶S. G. Rautian and I. I. Sobelman, *Usp. Fiz. Nauk* **90**, 209 (1966) [English transl.: *Soviet Phys. - Usp.* **9**, 701 (1967)].

¹⁷S. G. Rautian, *Zh. Eksperim. i Teor. Fiz.* **51**, 1176 (1966) [English transl.: *Soviet Phys. - JETP* **24**, 788 (1967)].

¹⁸D. W. Ross, *Ann. Phys. (N. Y.)* **36**, 458 (1966).

¹⁹V. V. Yakimets, *Zh. Eksperim. i Teor. Fiz.* **51**, 1469 (1966) [English transl.: *Soviet Phys. - JETP* **24**, 990 (1967)].

²⁰B. Bezzerides, *J. Quant. Spectry. Radiation Transfer* **7**, 353 (1967).

²¹J. Cooper, *Rev. Mod. Phys.* **39**, 167 (1967).

²²E. I. Duman, B. M. Smirnov, and M. I. Chibisov, *Zh. Eksperim. i Teor. Fiz.* **53**, 314 (1967) [English transl.: *Soviet Phys. - JETP* **26**, 210 (1968)].

²³W. R. Hindmarsh, A. D. Petford, and G. Smith, *Proc. Roy. Soc. (London)* **A297**, 296 (1967).

²⁴E. L. Lewis, *Proc. Phys. Soc. (London)* **92**, 817 (1967).

²⁵M. Mizushima, *J. Quant. Spectry. Radiative Transfer* **7**, 505 (1967).

²⁶A. Omont, Ph.D. thesis, Paris, 1967 (unpublished).

²⁷C. J. Tsao and B. Curnette, *J. Quant. Spectry. Radiative Transfer* **2**, 41 (1962).

²⁸Y. A. Vdovin and V. M. Galitskii, *Zh. Eksperim. i Teor. Fiz.* **52**, 1345 (1967) [English transl.: *Soviet Phys. - JETP* **25**, 894 (1967)].

²⁹J. I. Gersten and H. M. Foley, *J. Opt. Soc. Am.* **58**, 933 (1968).

- ³⁰B. L. Gyorffy, M. Borenstein, and W. E. Lamb, Jr., Phys. Rev. 169, 340 (1968).
- ³¹A. Omont and J. Meunier, Phys. Rev. 169, 92 (1968).
- ³²H. R. Zaidi, Phys. Rev. 173, 123 (1968).
- ³³The paper of W. Fursow and A. Wlassow [Physik Z. Sowjetunion 10, 378 (1936)] was instrumental in guiding the theoretical approach to the problem of resonant broadening.
- ³⁴T. Holstein, Phys. Rev. 72, 1212 (1947).
- ³⁵J. P. Barrat, J. Phys. Radium 20, 541 (1959); 20, 633 (1959); 20, 657 (1959).
- ³⁶M. I. Dyakonov and V. I. Perel, Zh. Eksperim. i Teor. Fiz. 47, 1483 (1964) [English transl.: Soviet Phys. - JETP 20, 997 (1965)].
- ³⁷A. Omont, J. Phys. (Paris) 26, 576 (1965).
- ³⁸F. W. Byron, Jr., M. N. McDermott, and R. Novick, Phys. Rev. 134, A615 (1964).
- ³⁹H. G. Kuhn and J. M. Vaughan, Proc. Roy. Soc. (London) A277, 297 (1963).
- ⁴⁰C. A. Piketty-Rives, F. Grossetete, and J. Brossel, Compt. Rend. 258, 1189 (1964).
- ⁴¹A. Szöke and A. Javan, Phys. Rev. Letters 10, 521 (1963).
- ⁴²D. N. Stacey and J. M. Vaughan, Phys. Letters 11, 105 (1964).
- ⁴³G. Attal and F. Schuller, Compt. Rend. 262, 807 (1966).
- ⁴⁴J. P. Barrat, D. Casalta, J. L. Cojan, and J. Hamal, J. Phys. (Paris) 27, 608 (1966). We are thankful to Dr. W. Happer for bringing this reference to our attention.
- ⁴⁵J. M. Vaughan, Proc. Roy. Soc. (London) A295, 164 (1966).
- ⁴⁶R. L. Barger, Phys. Rev. 154, 94 (1967).
- ⁴⁷J. P. Faroux and J. Brossel, Compt. Rend. 265, 1412 (1967).
- ⁴⁸W. Happer and E. B. Saloman, Phys. Rev. 160, 23 (1967).
- ⁴⁹H. G. Kuhn and E. L. Lewis, Proc. Roy. Soc. (London) A299, 423 (1967).
- ⁵⁰B. Lanjepce and J. P. Barrat, Compt. Rend. 264, 146 (1967).
- ⁵¹Y. Lecluse, J. Phys. (Paris) 28, 785 (1967).
- ⁵²W. J. Tomlinson and R. L. Fork, Phys. Rev. Letters 20, 647 (1968).
- ⁵³J. M. Vaughan, Phys. Rev. 166, 13 (1968).
- ⁵⁴J. M. Vaughan and G. Smith, Phys. Rev. 166, 17 (1968).
- ⁵⁵The Weisskopf or optical collision radius is commonly defined as that impact parameter for which a collision produces a relative phase shift of unity in the atomic levels.
- ⁵⁶D. M. Brink and G. R. Satchler, Angular Momentum (Clarendon Press, Oxford, 1962).
- ⁵⁷We use the definition
- $$\langle \alpha j \| T^K \| \alpha' j' \rangle = T^K(\alpha j; \alpha' j')_{\alpha_0}$$
- $$= \langle \alpha j m | T^K_Q | \alpha' j' m' \rangle \begin{bmatrix} j' & K & j \\ m' & Q & m \end{bmatrix},$$
- where T^K is an irreducible tensor of rank K .
- ⁵⁸The fine-structure splitting is not so large for some

of the laser atoms to be considered. However, for these cases the quenching (transfer of population between fine-structure levels) is still relatively small. The opposite limit is the case of hydrogen where the various fine-structure states of a given electronic level are effectively degenerate with regards to a collision.

⁵⁹Note that $\rho(t)$ is defined in the interaction representation.

⁶⁰If no time argument is displayed in T, R , or S elements, the assumed time is $t = \infty$.

⁶¹The symbol $[\dots]_{av}$ indicates an average over all histories up to time $t + \delta t$ while the symbol $\langle \dots \rangle_c$ indicates an average over all histories to time t . At impact broadening pressures, these quantities may be taken as equal.

⁶²U. Fano and G. Racah, Irreducible Tensorial Sets (Academic Press Inc., New York, 1962).

⁶³After removing $V(t')$ and $\vec{a}(t')$ from the t'' integral, one is left with $\int_{-\infty}^{t'} \exp[-i\tilde{\omega}_{pS}(t' - t'')] = (i\tilde{\omega}_{pS})^{-1}$ since it is assumed that $\tilde{\omega}_{pS} \neq 0$. [See, for example, W. Heitler, Quantum Theory of Radiation (Oxford University Press, England, 1954), 3rd ed., p. 69].

⁶⁴If level a lies below level b , the direction of shift is reversed.

⁶⁵F. London, Z. Physik Chem. B11, 222 (1930); see also H. Margeneau, Rev. Mod. Phys. 11, 1 (1939).

⁶⁶H. B. G. Casimir and D. Polder, Phys. Rev. 73, 360 (1948).

⁶⁷In obtaining the effective Hamiltonian $H^C(t)$, we have assumed (in addition to adiabaticity) that the radiation field does not act during a collision time, i.e., $\gamma\tau_c \ll 1$, where γ is some decay parameter of the perturber. In general, this is a good approximation.

⁶⁸A problem of normalization is involved here. In Eq. (112), the factor $H^V_{sk\lambda}; m^H{}^{V*}_{sk\lambda}; m'$, when summed over \hat{k} and λ , will give a value proportional to the natural width Γ_a of level a . Thus, if spontaneous emission is ignored (i.e., $\Gamma_a = 0$) one is actually multiplying Γ_a by an expression which diverges as Γ_a^{-1} and the total expression is finite and nonzero. By neglect of these considerations and proper normalization of the resultant line shapes, agreement with this more systematic treatment is obtained.

⁶⁹Note that the collision argument c has been dropped. In what follows, it will be more convenient to express the average value of $\rho_{mm'}(c)$ by $\langle \rho_{mm'}(t) \rangle_c$.

⁷⁰Even if recoil is neglected, deviations from a Voigt profile might occur. This effect can be understood by consideration of Eq. (114). The impact effects on a given emitter are averaged over all collision histories which corresponds to an average over all perturber velocities and impact parameters. In general, this will give rise to an exponential decay for $\langle \rho(t)\rho(t+\tau) \rangle$ perturbors with a decay parameter dependent on the emitter velocity u . Then, the subsequent average over emitter velocity will not yield a Voigt profile. Approximate calculations (see Refs. 25, 26, and 32) of this effect for the case of resonant broadening have indicated that it might be significant in the line wings and at high pressures. Its effect on nonresonant broadening pro-

files is not known but may prove to be somewhat important at high pressures. We shall refer to the line shapes obtained neglecting recoil as Voigt profiles, but this designation is subject to the above reservations.

⁷¹G. Breit, *Rev. Mod. Phys.* **5**, 91, (1933).

⁷²W. E. Lamb, Jr., *Phys. Rev.* **134**, A1429 (1964).

⁷³M. Sargent, III, W. E. Lamb, Jr., and R. L. Fork, *Phys. Rev.* **164**, 436 (1967).

⁷⁴In Ref. 36, Omont, in effect, has also calculated these elements. We have obtained the same results by a simplified form of radiation trapping theory.

⁷⁵It can be shown that if $v\gamma aS^{-1} \gg \lambda$ (λ = resonant wavelength) the major contribution to radiation trapping will come from atoms with $R \gg \lambda$ so that the values in Eqs. (140) and (141) may be valid at impact broadening pressures. [See also Eq. (135).]

⁷⁶The operators $H(r, t)$ and $H(c, t)$ have been sometimes termed operators in Liouville space (see Refs. 7 and 14).

⁷⁷Strictly speaking, we must also require that $H(r, t)$ be rapidly varying with respect to $[\Gamma(\text{col})]^{-1}$ if we wish to neglect all correlation effects in $H(r, t)$. However, this additional requirement becomes important only at pressures where $\Gamma(\text{col}) \gg \Gamma(\text{rad})$ in which case any modifications of $\Gamma(\text{rad})$ due to correlation effects can produce only a relatively small influence in the resultant line shapes.

⁷⁸Vdovin and Galitskii, Ref. 28, also pointed out this error.

⁷⁹The calculation of Zaidi (Ref. 32) is consistent with this experimental result. He predicts only small deviations from a Voigt profile for this experimental situation.

⁸⁰H. G. Kuhn, E. L. Lewis, and J. M. Vaughan, *Phys. Rev. Letters* **15**, 687 (1965).

⁸¹R. L. DeZafra and A. Marshall, *Phys. Rev.* **170**, 28 (1968).

⁸²A somewhat more realistic model for recoil in laser theory is being investigated by M. Borenstein at Yale University.

⁸³The case of hyperfine structure has been treated by Omont in Refs. 10 and 25.

⁸⁴L. Spitzer, Jr., *Phys. Rev.* **58**, 348 (1940).

⁸⁵V. N. Rebane and T. K. Rebane, *Opt. i Spectroskopiya* **20**, 185 (1966) [English transl.: *Opt. Spectry. - USSR* **20**, 101 (1966)].

⁸⁶The factor $(8\pi^2)^{-1}$ arises as follows: The direction of the impact parameter b can lie anywhere within a solid angle of 4π sr. In addition, the relative velocity vector can lie in anywhere in a circle of 2π rad in a plane perpendicular to b . The inverse product of these two numbers gives the probability density $F(\Omega)$ for a collision orientation Ω .